The University Of Sheffield.

Mapping mRNA export complex formation in living cells

Thesis submitted to obtain the degree of Doctor of Philosophy

by

I-Fang Teng

Department of Molecular Biology and Biotechnology

University of Sheffield

Sheffield, United Kingdom

July 2013

Acknowledgements

I would like to thank all the people who offered the assistance and support for the completion of this thesis. In particular, I would like to express my deepest gratitude to my supervisor, Prof. Stuart A Wilson. Thank you very much, Prof. Wilson for all of your professional and scientific guidance and advice, patience encouragement and support during my study at University of Sheffield. I deeply appreciate all the efforts you put forth to guide and help me complete this thesis within three years by all means. I would also like to thank Prof. Alastair Goldman and Prof. Dean Jackson for taking their time and offering professional and scientific advice, suggestion and guidance to support and help me improve and complete this thesis. Besides, I would like to acknowledge all the laboratory members: Dr. Guillaume Hautbegue, Dr. Nicolas Viphakone, Dr. Matthew Walsh, Dr. Chung-Te Chang, Vicky Porteous and Arthur Holland and also Dr. Collin Gray who had been offering assistance and guidance during my study at University of Sheffield. Finally, I would greatly appreciate my beloved parents and family members and friends who are always being there for me, encourage me and support for me in my life. Thank you very much!

INDEX OF CONTENTS

INDEX OF CONTENTS **I**

INDEX OF FIGURES **V**

ABSTRACT **VIII**

ABBREVIATIONS **IX**

CHAPTER I **1**

INTRODUCTION **1**

1.1 Global Chromatin-transcription network 1

1.1.1 Chromosome architecture 1

1.2 Transcription 2

1.2.1 RNA Polymerases in Eukaryotes and Prokaryotes 2

1.2.2 Laboratory Methods 4

1.3 Transcriptional Sites 6

1.3.1 Transcription factories 6

1.3.2 DNA elements 7

1.4 NUCLEAR PORE COMPLEX **9**

1.4.1 STRUCTURE 9

1.4.2 CARGO TRANSLOCATION 10

1.5 NUCLEAR SPECKLE 11

1.5.1 CHARACTERIZATION 12

1.5.2 COMPOSITION 12

1.5.3 BIOGENESIS 13

1.5.4 LOCALIZATION OF SC35 DOMAIN IN GENE EXPRESSION 14

1.6 RAN-DEPENDENT NUCLEAR EXPORT OF RNAS 15

1.6.1 snRNA AND rRNA EXPORT BY CRM1 16

1.6.2 tRNA EXPORT BY EXPORTIN-T 18

1.6.3 miRNA EXPORT BY EXPORTIN-5 19

1.7 mRNA EXPORT 22

1.7.1 THE mRNA EXPORT RECEPTOR 22

1.7.2 THE TREX COMPLEX 24

1.7.2.1 THE CONSERVED THO COMPONENTS IN TREX COMPLEX 24

1.7.2.2 THE mRNA EXPORT FACTORS IN TREX COMPLEX 25

1.7.2.2.1 YRA1/ALY/REF ADAPTOR 25

1.7.2.2.2 UIF (UAP56-INTERACTING FACTOR) ADAPTOR 26

1.7.2.2.3 CHTOP CO-ADAPTOR 27

1.7.2.3 TREX COMPLEX COUPLING PRE-mRNA PROCESSING 28

1.7.3 SR ADAPTOR 30

1.7.4 ROLE OF 3’END PROCESSING AND mRNA EXPORT 31

1.7.4.1 THE YEAST SR-LIKE PROTEIN NPL3 32

1.7.4.2 THROUGH THE NPC WITH YEAST NAB2 35

1.7.4.3 YRA1 RECRUITMENT VIA PCF11 34

1.7.5 EXPORT OF VIRAL RNAS 35

1.7.6 POST-TRANSLATIONAL MODIFICATION 37

1.7.7 CO- VERSUS POST-TRANSCRIPTIONAL SPLICING 38

1.7.8 MODEL OF mRNA EXPORT 39

1.8 AIM OF THIIS STUDY 42

CHAPTER II 46

MATERIAL AND METHODS 46

2.1 Plasmids, antibodies and cell cultures 46

2.2 Immunoprecipitation 47

2.3 Immunofluorescence microscopy 48

2.4 Acceptor photobleaching fluorescence resonance energy transfer microscopy 49

2.5 Confocal microscopy and fluorescence resonance energy transfer analysis 50

2.6 TCSPC fluorescence lifetime imaging microscopy 51

2.7 Fluorescence recovery after photobleaching 53

CHAPTER III **55**

3.1 INTRODUCTION: Investigation of nuclear mRNA circularization 55

3.2 RESULTS: FRET based RNA reporter constructs 56

CHAPTER IV **68**

RESULTS **68**

4.1 Subnuclear localization of mRNA export proteins 72

4.2 Detection of the Chtop:Nxf1 interaction in living cells 72

4.3 Spatially mapping the interaction between Chtop and Nxf1 by FLIM-FRET 80

4.4 Alyref interacts with Nxf1 in living cells 84

4.5 Intermolecular interactions between mRNA export factors Chtop and Alyref *in vivo* 90

4.6 Nuclear dynamics of mRNA export proteins 101

CHAPTER V **108**

DISCUSSION **108**

REFERENCES **114**

INDEX OF FIGURES

CHAPTER I: INTRODUCTION **1**

FIGURE I THE DIFFERENT RNA EXPORT PATHWAYS 21

FIGURE II A MODEL FOR mRNA EXPORT 41

CHAPTER II: MATERIALS AND METHODS **46**

CHAPTER III: RESULTS **55**

FIGURE 3-1 Schematics of tethered mRNA reporter constructs 59

FIGURE 3-2 Functional analysis of tethered messenger RNA export assay 60

FIGURE 3-3 A FRET-based RNA reporter system 61

FIGURE 3-4 An effect of a FRET-based RNA reporter system 64

FIGURE 3-5 An effect in the presence of 5’end or 3’end of reporter mRNA 65

FIGURE 3-6 A comparison of FRET Efficiency (%) with various expression vectors **67**

CHAPTER IV: RESULTS **68**

FIGURE 4-1 mRNA export protein Chtop localizes to the vicinity of nuclear speckles 69

FIGUER 4-2 Chtop colocalizes with poly (A)+ RNA in nuclear speckle 70

FIGURE 4-3 Nxf1 localizes to the vicinity of nuclear speckles 71

FIGURE 4-4 Chtop associates with TREX complex 73

FIGURE 4-5 Chtop interacts with Nxf1 in living cells 74

FIGURE 4-6 Chtop associates with Nxf1 near nuclear speckle 76

FIGURE 4-7 Chtop associates with Nxf1 near nuclear speckles 78

FIGURE 4-8 mRNA export is coupled to ongoing transcription process near nuclear speckles 79

FIGURE 4-9 The interaction between Chtop and Nxf was analyzed by FLIM-FRET 81

FIGURE 4-10 The FLIM image of Chtop and EYFP 83

FIGURE 4-11 The topological relationship between Chtop and Nxf1 84

FIGURE 4-12 The topological relationship between Chtop and Nxf1 following transcription inhibition 85

FIGURE 4-13 FLIM image between Chtop and Nxf1-Cterminus 87

FIGURE 4-14 Analysis of the Nxf1 and Alyref interaction in living HeLa cells 88

FIGURE 4-15 FRET images of Nxf1 and Alyref in living HeLa cells 89

FIGURE 4-16 FRET images of Nxf1 and Alyref after transcription

stops 91

FIGURE 4-17 The interactions of Nxf1 and Alyref by FLIM-FRET 92

FIGURE 4-18 The spatial interactions of Nxf1 and Alyref by FLIM-FRET 93

FIGURE 4-19 The interactions between Chtop and Alyref 95

FIGURE 4-20 The interactions between Chtop and Alyref by FLIM-FRET 97

FIGURE 4-21 The spatial interactions between Chtop and Alyref by FLIM-FRET 98

FIGURE 4-22 The interaction between Alyref and Chtop analyzed by NFRET 99

FIGURE 4-23 The spatial interaction between Alyref and Chtop in living cells 100

FIGURE 4-24 The spatial interaction between Alyref and Chtop in living cells 102

FIGURE 4-25 Nuclear dynamics of Chtop were measured by FRAP 103

FIGURE 4-26 Nuclear dynamics of Alyref were measured by FRAP 105

Table 1 FRAP measurement of export factors in living cells 106

CHAPTER IV: DISCUSSION **108**

ABSTRACT

The TREX ('transcription/export') complex couples nuclear RNA processing events and undergoes substantial rearrangements with mRNA export receptor Nxf1 during assembly and maturation for efficient mRNA export. However, it is not clear where TREX assembly takes place and where Nxf1 is recruited to TREX to form the export competent mRNP. Here we have used sensitized emission Förster resonance energy transfer (FRET) and fluorescence lifetime imaging (FLIM)-FRET, to produce a spatial map in living cells of the sites for the interactions of two TREX subunits, Alyref and Chtop, with Nxf1. In addition, we have performed fluorescence recovery after photobleaching (FRAP) to monitor the dynamic behaviors of export factors in the nucleus, showing Chotp and Alyref have distinctive attributes between speckle and nucleoplasm. Together, our results have been shown that prominent assembly sites for export factors are found in the vicinity of nuclear speckles in regions known to be involved in transcription, splicing and exon junction complex formation highlighting the close coupling of mRNA export with mRNP biogenesis.

ABBREVIATIONS

aa	amino acid
Ad5	adenovirus 5
APS	ammonium persulfate
ATP	adenosine triphosphate
BSA	bovine serum albumin
CAT	chloramphenicol acetyl transferase
CSK	cytoskeletal
dCTP	deoxy-cytidine triPhosphate
DEPC	diethylpyrocarbonate
dH2O	distilled water
DMEM	Dulbecco's modified Eagles' medium
DMSO	dimethyl sulfoxide
DNA	deoxynucleic acid
DNA-AD	DNA-activator domain
DNA-BD	DNA-binding domain
DTT	dithiotreitol
E. coli	*Escherichia coli*
E1B-AP5	early 1B associated protein 5

EDTA	ethylendiaminetetraacetic acid
EJC	exon junction complex
Env	envelope glyco-protein
F.I.S.H	fluorescence *in situ* hybridization
FRAP	fluorescence recovery after photobleaching
g	gram
GAP	guanine activator protein
GDP	guanosine diphosphate
GEF	guanine exchange factor
GFP	green fluorescent protein
GST	gluthathione-S-transferase
GTP	guanosine triphosphate
HIV	human immunodeficiency virus
hnRNP	heterogeneous ribonucleoprotein
HRP	Horse Radish Peroxidase
IP	immunoprecipitation
L	liter
mg	milligram
min	minute

miRNA	micro RNA
ml	milliliter
mM	millimolar
mRNA	messenger RNA
NBD	nucleotide binding domain
NES	nuclear export signal
ng	nanogram
NLS	nuclear localisation signal
nm	nanometres
NPC	nuclear pore complex
nt	nucleotides
NTF2	nuclear transport factor 2
NTP	nucleoside 5’ triphosphate
Nups	nucleoporins
OD	optical density
ORF	open reading frame
PCR	polymerase chain reaction
PEG	polyethylene glycol
PMSF	phenylmethylsulfonylfluoride

Pol.	polymerase
RNA	ribonucleic acid
RNAi	RNA interference
RNPs	ribonucleoprotein complexes
ROI	region of interest
rpm	revolutions per minute
RT	room temperature
RT-PCR	Reverse Transcriptase-Polymerase Chain Reaction
SDS-PAGE	sodium dodecyl sulphate polyacrylamide gel electrophoresis
sec	seconds
siRNA	small interference RNA
SSC	sodium saline citrate
TEMED	N,N,N’,N’-tetramethylethylenediamine
TRIS	tris (hydroxymethyl)-aminomethane
UTR	untranslated region
TB	terrific broth
µg	microgram
µL	microliter

CHAPTER I

INTRODUCTION

Gene expression in eukaryotic cells is compartmentalized between the nucleus and cytoplasm, with transcription, RNA processing and translation taking place in the nucleus and cytoplasm. This means mRNA has to translocate across the nuclear pore during the gene expression pathway. In a variety of outlooks on how and where gene expression occurring have been reported though the global pictures of coordinated work remain to be unraveled in the near future. In this thesis I have mainly introduced the architecture of the nucleus and protein complexes involved in nucleocytoplasmic transport.

1.1 Global Chromatin-transcription network

1.1.1 Chromosome architecture

Under light and electron microscopy, it is observable that nuclear architecture encompasses tons of distinct compartments for instance nucleoli, euchromatin, heterochromatin, interchromatin granule clusters (IGC, nuclear speckles or SC-35 domain) and perichromatin granules (PF). Chromosome could be observed at particular zones discretely in which so called

chromosome territories during interphase by using the method of fluorescent *in situ* hybridization (FISH). It has been shown that chromatin is able to form a looped shape with 1~2 μm into the nucleoplasm recognized as interchromatin spaces to slip away from the restraint territories. The shape of chromatin loop is thought to be likely a transcription area where chromosome with high expression level of genes (Jackson, 2003; Jackson, 2005). The earlier finding pointed out that gene clusters could appear at chromosomal bands which were topologically close to nuclear speckle SC-35 domain. It also provides an insight of SC-35 domain could be as a functional center in recruitment of clusters of genes close by and also it could be a neighborhood of euchromatin at particular regions in the nucleus (Shopland et al, 2003).The more introductions for nuclear speckles will be described in the other sessions.

1.2 Transcription

1.2.1 RNA Polymerases in Eukaryotes and Prokaryotes

Generally in eukaryotes, transcription is believed of the first stage of gene expression which can be regulated spatial separately by three types of RNA polymerase I, II and III. The phosphorylated form of RNA polymerase is regarded as the transcription event occurring actively. The RNA polymerase I

is of particular known for taking charge of the synthesis of 45S ribosomal RNA, which is a precursor of 18s and 28s rRNA, in the nucleoli. The messenger RNA is synthesize by RNA polymerase II, comprising 12 subunits (RPB1~12) and taking charge of transcribing most of genes in eukaryotes. The RNA polymerase III has a role in synthesis of such as ribosomal 5s rRNA, tRNA and small RNAs. In the case of the time for 13 kilobase transcripts completed by RNA polymerase I have been reported for approximately 2.5 minutes when transcription events take place and this could match a line with evidence for an interval of re-initiation, 1.5 seconds, in transcriptional process (Dundr et al, 2002; Jackson, 2003; Jackson, 2005; Melnik et al, 2011). Many of human genes are more than 150 kilobases; nevertheless, the TNF-α responsive genes in the tilting microarray, the time of transcription for long as 220 kilobase gene were measured by more than one hour (Papantonis & Cook, 2010).

The transcriptional process in prokaryotes takes place while transcribing DNA into RNA which is controlled via RNA polymerase (RNAP or core enzyme), including five subunits: α, α, 1β, 1β' and 1ω. There are five stages are included in the process of prokaryotic transcription: (1) pre-initiation, (2) initiation, (3) elongation, (4) promoter clearance and (5) termination. It is of Importance a variety of the transcriptional factor σs function in the regulation of

transcription process in prokaryote. Whilst the beginning of transcription which also called pre-initiation stage, RNAP would bind to promoter elements, which locates between -10 and -35 of an upstream region on the DNA sequence. Once start of the initiation stage, the transcriptional factor σ coming to interact with RNAP forms functional holoenzyme, dependent on the recognition of -10 and -35 sequences of the DNA. The example for housekeeping factor σ^{70} of E.coli, recognizing the six consensus sequences of TATTAAT at -10 and TTGACA at -35 positions on DNA promoters. Another example of transcriptional factors σ^{32} and σ^{54} family in E.coli usually regulates particular genes in response to environmental stimuli. In the beginning of promoter clearance, mRNA is synthesized via the first DNA base. It leads abortive initiation to happen, representing the incomplete transcripts produced by DNA template because of RNAP slipping. Nevertheless, the elongation of mRNA starts proceeding when RNAP stops to slip and 23 base-pair transcripts are being synthesized. Finally, the termination of mRNA transcription is influenced by Rho proteins and the DNA hairpin structures (also known as Rho-independent termination) which cause the release of mRNA from DNA template (Nickels et al, 2004; Wade et al, 2006; Van Hijum et al, 2009).

1.2.2 Laboratory Methods

The various methods to detect transcription events have been developed, and new techniques and tools keep in progress nowadays. The classic biochemistry methods used in the laboratory are briefly exampled as follows. (1) Northern blotting has been used in the quantitative measurement for the probed RNA, (2) RT-PCR is commonly analyzed for the abundance of total RNA, (3) Nuclear run-on assay has been manipulated for the measurement of newly transcripts, (4) DNA microarray, designed for analysis of collections and rates of RNA synthesis, (5) fluorescent *in situ* hybridization, detecting the localization of RNA transcripts, (6) MS2-CP tagging, a strategy that MS2 coat protein (MS2-CP) capable of being integrated within MS2-CP recognition sites, allowing to track and detect the RNA activity in living cell, (7) RNA-seq assay, one method of high-throughput sequencing in used of detecting sequence of cDNA. Additionally, three kinds of transcriptional inhibitors have been commonly used in the laboratory, for instance 6-Dichloro-1-β-d-ribofuranosylbenzimidazole (DRB) in inhibition of elongation kinase CDK of RNA polymerase II, Actinomycin D with intercalating into DNA base pairs, and α-Amantin interference with the large subunit of RNA

polymerase to block nascent transcript synthesis (Jackson, 2000; Jackson, 2003; Céline Cassé et al, 1999).

1.3 Transcriptional Sites

It is of interest to know where transcriptional sites occur for gene expression in the nucleus. Many views of models will be more clarified in the near future dependent on the rapid development of technologies. In this thesis a model of transcription factories is given as an example.

1.3.1 Transcription factories

The concept of transcription factories was evolved from the detectable and noticeable foci in the nucleus where the active genes coordinated transcription events, and in which active and phosphorylated form of RNA polymerase II was incorporated. The number of transcription factories could be different and measurable from which material sources obtained such as primary cells or adult tissues. It is generally thought that RNA polymerase I, II and III have a various and distinct kinds of transcription factories on their own (Iborra et al, 1996; Osborne et al, 2004; Sutherland & Bickmore, 2009). Detection of the transcription factories at subcellular level is achievable by

several methods such as (1) 5-bromouridine 5'-triphosphate (Br-UTP or Br-U) labeling for nascent transcripts, (2) immunofluorescence antibody staining RNA polymerase II, (3) fluorescent *in situ* hybridization (FISH) probing for the localization of RNAs, (4) MS2-CP tagging, incorporated within MS2 coat protein recognition sites on RNA transcripts. (5) Native chromosome conformation capture (3C) assay, using biochemistry purification method to detect the relationship between genome and transcription factories. Furthermore, under electron microscopy, the estimated diameter of a transcription factory was observed 45~100 nm in the nucleus (Jackson et al, 1998; Iborra et al, 1996; Jackson, 2000; Jackson, 2003; Martin & Pombo, 2003). The earlier studies reported that, for example, in the nucleoplasm of HeLa cell there are approximately 10,000 transcription factories, including ~8,000 RNA polymerase II and ~2,000 RNA polymerase III of transcription factories. One model has been proposed that each one transcription factory which could own ~8 distinguished RNA polymerase II molecules functions in transcribing a DNA template from each RNA polymerase molecule (Osborne et al, 2004; Sutherland & Bickmore, 2009; Papantonis & Cook, 2010; Edelman & Fraser, 2012).

1.3.2 DNA elements

The functional role of DNA elements is thought to be involved in gene expression regulation such as enhancers, silencers, promoters, barriers, locus control regions (LCRs) and nuclear matrix attachment regions (MARs). How do these DNA elements function and work? Their roles in chromosome territories remain unclear; however, some studies have been shown the functional relationships between transcription factors and DNA elements. For example, the LCR function is of interest that the genes expressed from the locus control regions (LCRs) of human beta-globin which were integrated into genome has an effect on the chromatin loop formation, with helping a loop shaped gene slid back to a factory for transcription initiation. Accordingly, a new point of view is mentioned that transcription factories appear to be a functional but immobilized space for active RNAP polymerase II to attract particular DNA elements for transcription start via forming loop shaped genes. In other case of DNA promoters, when plasmids which have promoters designed from RNA polymerase II were injected into cells, the plasmids with different promoters would be led to various factories (Jackson, 2003; Jackson, 2005; Noordermeer et al, 2008; Papantonis & Cook, 2010; Xu & Cook, 2008; Edelman & Fraser, 2012).

1.4 NUCLEAR PORE COMPLEX

1.4.1 STRUCTURE

Nuclear pore complexes (NPC) found in the nuclear envelope are an evolutionarily conserved structure and contain three major parts: a core structure, a basket and filaments. The core structure of the NPC which is also called the spoke complex has a cylinder-like structure with eight spoke-ring complexes symmetrically embedded between a nuclear ring and a cytoplasmic ring. Another structure is recognized as the nuclear basket on account of the filaments extending from the nuclear ring of the NPC. Besides, the eight short flexible fibrils protruding forward from the cytoplasmic ring of the NPC, constitute the third part of the NPC (Fahrenkrog et al, 2001; Rout & Aitchison, 2001). Normally, the channel in the core structure of the NPC appears to be around 10nm diameter, but the diameters of the core structure and nuclear basket of NPC are able to dilate up to 40nm when mobilizing large cargoes through the NPC (Kiseleva et al, 1998).

The yeast or metazoan NPC is formed by around 30 different nucleoporins which consists of 8, 16, 32 or 56 copies per NPC in its symmetrical octagon structure (Cronshaw et al, 2002; Rout et al, 2000). There

are three major groups of nucleoporins. The first group is the FG nucleoporins which are characterized by the repeats of the amino acid sequence FG, GLFG and FXFG, interacting with transport receptors such as importins and exportins to mediate the nuclear and cytoplasmic transport (Bednenko et al, 2003). The second group is the nucleoporins lacking FG-repeat amino acid sequences but present of a variety of motifs which are the primarily structural part of the NPC. The third group is the integral membrane proteins Nups which anchored the NPC within the double nuclear membrane. Though most nucleoporins are found symmetrically on both sides of the NPC, a few nucleoporins are located asymmetrically on either side of the NPC. It is believed that these assymetrical nucleoporins function in directional transport processes from receptors targeting through to the transport termination; in addition, they may have a compartment-specific role at the NPC by interacting with chromatin or transcription factors, or as checkpoint proteins for the quality control of the nucleocytoplasmic transport (Kohler & Hurt, 2007).

1.4.2 CARGO TRANSLOCATION

Although nuclear transportation requires the RanGTP system for recycling of the transport receptors importins and exportins, the translocation of cargo

and receptor proteins are independent of the energy of NTP hydrolysis. Thus, two main models, “Brownian affinity gate model” and the “selective phase model” have been proposed to illustrate how FG-nucleoporins interact with the cargo and receptor proteins in a direction to pass through the NPC.

The “Brownian affinity gate model” proposes that Brownian motion facilitates the binding affinity of transport receptors with the flexible filaments of FG-nucleoporins at both sides of the NPC. Therefore, the dwelling time of transport receptors at the nuclear pore is increased and it also enhances the chance of passing through the NPC channel. Upon the sequential low affinity of binding with FG-nucleoporins, the transport receptor and cargo are able to be released from the NPC pore (Rout et al, 2003; Rout et al, 2000). Another model is the “selective phase model” whereby FG-nucleoporins constitute a mesh in the NPC channel via the low affinity of FG-repeat domain which forms a barrier to diffusive movement. The low affinity between FG-repeat domain and cargo-receptor proteins facilitates the distribution of movement in the channel, promoting the cargo-receptor proteins being released from the NPC channel by the enhanced diffusion (Ribbeck & Gorlich, 2001; Ribbeck & Gorlich, 2002).

1.5 NUCLEAR SPECKLES

1.5.1 Characterization

Interchromatin granule clusters (IGCs) known as nuclear speckles localize in the interchromatin areas of the nucleoplasm. Nuclear speckles are thought to be storage and assembly sites for the pre-mRNA splicing machinery such as small nuclear ribonucleo protein particles, spliceosomes, and other non-snRNP protein splicing factors. IGCs have variable sizes from one to several micrometers in diameter and are formed by 20-25nm granule particles which are linked by a thin fibril observed by electron microscopy making them look like a beaded chain, including little or no DNA (Spector & Lamond, 2011; Thiry, 1995).

1.5.2 Composition

The hypothesis has been proposed that nuclear speckles play a role in regulation of many factors to facilitate the proper coupling of the processes of transcription and pre-mRNA splicing in subcellular compartments (Misteli et al, 1998). Proteomic analysis and localization studies have provided the evidence that many non pre-mRNA splicing factors can be detected at nuclear speckles including transcription factors, 3’-end RNA processing factors, eukaryotic

translation initiation factor eIF4E, translation inhibitor eIF4AIII and structural proteins (Rappsilber et al, 2002; Zhou et al, 2002) However, whether RNA polymerase II is present at nuclear speckle or not, it still has different points of view. Several studies showed that RNA polymerase II can not been observed at nuclear speckles (Doyle et al, 2002; Grande et al, 1997; Kimura et al, 2002), but other studies identified that the subunits of RNA polymerase II were located at nuclear speckles by the biochemical analysis of the IGC proteome and localization studies (Bregman et al, 1995; Mortillaro et al, 1996; Saitoh et al, 2004). Nevertheless, it has been shown that a population of poly(A) RNA can be detected its accumulation within nuclear speckles when transcription is inhibited (Huang et al, 1994).

1.5.3 Biogenesis

Nuclear speckles appeared to round-up after the inhibition of transcription, implying that those factors may have a consistent movement from all directions (Spector, 1993). In addition, other research indicated that it is necessary to phosphorylate the splicing factor SR proteins before recruiting the SR proteins from nuclear speckle to the active transcription site where pre-mRNA processing occurs (Misteli et al, 1998). It has been suggested that regulation

between phosphorylation and dephosphorylaiton may have a function in the exchange rate of factors at nuclear speckles (Spector & Lamond, 2011). Additional studies have pointed out that the treatment of kinase inhibitors in cells led to the limitation of mobility on the periphery of speckles and overexpressing of mutations of Clk/StY kinase accumulated on the periphery of speckles, suggesting the restriction on the release of these factors (Misteli et al, 1998; Sacco-Bubulya & Spector, 2002). It has raised the possibility that nuclear speckle may be formed by a self-assembly process independent of other scaffold proteins and can be a place, a nonmembrane-bound nuclear organelle, storing one important population of factors which are not in use functionally. However, the ability of proteins to move in and out of speckles provides a means to allow pre-mRNA processing at the site of transcription. (Lamond & Spector, 2003; Spector & Lamond, 2011).

1.5.4 Localization of SC35 domain in gene expression

Several studies have showed that highly active transcription sites of many genes prefer to localize in the vicinity of nuclear speckle domains (Brown et al, 2008; Moen et al, 2004). Other study also indicated that the gene-rich R bands were generally observed around SC35 domains, suggesting nuclear speckles

may develop as functional centers for the local euchromatic neighborhoods to gather the active genes close by (Shopland et al, 2003). However, there is discrepancy between the views that location of mRNA processing takes place near or within nuclear speckles domains. Some studies supported the view that nuclear speckles service as places of storage and/or assembly and/or modification for mRNA processing machinery such as splicing factors and export factors supplied to the active transcription sites where near to speckles (Cmarko et al, 1999; Daguenet et al, 2012; Fakan, 1994; Lamond & Spector, 2003; Melcak et al, 2000; Sacco-Bubulya & Spector, 2002; Zhao et al, 2009). On the other hand, some studies suggest that nuclear speckles function as sites of RNA processing, where pre-mRNAs are able to be assembled and spliced by splicesomes (Girard et al, 2012; Hall et al, 2006; Johnson et al, 2000; Melcak et al, 2000; Shopland et al, 2003; Wei et al, 1999).

1.6 RAN-DEPENDENT NUCLEAR EXPORT OF RNAS

In a general receptor-mediated active transport system, a conserved group of nuclear transport receptors, known as the karyopherins-β family of transport receptors or importins/exportins, recognize a nuclear localization signal (NLS) or a nuclear export signal (NES) of cargo proteins and the

structural motifs of nucleotides of cargo RNAs for the import or export. Karyopherins are regulated by the small GTPase Ran (Gorlich & Kutay, 1999; Mattaj & Englmeier, 1998; Pemberton et al, 1998). There are two major forms of Ran which exist in the cell; a GTP-bound state of Ran, RanGTP, is generated by the Ran guanine nucleotide exchange factor (RanGEF or RCC1) in the nucleus and a GDP-bound state of Ran, RanGDP, is produced by the Ran GTPase activating protein (RanGAP) in the cytoplasm. In other words, importins transport cargo from the cytoplasm to the nucleus where they release cargo dependent on binding with RanGTP; on the other hand, exportins assemble with nuclear cargo while binding together with RanGTP in the nucleus. Therefore, the asymmetric distribution of the RanGTP and RanGDP gradient provides a driving force to convey the direction of transport receptors karyopherin or importins/exportins (Gorlich & Kutay, 1999). Typically, exportins and RanGTP involve the export of tRNA, microRNA (miRNA), small nuclear RNA (snRNA) and ribosomal RNA (rRNA) through the NPC with the exception of messenger RNA (mRNA) (Rodriguez et al, 2004). The RNA export pathway of karyoptin-β family of transport receptors is overviewed as follows.

1.6.1 snRNA and rRNA EXPORT BY CRM1

The spliceosomal snRNAs involve the intron removal of pre-mRNAs in the nucleus. The majority of spliceosomal snRNAs (U1, U2, U4 and U5) are transcribed by RNA Polymerase II in the nucleus and transported to the cytoplasm with the exclusion of U6 snRNA, which is transcribed by RNA Polymerase III and retained in the nucleus. The cap-binding complex (CBC) associates with the 5' cap of snRNAs and recruits a NES-containing adaptor protein called PHAX, which in turn recruits CRM1 and RanGTP to promote export (Ohno et al, 2000). Once arrived in the cytoplasm, the interaction between snRNAs and Sm proteins induce trimethylation of the cap and 3' trailer sequence removals, providing a nuclear signal for the mature and functional snRNPs to be re-imported into the nucleus. (Huber et al, 1998).

Ribosomes are formed from a large subunit (60S) and a small subunit (40S) together consisting of 4 rRNAs (28S/25S rRNA, 5.8 rRNA, 5S rRNA and 18S rRNA) and around 80 ribosomal proteins. In the nucleolus, these ribosomal subunits are synthesized from 35S rRNA by RNA polymerase I and assembled, and then transported to the cytoplasm. The major role of the ribosome serves as a protein-synthesizing machine to translate mRNAs in the cytoplasm, but the mitochondria and chloroplasts have their specific ribosomes.

Though the mechanism of export of 40S is not clear yet, it is known that the export of both 40S and 60S subunits are dependent on Crm1 and RanGTP. The pre-60S particle recruits an adaptor protein Nmd3 containing a conserved NES sequence for nuclear exit at a late stage of pre-ribosome assembly (Ho et al, 2000). Unexpectedly, an additional receptor protein Mex67-Mtr2 was found to participate in the export of pre-60S subunit in yeast (Yao et al, 2007). Another export factor Arx1 is also recruited to the late stage of pre-60S particle with Nmd3 and Mex67-Mtr2 (Nissan et al, 2002). The 60S subunit is a large RNA-containing particle, similar in size to the NPC diameter ~26nm, and therefore it needs to recruit several types of export receptor to assist the transport through the NPC (Reed & Hurt, 2002).

1.6.2 tRNA EXPORT BY EXPORTIN-T

The aminoacylated tRNAs which have the amino acids attached with its additional CCA-nucleotide at 3' termini functions in ribosomal translation in the cytoplasm. The genes encoding tRNAs are transcribed by RNA polymerease III in the nucleus and they are characterized by the cloverleaf structures with single-stranded loops and double-stranded minihelix regions. The metazoan exportin-t, a karyotin-β family of transport receptor, is capable of binding tRNA

cargo together with RanGTP for nuclear exit and so does its yeast homolog Los1p (Hellmuth et al, 1998; Kutay et al, 1998). Unlike the CRM1-dependent nuclear export pathway, the interaction of tRNA and exportin-t for export is independent of any adaptors. Moreover, exportin-t plays a role in a quality control checkpoint by preventing its interaction from the improperly processed 5' or 3' termini of tRNAs or the mutant tRNAs with incorrect structured nucleotides prior to their export. Nevertheless, export-t proteins do not distinguish between the intron-containing tRNAs and spliced tRNAs, allowing the unspliced tRNAs to be exported to the cytoplasm (Arts et al, 1998).

1.6.3 miRNA EXPORT BY EXPORTIN-5

The pre-miRNAs (microRNAs) can be transcribed from genes containing introns or without introns by RNA Pol II or RNA Pol III and then a 60-70 nucleotides of pre-miRNA with minihelix structural motif, including a double-stranded stem with a 3-8 nucleotides 3' overhang, is produced by the RNaseIII endonuclease Drosha (Borchert et al, 2006; Lee et al, 2003). Therefore, exportin-5, a karyopherin-β family of transport receptor, is able to recognize this minihelix structure of pre-miRNA for the nuclear export upon a RanGTP-dependent manner. Once it is relased to the cytoplasm, the

cytoplasmic RNaseIII endonuclease Dicer cleaves the pre-miRNA to a final product of a ~22-nucleotide miRNA with mismatched base pairings (Bernstein et al, 2001). This unstable mismatches lead to one strand degradation and other strand assembling with the RNAi-induced silencing complex (RISC) (Bernstein et al, 2001; Schwarz et al, 2003). The 3' untranslated region of target mRNA is recognized by the miRNA on the RISC and causes mRNA cleavage, translation inhibition or mRNA degradation independent of cleavage (Valencia-Sanchez et al, 2006). The different RNA export pathways described are summarized in Figure I.

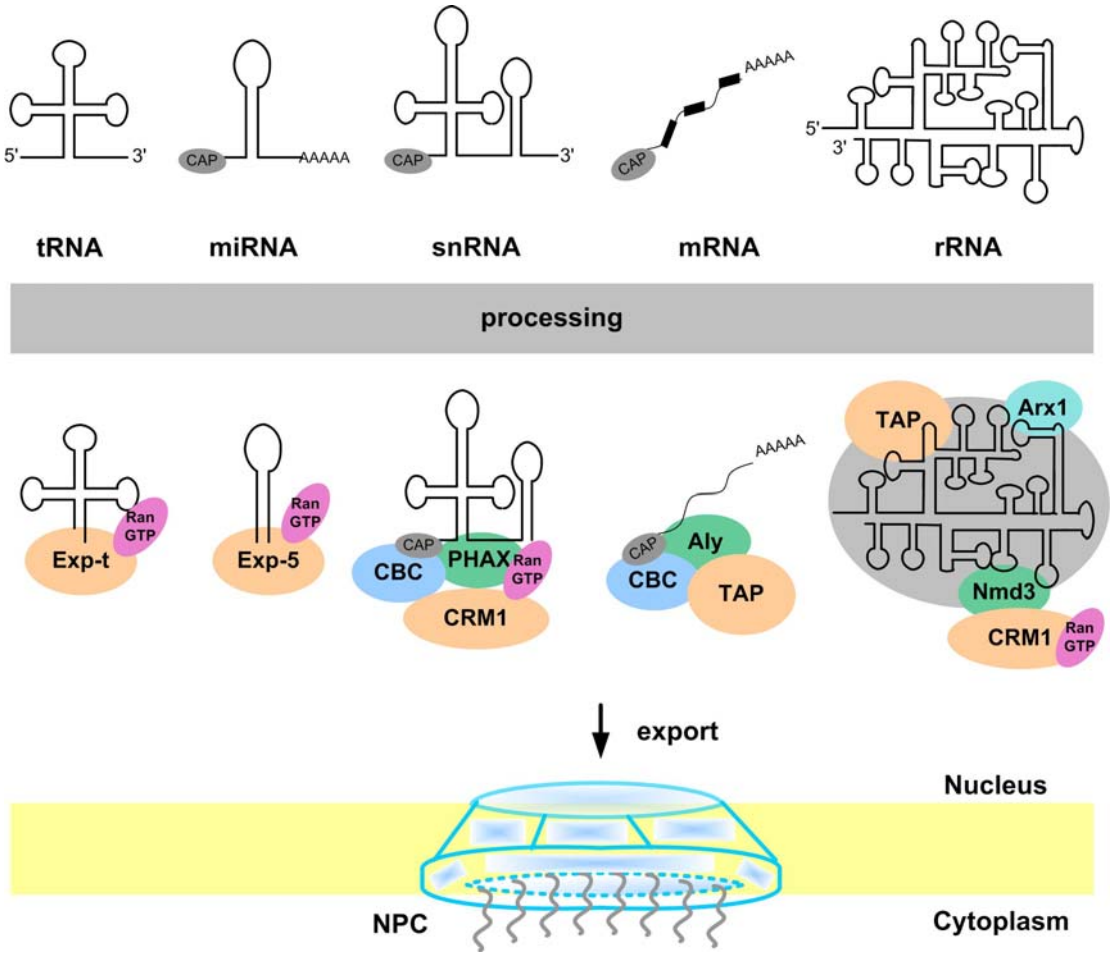

[Figure I] THE DIFFERENT RNA EXPORT PATHWAYS

1.7 mRNA EXPORT

Nuclear mRNA export involves the pathway of gene expression from both "upstream events" and "downstream events" through nuclear pore complexes (NPCs); the upstream events include mRNA transcription, 5' capping, elongation, splicing, mRNP formation, 3' end processing/polyadenylation and NPC recruitment whereas mRNP modification and translation are included in "downstream events" (Kohler & Hurt, 2007; Rodriguez-Navarro & Hurt, 2011). The recent studies on genome-wide analyses have suggested that different functional classes of mRNAs preferentially interact with particular RNA-binding proteins, suggesting that each population of mRNAs may have a distinctive pathway in the regulation of biogenesis, export and translation (Hieronymus & Silver, 2003; Kim Guisbert et al, 2005). Also, it has been shown that some conserved export receptors and specific factors involve the successive processes while mRNAs are being exported from the nucleus to the cytoplasm. These factors are classified and discussed in more detail below.

1.7.1 The mRNA export receptor

There is a general, specific and conserved mRNA receptor called

Mex67-Mtr2 in *Saccharomyces cerevisiae* or TAP-p15 complex (also known as NXF1-NXT1) in metazoan (Kohler & Hurt, 2007; Reed & Hurt, 2002). The general mRNA export receptor plays an important role in assisting mRNP transport from the nucleus through the nuclear pore complexes (NPCs), and the mRNA receptor binds directly to the phenylalanine-glycine-rich repeats of FG nucleoporins which form nuclear pore complexes to overcome the permeability barrier in order to get access to the cytoplasm (Conti & Izaurralde, 2001). The large subunit MEX67/TAP has three conserved domains: a N-terminal LRR (leucine-rich repeat) domain, a NTF2-like domain whereas NTF2 is an important receptor for RanGDP, and a C-terminal UBA (ubiquitin associated) domain (Conti & Izaurralde, 2001; Iglesias & Stutz, 2008) whereas the small subunit p15 has an NTF2 associated domain (Fribourg et al, 2001). The LRR domain functions as binding with mRNA adaptor proteins such as Yra1/REF whilst the C-terminal UBA domain and NTF2-like domain of MEX67/TAP have function in shutting and interacting with the FG nucleoporins of NPC components (Fribourg et al, 2001; Reed & Hurt, 2002). In addition, the C-terminal UBA domain of MEX67/TAP has an additional helix 4 (H4) in the last 10 amino acids whereas other UBA domains are usually composed of three α-helices (Gwizdek et al, 2006; Hobeika et al, 2007; Iglesias & Stutz,

2008), thus, allowing MEX67/TAP to make use of this additional helix 4 to interact with a specific substrate such as an ubiquitinated Hpr1 and protects ubiquitinated Hpr1 from proteasomal degradation (Gwizdek et al, 2005).

1.7.2 The TREX complex

TREX is abbreviated from transcription/export complex, and TREX complex integrates signals from the major nuclear mRNA processing events such as capping, splicing and polyadenylation and licenses mRNA for export from the nucleus to the cytoplasm. There has been two major parts of TREX complex identified, the stable multi-subunit THO components and the mRNA export factors Sub2/UAP56 and Yra1/Aly, and THO components of TREX complex have function in recruiting the mRNA export factors to load onto the mRNA in yeast and human (Reed & Cheng, 2005). Some studies have found the conserved TREX complex in yeasts and even in higher eukaryotes such as *Drosophila melanogaster* and humans might have their particular function in the regulation of pathway of pre-messenger RNA processing in the nucleus by coupling with transcription, elongation, splicing, 3'end processing or export of nascent transcripts as described below.

1.7.2.1 The conserved THO components in TREX complex

The conserved multisubunit THO components of TREX complex in yeast and in metazoan have been characterized, showing three homologous THO components, Tho2 (THOC2), Hpr1 (THOC1) and Tex1, though the cellular function of Tex1 is still unknown. Three another parts of THO components, fSAP79 (THOC5), fSAP35 (THOC6) and fSAP24 (THOC7) are conserved in metazoan but not in yeast. However, the other two THO components Mft1 and Thp2 are found conserved in yeast but not in metazoan (Masuda et al, 2005; Rehwinkel et al, 2004; Strasser et al, 2002; Zhou et al, 2002)

1.7.2.2 The mRNA export factors in TREX complex

1.7.2.2.1 Yra1/ALY/REF adaptor

One important mRNA export adaptor in mRNA export is the conserved protein Yra1/ALY adaptor, also named the REF (Strasser & Hurt, 2000). The REF family has a RRM/RBD (RNP-motif RNA binding domain/RNA binding domain) which was flanked by variable length of RGG-rich regions (N-vr and C-vr); the short N and C termini of REF family have highly conserved sequence, designated REF-N and REF-C boxes, interacting directly with MEX67/TAP in *Saccharomyces cerevisiae* and in metazoan (Rodrigues et al,

2001; Strasser et al, 2000; Stutz et al, 2000). The Yra1 adaptor asociates with another conserved mRNA export factor Sub2 in *Saccharomyces cerevisiae* similarly ALY/REF binds the Sub2 orthologue UAP56 in metazoan and regulates the mRNA export pathway (Strasser & Hurt, 2001; Zenklusen et al, 2002). ALY, TAP-p15 and UAP56 form a stable complex with EJC (exon-junction complex) located in the ~20-24 nucleotides upstream of every exon-exon junction during late splicing (Le Hir et al, 2001; Le Hir et al, 2000). Since Sub2 and UAP56 have been characterized are RNA helicases, their cellular function is also related to the process of mRNP biogenesis, binding to TREX ('transcription/export') complex and the spliceosome complex and may help couple splicing and mRNA export.. The Yra1/ALY/REF adaptor play a role in being a bridge between RNA and the downstream-acting mRNA export receptor (Kohler & Hurt, 2007; Reed & Hurt, 2002).

1.7.2.2.2 UIF (UAP56-interacting factor) adaptor

In light of evidence that not only one mRNA export adaptor exists in metazaon since REF/Aly is not essential for bulk mRNA export (Gatfield & Izaurralde, 2002; Longman et al, 2003). However, Yra1 in yeast has been shown to interact with only a subset of mRNAs in yeast (Hieronymus & Silver,

2003). One new protein, UAP56- interacting factor (UIF), was identified in 2009 as an mRNA export adaptor. UIF, interacting with TAP, is recruited to mRNA via the FACT histone chaperone complex, SSRP1 subunit (Hautbergue et al, 2009b). This article points out that more than one adaptor involve mRNA export pathway. Nevertheless, export adaptors are capable of working with export co-adaptors for efficient mRNA export.

1.7.2.2.3 CHTOP co-adaptor

A finding of mRNA export co-adaptor, CHTOP (Small protein Rich in Arginine and Glycine; also known as FOP or CHTOP), positioned at the human C1orf77 gene was characterized as a novel TREX component in 2012. CHTOP and REF bind to UAP56 in a mutually exclusive manner and this leads to the activation of ATPase and RNA helicase activity in UAP56. The methylation of CHTOP regulates its associations with Aly, TAP and RNA but not UAP56 while CHTOP is able to cooperate with Aly to facilitate the RNA binding activity of TAP. Moreover, CHTOP binds to TAP in a mutually exclusive manner with THOC5 in the same complex to export specific mRNA. This finding reveals that the interaction of TREX complex with UAP56 is dependent on an ATPase cycle during the assembly stage, followed by loss of UAP56 and

recruiting TAP during maturation stage to undergo subsequent rearrangement for efficient mRNA export from the nucleus to the cytoplasm (Chang et al, 2013).

1.7.2.3 TREX complex coupling pre-mRNA processing

In yeast TREX complex is thought to be recruited co-transcriptionally on nascent transcripts, but in metazoan the recruitment of TREX complex is coupled to pre-mRNA splicing (Reed & Cheng, 2005).

The first *in vivo* evidence in mammalian revealed that pre-mRNA splicing requires the recruitment of mRNA export proteins UAP56, ALY and EJC onto the mRNA by using *in situ* hybridization to analyze HeLa cells infected with adenovirus and murine erythroleukemia (MEL) cells stably transfected with the human β-globin gene (Custodio et al, 2004). A close link between pre-mRNA splicing and mRNA export is connected by the interaction of ALY and UAP56, where Aly is recruited by UAP56 to the spliced mRNP (Luo et al, 2001). The C-terminal of ALY is indispensable to directly interact with UAP56 whilst the C-terminal of UAP56 is sufficient to associate with ALY, but the N-terminal of UAP56 associates with the THO components at a low level of affinity (Masuda

et al, 2005). In addition, it has been proposed that TREX complex is recruited to a region close to 5' end of pre-mRNA via the cap-binding subunit CBP80 directly associating with ALY/REF. It is dependent on splicing, whereas the recruitment of EJC (exon-junction complex) is not required. Since TREX is recruited to the 5' end of mRNA this has led to the suggestion that TREX ensures that mRNA is exported in a 5' to 3' direction through the nuclear pore (Cheng et al, 2006).

In yeast, the TREX complex can be recruited to either intron-containing or intronless transcripts. Once transcription occurs on the intronless transcripts in yeast, the TREX complex is recruited to the transcription sites via the transcription machinery, and it facilitates Sub2 and Yra1 transfer to the nascent transcript (Abruzzi et al, 2004). However, on the intron-containing transcripts, the move of Sub2 and Yra1 to the nascent RNA may be presumably hampered due to the large spliceosome complex (Abruzzi et al, 2004). Therefore, TREX complex might be recruited to active genes whereas it uses the THO complex to interact with RNA polymerase II to help deliver Sub2 and Yra1 to the nascent transcript (Reed & Cheng, 2005). Furthermore, the yeast THO component, Hpr1, does not associate with Yra1 directly, but it interacts with Sub2 directly after the recruitment to the active genes, and therefore Yra1 is

connected to THO components by Sub2 (Zenklusen et al, 2002). In addition, as it can cause misfolding transcripts, transcriptional suppression and failing to be exported in the absence of a THO subcomplex (Huertas & Aguilera, 2003), and these defects can be rescued after slowing down transcription (Jensen et al, 2004). Therefore, TREX function is thought to co-transcriptionally load RNA binding proteins onto the nascent transcript just at a limited time.

1.7.3 SR adaptor

In metazoan, SR (Ser/Arg-rich) proteins play multiple roles in the mRNA metabolism pathways, such as pre-mRNA splicing, mRNA export, stability and translation. SR proteins are loaded onto the exon regions of pre-mRNA and play a role in the recruitment of the large splicesome complex to the flank of 5' and 3' splicing sites, and therefore, dependent on the interaction of U1 snRNP and SR proteins working with RNA polymerase II, it organizes splicing factors in an appropriate arrangement during the early spliceosome assembly and also facilitates the spliceosome machinery to be close to the nascent pre-mRNA (Das et al, 2007). A role of SR protein in the splicing process is dependent upon the regulation of its phosphorylation states, and hence, even when splicing is accomplished, SR protein can be still kept binding on the

spliced mRNA (Graveley, 2000). In metazoans, the hypophosphorylated form of SR proteins 9G8 and ASF/SF2 are involved in the export of spliced mRNAs with TAP from nucleus to the cytoplasm whereas SR proteins dissociate from the mRNP complex in the hyperphosphorylated form to return from cytoplasm to nucleus (Huang et al, 2004). However, another type of SR protein SC35 appears not to function as a shuttle protein between nucleus and cytoplasm, but it can be observed on the nuclear domain which is known as nuclear speckle domain (Sapra et al, 2009).

In yeast, there are three SR-like proteins: Npl3, Gbp2 and Hrb1. These proteins are considered to be participating in mRNA export but not a role in pre-mRNA splicing (Reed & Cheng, 2005). Nevertheless, Npl3 is highly related to pre-mRNA splicing in *Saccharomyces cerevisiae* by using the method of high-density genetic interaction profiling and genome-wide splicing-sensitive microarray, plus, the result of chromatin immunoprecipitation showed that the U1 and U2 snRNPs were reduced following the NPL3 gene mutation (Kress et al, 2008). Therefore, the yeast SR-like protein, Npl3, is thought to be able to function in assist the recruitment of spliceosome complexes to pre-mRNA which is quite similar to the situation in metazoa (Reed & Cheng, 2005).

1.7.4 Role of 3'end processing and mRNA export

1.7.4.1 The yeast SR-like protein Npl3

The yeast SR-like protein plays a role at 3' end processing machinery and in the mRNA export pathway by engaging in the formation and regulation of 3' end of mRNA at the polyadenylation site (Bucheli et al, 2007). The Npl3 protein associates with mRNA in the nucleus in hyperphosphorylated form, once Glc7 is stimulated by the 3' end processing machinery of mRNA, it helps dephosphorylate Nlp3 protein and leads to mRNA and Npl3 releasing from 3' end processing machinery Rna15p and bind to Mex67-Mtr2, facilitating mRNA export from nucleus to cytoplasm; however, whilst in the cytoplasm Npl3 dissociates from mRNPs in phosphorylated form stimulated by Sky1, recycling back to the nucleus and start over its work (Gilbert & Guthrie, 2004; Kress et al, 2008).

1.7.4.2 Through the NPC with yeast Nab2

Both nuclear poly (A) binding protein 2 (Nab2) in *Saccharomyces cerevisiae* and its orthologue, ZC3H14 (also known as NY-REN-37 or UKp68), in higher eukaryotes have a conserved CCCH zinc finger domain which can specifically bind with polyadenosine RNA. This zinc finger domain of Nab2

includes seven CX5CX4-6C3H motifs in *Saccharomyces cerevisiae* and five analogous motifs in human. In addition, the homologous N-terminal domain of Nab2 and ZC3H14 assists export inside the nucleus in binding with Mlp, and associates with other mRNA export factors such as Yra1 and Mex67. The human ZC3H14 have a NLS domain to regulate the function of the nuclear import, and it contains RGG (arginine-glycine-glycine) repeat domain performing this function (Kelly et al, 2010; Kelly et al, 2007). Besides, the DEAD-box protein Dbp5 has function of ATPase activity in removing Nab2 from RNA in ADP-bound form by NPC-associated factor Gle1 and this process also requires the small molecule inositol hexakisphosphate (IP6) (Tran et al, 2007).

On the other hand, a recent study has proposed that Nab2 plays a role as an adaptor to assist Mex67 export from nucleus to cytoplasm whereas Yra1/REF functions as a cofactor to stabilize the interaction between the adaptor Nab2 and the receptor Mex67, representing that Nab2 interacts with Mex67 by working with Yra1/REF (Iglesias et al, 2010). Interestingly, Yra1/REF is dispensable after overexpressing Nab2 and Mex67 in cells; in addition, Yral dissociates from Nab2 following the ubiquitination by E3 ligase Tom1. (Iglesias et al, 2010).

1.7.4.3 Yra1 recruitment via Pcf11

The yeast 3' end of cleavage/polyadenylation complex is recruited to the active genes co-transcriptionally by binding the Pcf11 subunit of CF1A with RNA polymerase II (Sadowski et al, 2003). Pcf11, a conserved 3' end processing factor, functions in coupling 3' end processing with transcription via its N-terminal CTD interaction domain (CID) to associate with Ser2 phosphorylated C-terminal domain of heptad repeats of RNA polymerase II and nascent transcript (Sadowski et al, 2003). Yeast Pcf11 associates with Clp1, Rna14 and Rna15 subunits of CF1A while the homolog of human Pcf11 is a subunit of CFIIm in the 3'end cleavage-polyadenylation processing complex (Proudfoot, 2004). Recently, a study points out that the recruitment of Yra1 to the nascent transcript is independent on Sub2 but dependent on the cleavage-polyadenylation factor CF1A by interacting directly with the Zn finger/ Clp1 binding region of Pcf11 (Johnson et al, 2009b). Moreover, Yra1 plays a role in regulation of the 3'end cleavage-polyadenylation processing, competing with Clp1 subunit of CF1A for interacting with Pcf11, to modulate the co-transcriptional assembly of the 3'end processing factor CF1A/B (Johnson et al, 2011). In summary, the Yra1 subunit of TREX complex is recruited to the

nascent transcripts via binding Pcf11 subunit of CF1A/CFIIm, providing a major link between export and 3'end processing independent of Sub2 in a co-transcriptional pathway.

1.7.5 EXPORT OF VIRAL RNAS

Spliced or intronless mRNAs can be exported efficiently via the mechanisms of splicing and export and therefore, a variety of incompletely spliced RNAs are retained within the nucleus. However, viruses have evolved the mechanism to prevent the retention of unspliced mRNA and overcome the inefficient export of intronless mRNAs. For example, lentiviruses and simple retroviruses can encode viral proteins to export the incompletely spliced or unspliced mRNAs as herpeviruses do for intronless mRNAs.

Rev and CRM1 dependent transport

Human immunodeficiency virus (HIV) is a complex retrovirus or lentivirus, including a single proviral transcript expressing nine genes by alternative splicing. The incompletely spliced viral mRNAs are exported dependent on CRM1 pathway through the HIV Rev protein. Rev protein consists of nuclear localization signal (NLS) and the Rev response element (RRE) binding domain

at its N-terminus of arginine-rich sequences, which is required to bind with a highly structured RRE of incompletely spliced HIV mRNA. At its C-terminus, the nuclear export signal (NES) of leucine-rich sequence of Rev protein functions to interact with a nuclear export factor CRM1, a karyopherin or importin/exportin family of nuclear transport receptors which requires Ran GTPase system for transport (Sandri-Goldin, 2004).

CTE (constitutive transport element) dependent transport

Simple retroviruses, like Mason-Pfizer monkey virus (MPMV), which requires the transport of partly spliced RNAs or unspliced RNAs dependent on the constitutive transport element (CTE) but not the Rev protein. This *cis*-acting RNA element CTE binds directly to TAP/NXF1 for mRNA transport; on the contrary, the cellular mRNAs requires the export adaptor protein Aly/REF or UIF to associate with TAP/NXF1 in transport pathway (Braun et al, 1999; Jackson et al, 2011).

ICP27 dependent transport

The ICP27 protein is encoded by Herpes simplex virus type 1 (HSV-1) and has been found to be involved in the transport of viral intronless RNAs. ICP27

protein abolishes a splicing process of the host cell by binding to SR protein kinase 1 (SRPK1), so the improper phosphorylation of SR protein leads to the retention of stalled spliceosomal complex and incompletely spliced RNAs within the nucleus (Sciabica et al, 2003). Thus, ICP27 protein is able to recruit the export factor Aly/REF to the transcriptional site of HSV-1 and export viral RNAs to cytoplasm via TAP/NXF1 pathway (Chen et al, 2005; Chen et al, 2002; Johnson et al, 2009a; Johnson & Sandri-Goldin, 2009).

1.7.6 Post-translational modification

Several studies have been shown that post-translational modification of mRNA export factors regulates the process of mRNP biogenesis and export pathway. Modification of methylation in REF facilitates handing over of mRNA to TAP due to the reduced RNA-binding activity of methylated REF (Hung et al, 2010a), and in addition, methylated Npl3p functions in the regulation of transcription elongation and termination (Wong et al, 2010).

Another thought on the modification of ubiquitination plays a role between an mRNP surveillance system and nuclear export pathway. A new finding that the modification of ubiquitination of Yra1 by Tom1, an E3 ligase, stimulates the release itself from the triple complex of Mex67, Yra1 and Nab2 prior to nuclear

export (Iglesias et al, 2010). Moreover, the ubiquitinated Hpr1, a component of TREX complex, which associates with the C-terminal UBA domain of MEX67, not only protects itself from proteasomal degradation but also recruits Mex67 to the nascent transcript (Gwizdek et al, 2006).

As mentioned earlier, the yeast SR-like protein Npl3 is dependent on the phosphorylation mechanism, which is dephosphorylated by Glc7p in the nucleus and phosphorylated by Sky in the cytoplasm, and this mediates its interaction with Mex67-Mtr2 in the mRNA export pathway (Gilbert & Guthrie, 2004). Furthermore, a finding that the poly(A)+ binding protein Nab2 is phosphorylated by MAP kinase Slt2/Mpk1 during heat shock stress. The phosphorylated Nab2 displacing from Mex67 appears to colocalize with Yra1 in nuclear foci (Carmody et al, 2010), representing another example that phosphorylation modification of mRNA export proteins regulates the mRNP in export pathway.

1.7.7 Co- versus post-transcriptional splicing

While a nascent transcript is being transcribed by RNA Polymerase II, the event called co-transcriptional splicing can occur where the introns are being removed and the exons are being spliced. On the other hand, once nascent

transcripts have accomplished the process of 3’ end cleavage and formation which infers to transcription termination, some introns would be subject to being excised. This event is therefore called post-transcriptional splicing (Girard et al, 2012).

1.7.8 A MODEL OF mRNA EXPORT

Shown in Figure II is a model for mRNA export pathway proposed from Prof. Wilson group. At the early transcription stage, the Pcf11 subunit of 3’ end processing complex CFIIm is recruited together with REF to the CTD (C-terminal domain) of RNA polymerase II. During transcriptional elongation or termination stage, Clp1 binds to Pcf11 by competing with REF, forming a functional 3’ end processing complex. In turn REF interacts with CBP80 subunit of cap-binding complex by loading close to 5’ end region of pre-mRNA with the removal of intron during splicing. At this stage, REF links to the components of TREX complex via UAP56 whereas SR protein interacts with mRNA in hypophosphorylated form. After the completion of pre-mRNA processing, the recruitment of TAP to TREX complex facilitates the release of UAP56, leading to mature messenger RNA being handed over from REF to TAP in mRNP complex. Whilst mRNP reaches the nuclear pore, REF

dissociates from TAP and mRNA. Once passing through the cytoplasmic side of the nuclear pore, SR protein forms hyperphosphorylated, allowing its dissociation from TAP, and TAP is therefore displaced from mRNA by DEAD-box protein Dbp5 (Walsh et al, 2010).

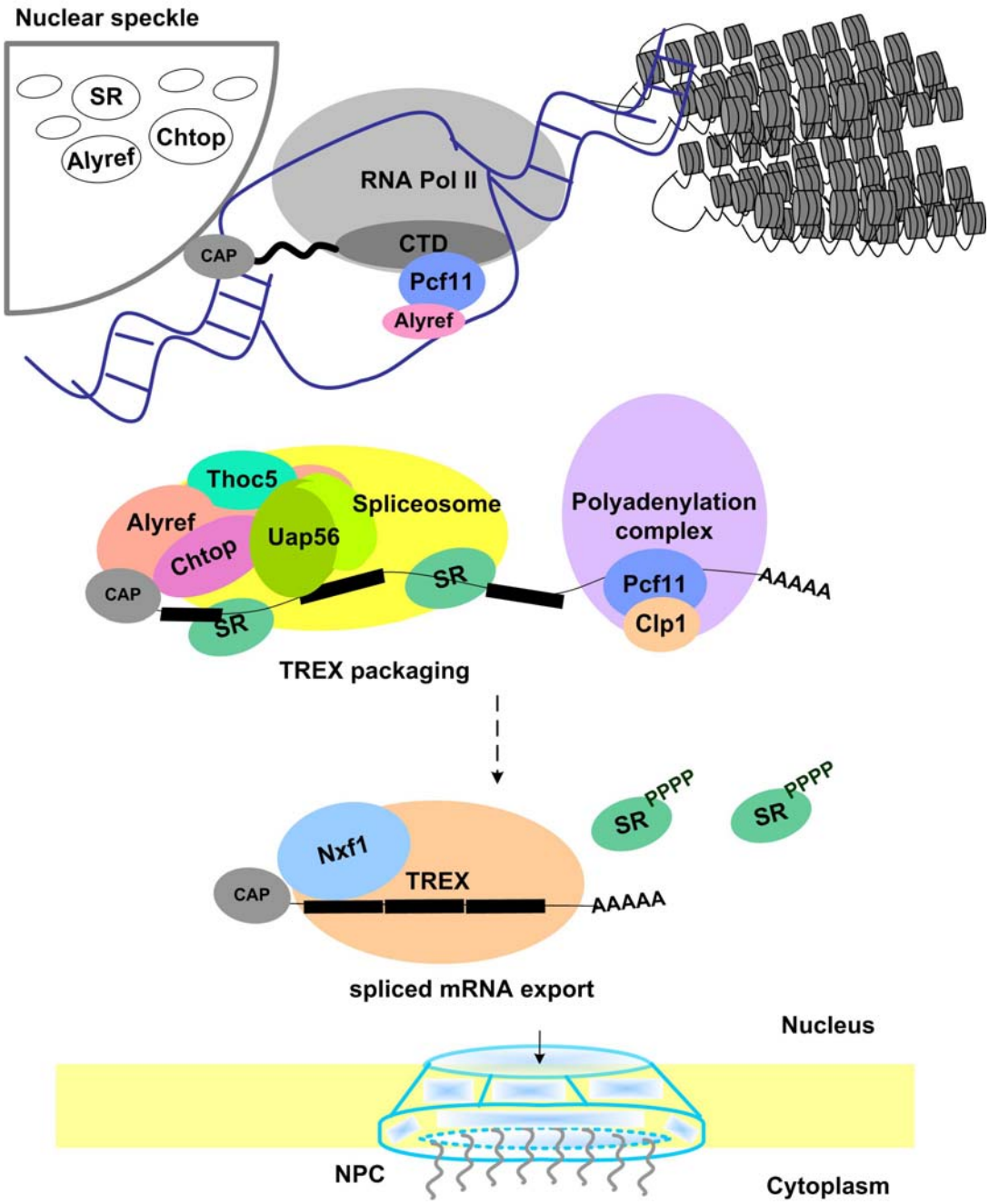

[Figure II] A MODEL FOR mRNA EXPORT

1.8 AIM OF THIS STUDY

The TREX complex couples transcription and nuclear processing of mRNA with its subsequent export to the cytoplasm (Reed & Hurt, 2002). Once assembled on mRNA, TREX has the ability to release the RNA binding domain of the mRNA export receptor Nxf1, allowing the stable association of Nxf1 with mRNA which subsequently leads to transport of the mRNA to the cytoplasm (Viphakone et al, 2012). Thus TREX acts to license mRNA export, informing the cell when an mRNA is processed and suitable for export. TREX is a multisubunit complex whose assembly requires ATP (Dufu et al, 2010). Four subunits of TREX are known to make contact with Nxf1, these are Alyref, Thoc5, Hpr1 and Chtop (Katahira et al, 2009) (Chang et al, 2013). Chtop and Thoc5 both bind to the same domain of Nxf1 and both cooperate with Alyref to enhance the RNA binding activity of Nxf1. However, Nxf1, Chtop and Alyref all exist in a single complex *in vivo*, indicating that the TREX complex is likely to undergo significant structural rearrangements during maturation of the mRNP. Both Chtop and Alyref are regulated by arginine methylation (Chang et al, 2013) (Hung et al, 2010b) and in the case of Chtop, the methylation of arginines allows it to bind Nxf1.

Although many biochemical approaches have been used to study the TREX complex function in gene expression, the sites within the nucleus where TREX recruits Nxf1 to mRNA are still unclear. The nuclear speckles are thought to be storage, assembly and modification sites for splicing and export factors (Spector, 2003) (Spector & Lamond, 2011) and a number of TREX subunits have been mapped to nuclear speckles in fixed cells (Chang et al, 2013) (Zhou et al, 2000) (Hautbergue et al, 2009a). mRNA splicing has been shown to take place in the vicinity of the perichromatin fibrils which surround nuclear speckle domains (Fakan, 1994) (Hall et al, 2006) and several studies have shown that splicing factors can be recruited from speckles to actively transcribed genes at the periphery of a speckle (Lamond & Spector, 2003; Misteli et al, 1997; Zhao et al, 2009). However, recent work has shown that post-transcriptional splicing occurs within the nuclear speckle and that release of mRNA from nuclear speckles and subsequent export to the cytoplasm requires the TREX complex (Dias et al, 2010; Girard et al, 2012). Despite all these studies, the site within the nucleus where Nxf1 assembles with the TREX complex remains unknown.

We have used two fluorescent imaging techniques to study the interaction of TREX components with Nxf1, sensitized emission FRET and FLIM-FRET.

Both techniques have the advantage that they rely on molecules being within 1-10nm and therefore are likely to report genuine protein-protein interactions (Sekar & Periasamy, 2003). In sensitized emission FRET the donor is excited with light of a suitable wavelength and fluorescence is measured in the acceptor channel. However, the signal in the acceptor channel does not only arise from FRET. The light used to excite the donor also causes some excitation of the acceptor due to spectral overlap between the donors and acceptors commonly used. To alleviate this problem images are also collected for donor only and acceptor only, excited with the same wavelengths used to excite the donor when measuring FRET. These control images are used to substract the fluorescence caused by spectral bleedthrough, which should in principal just leave the FRET signal, though correct acquisition of control images and substraction is vital to ensure an accurate FRET image is produced. In FLIM-FRET, the time it takes for a fluorophore to become excited and then return to ground state is measured. The lifetime of the fluorescence of the donor molecule decreases when the donor molecule is engaged in FRET with an acceptor molecule, therefore the fluorescence lifetime of the donor molecule provides a read out of molecules engaged in FRET and are likely to be interacting. Since FLIM-FRET only measured donor fluorescence

and is not subject to potential problems associated with spectral crosstalk it provides a robust readout of protein interactions in living cells. In addition, FLIM-FRET allows quantification of the number of interacting molecules at specific sites within the cell with nanometer resolution (Becker, 2012). By using both FRET techniques we aimed to produce an accurate and coherent view of the interactions between mRNA export factors in human cells. Our results provide the first intranuclear spatial map of the assembly of the export competent mRNP. We show that TREX assembly with Nxf1 predominantly occurs outside nuclear speckles, despite a large proportion of TREX subunits residing within nuclear speckles at steady state.

I also established a novel in vivo reporter assay to address the hypothesis that mRNA circularizes in the nucleus prior to mRNA export.

CHAPTER II

MATERIALS AND METHODS

2.1 Plasmids, antibodies and cell cultures

The full-length Nxf1, Chtop, Alyref, the C-terminus of Nxf1 (the 372-619 fragment), deletion mutants of Chtop (fragments corresponding to amino acids 1-87 and 92-213), coat proteins PP7 and MS2 were PCR amplified and cloned into pECFP-N1, pEYFP-N1 or pEGFP-N1 vectors. The reporter construct was created. First, EcoRV restriction site was created by using site-directed point mutation method on the mammalian expression vector pCI-Neo. Secondly, the six recognition binding sites of coat protein PP7 were introduced into EcoRV restriction sites on the mammalian expression vector pCI-Neo. Thirdly, the luciferase DNA with six recognition biding sites of coat protein MS2 were cloned into the mammalian expression vector pCI-Neo by specific primers introduced MluI and NotI restriction sites. Finally, another NotI restriction site was created behind the six recognition binding sites of coat protein MS2 by site-directed point mutation method. Therefore, eighty-six base pairs were cut out using NotI restriction enzyme. Human HeLa cells were grown on 35 mm glass bottom dishes with DMEM (Invitrogen) supplemented with 10% Fetal

Calf Serum and 100 U/ml of penicillin and streptomycin (Invitrogen) and incubated at 37 °C with 5% CO_2. Cells were transfected using Turbofect (Fermentas). The Nxf1 and Hpr1 antibodies were from Abcam. The Alyref monoclonal antibody (11G5) was from Sigma. The Thoc5 and Chtop (KT64) antibodies were described (Hautbergue et al, 2009a) (van Dijk et al, 2010). The Thoc5 antibody was described previously (Hautbergue et al, 2009a). For inhibition of transcriptional activity, cells were treated for 2 hours with 10 µg/ml actinomycin D (Sigma-Aldrich) prior to imaging analysis.

2.2 Immunoprecipitation

Cells were transfected with a construct expressing the target protein or mock transfected for 48 hours, each dish was lysed in 1 mL of IP lysis buffer (50 mM HEPES pH 7.5, 100 mM NaCl, 1 mM EDTA, 1 mM DTT, 0.5 % Triton X-100, 10% Glycerol) containing protease inhibitors and 10 µg/mL RNase A. The supernatants of cell extracts were incubated for 1 hour with 30 µL Protein G-Sepharose beads in IP lysis buffer supplemented with 1% BSA. The anti-GFP monoclonal antibody (Roche) was bound to 30 µL Protein G-Sepharose beads for 1 hour prior to immunoprecipitation. The beads were then washed with 1 mL IP lysis buffer three times. The bound proteins were

finally eluted from the Protein G-Sepharose with 50 µL of buffer (0.2 M glycine pH 2.8, 1 mM EDTA), and analysed by SDS-PAGE and Western blotting with the indicated antibodies.

2.3 Immunofluorescence microscopy

HeLa cells were fixed in 4% paraformaldehyde in PBS for 15 mins and permeabilized with 0.1% Triton X-100 in PBS for 10 mins before immunostaining. After blocking with 2% bovine serum albumin (BSA) in PBS for 1 hour, cells were incubated with the primary antibodies for 1 hour at room temperature. Then cells were washed in PBS three times and incubated with the fluorescently labeled secondary antibody (Cy3-, AlexaFluor 488, AlexaFluor 555 and AlexaFluor 680) for 1 hour. Cells were washed in PBS three times and nuclei were counterstained with 4, 6-diamidino-2-phenylindole (DAPI) for microscopy analysis. For fluorescence *in situ* hybridization, cells grown on coverslips were fixed at room temperature for 30 min with 4% paraformaldehyde in PBS. Cells were washed in PBS then incubated for 2 h at 37°C with hybridisation solution (20% formamide (2×sodium saline citrate, 10% dextran sulphate and 1% bovine serum albumin) containing 1 ng/µl Cy3-labelled oligo $(dT)_{50}$, 0.5 µg/µl single-stranded DNA and 0.5 µg/µl tRNA

and subsequently washed in PBS three times before mounting on glass slides for microscopy analysis.

2.4 Acceptor photobleaching fluorescence resonance energy transfer microscopy

Measurements were conducted on a Zeiss LSM510 META confocal microscope. Images were collected using a 63× NA1.4 Plan-Apochromat Oil DIC lens. The filter sets were used to the signals: BP 440-505 for ECFP passes and LP525 for EYFP passes. The emission light at 514 nm was used for photobleaching YFP. In acceptor photobleaching FRET method, after obtaining prebleach images, a region of interest (ROI) was photobleached with a 100% laser power. A total of images were acquired before and after the bleach event. Images of donor (ECFP) and acceptor (EYFP) were taken in separate subsequent measurements, bleaching exactly the same spot before collecting postbleach images. The values for CFP signal before bleaching (CFPpre) and after each bleach exposure (CFPpost) were used to calculate the FRET efficiency (%) values: FRET Efficiency (%)= [(CFPpost – CFPpre) / CFPpost] X 100. The values for YFP signal before bleaching (YFPpre) and after each bleach exposure (YFPpost) were used to calculate the percent

decrease in YFP signal after each bleach exposure: % Decrease YFP = [1-(YFPpost – YFPpre)] X 100. FRET Efficiency (%)= [(CFPpost – CFPpre) / CFPpost] X 100. The pre-bleach image has values of 0% for both the decrease in YFP signal and the FRET efficiency. After each bleach exposure, the value for the percent decrease in YFP signal approached 100%.

Quantification of the effect on the percent FRET efficiency is shown by a Box-and-Whisker Plot in each condition. The boxes contain the 25th to 75th percentile of data, the lines within boxes represent the data median and the upper and lower whiskers indicate the 10th and 90th percentile of data, respectively. Data were presented as means ± SD of each conditon and *P*-values were obtained using Student's *t*-test. $P < 0.05$ was considered as statistically significant. Each condition contains at least 10 cells.

2.5 Confocal microscopy and fluorescence resonance energy transfer analysis

Cell images were collected using a Zeiss LSM 510 META microscope equipped with a Zeiss Plan-Apochromat 63x NA 1.4 oil immersion DIC lens. For Z-stack confocal images a micrometer step size was used for the z-scan. *In situ* characterisation of fluorescence emission spectra was performed using

the Zeiss META detection module with a 458 nm laser excitation. For sensitized emission FRET, a 30 mW Argon laser line 458 nm was used for ECFP (donor) and FRET excitation and laser line 514 nm for EYFP (acceptor) excitation. To effectively reduce background noise, emission fluorescence images of ECFP, EYFP, and FRET pairs were acquired with band pass filter BP 470-500, long pass filter LP530, and long pass filter LP530, respectively.

To measure the normalized FRET (NFRET) value, all three emission images from cells expressing FRET pairs were collected and processed using the Image J (National Institutes of Health) FRET plug-in based on this equation: $NFRET = 100 \cdot (I_{fret} - BT_{donor} \cdot I_{donor} - BT_{acceptor} \cdot I_{acceptor}) / N$. Cells expressing donor alone or acceptor alone were acquired to measure spectral bleed through coefficients BT_{donor} or $BT_{acceptor}$. N was determined by the square root of the product of donor and acceptor intensities. For quantitative analysis, mean NFRET values were determined by defining regions of interest (ROIs) for the whole nucleus. Data were presented as mean value ± SD of independent experiments and *P*-values were obtained using the Student's *t*-test. $P < 0.05$ was considered as statistically significant. An NFRET value of >5% was considered a significant protein-protein interaction.

2.6 TCSPC fluorescence lifetime imaging microscopy

FLIM was performed using an upright multiphoton Zeiss LSM510 NLO laser scanning microscope with a 60x NA1.0 water immersion lens. A Coherent Chameleon Verdi-pumped ultrafast tunable (690-1040nm) laser was used for multiphoton excitation by pumping a mode-locked Ti:Sapphire laser to produce sub-200 femtosecond duration pulses at a 90 MHz repetition rate. Fluorescence lifetimes were acquired by the high-speed Hamamatsu 5783P detector and each photon was delivered to B&H SPCM/SPC-830 TCSPC imaging module board. To measure the lifetime of fluorophore, ECFP fusion protein was excited by multiphoton laser at 850nm and emission fluorescence was collected to bandpass filter 435 ± 50nm. A mean photon count rate of each image was monitored at the order 10^4~10^6 photons per second and acquisition time was over 90 seconds. Time-correlated single-photon counting (TCSPC) measurement relies on the fluorescence decay histogram generated from accumulated photon counts at different times after the laser excitation pulse. The recorded data was analyzed using B&H SPCImage software. Measurements of FRET based on the analysis of the fluorescence lifetime of the donor by FLIM approach can resolve the FRET efficiency and the FRET population (concentration of FRET species) when analyzed using

bi-exponential decays model. In the analysis of FLIM-FRET data, a bi-exponential decay model ($f(t) = a \cdot e^{-t/\tau_{DA}} + b \cdot e^{-t/\tau_D}$) was fitted in ECFP fusion proteins and FRET pair specimens. The displayed X^2 value was optimized to close to one as possible to achieve a best fitting model. We obtain information about the lifetimes of two populations of molecules, τ_{DA} is the mean fluorescence lifetime of the donor in the presence of the acceptor and τ_D is the mean fluorescence lifetime of the donor expressed in the absence of acceptor as well as two decay components a and b. By fixing the non-interacting proteins lifetime τ_D using data from control experiments (in the absence of FRET) and by assuming invariance in the efficiency of interaction $\tau_{DA,}$ the population of FRET species can be estimated. From this model, the FRET efficiency was measured by the equation: $E = 1 - (\tau_{DA} / \tau_D)$. For quantitative analysis, the mean value for FRET efficiency was determined by defining regions of interest (ROIs) for the whole nucleus. Data were presented as means ± SD of independent experiments and *P*-values were obtained using Student's *t*-test. *P*< 0.05 was considered as statistically significant. A FRET efficiency of >5% is considered a significant protein-protein interaction.

2.7 Fluorescence recovery after photobleaching

HeLa cells expressing EGFP fusion proteins were grown in glass bottom dishes. FRAP experiments were performed using a Zeiss LSM 510 META microscope equipped with a Zeiss Plan-Apochromat 63x NA 1.4 oil immersion DIC lens. A small circular area within the nuclear speckle or nucleoplasm was bleached using 100% 488nm laser power. The four images were acquired before bleaching with 1.5~2.5 % 488nm laser power. A series of 76 post-bleached images for the Chtop-GFP in the nuclear speckles were captured at intervals of 15s. A series of 76 post-bleached images for Chtop-GFP or mutant Chtop-GFP in the nucleoplasm were collected at interval of 5 s and 98.9 ms. A series of 76 post-bleached images for Alyref-GFP or Nxf1-GFP in the nuclear speckles or nucleoplasm were captured at intervals of 58.8 ms. Fluorescent intensities of the bleached area collected at different series of time were normalized to pre-bleached fluorescent intensity. For the measurement of half-time of recovery ($\tau_{1/2}$) and immobile fraction, we used the mathematical equation: $I(t) = A(1 - e^{-\tau \cdot t})$, whereas A indicates the mobile fraction, I(t) is the fluorescent intensity at time (t), and τ is the lifetime of recovery to fit the frap curve and meanwhile the value of the immediate post-bleached intensity as 0 and the pre-bleached intensity as 1 were carried out.

CHAPTER III

3. 1 INTRODUCTION: Investigation of nuclear mRNA circularisation

It has been shown that in yeast the mRNA export factor Yra1 is recruited to mRNA via the 3' end processing factor Pcf11 (Johnson et al, 2009b). Another 3' end processing factor, Clp1 directly binds Pcf11 and displaces Yra1 which then associates with mRNA and this process is likely to occur at the 3' end of the mRNA. Moreover, the human orthologue of Yra1, ALY (or REF) interacts with human Pcf11. Furthermore it is known that human REF as part of the TREX complex is loaded onto the mRNA very close to the 5' end of the mRNA and this positioning of TREX is thought to occur in part because ALY associates with the 5' CAP binding protein CBP80 (Cheng et al, 2006). These observations lead to the hypothesis that REF is transferred from the 3' to the 5' end of the mRNA in the nucleus. Furthermore, this process may be facilitated by the RNA circularising in the nucleus such that the 5' and 3' ends were juxtaposed, allowing efficient relocation of REF form the 3' end processing complex to the TREX complex at the 5' end.

Circularisation of mRNA is not unprecedented. For example, mRNA is known to form a circular structure during the translation initiation process (Wells et al, 1998) whereby the translation initiation factors which associate

with the 5’ cap make contact with proteins associated with the poly A tail. This process of circularisation of the mRNA is thought to promote cycling of ribosomes on the mRNA i.e. a ribosome which has completed translation is released in very close proximity to the site where the next round of translation would initiate. Circularisation of the mRNA to initiate translation may also act as a quality control mechanism to ensure that only intact mRNAs are translated.

In order to test the hypothesis that mRNA may form circles in the nucleus with the 5’ and 3’ ends in close proximity I established a fluorescence resonance energy transfer (FRET) based RNA reporter assay.

3.2 **RESULES: FRET based RNA reporter constructs**

To establish whether RNA might form circles I developed a FRET based reporter system in which donor and acceptor FRET molecules would be tethered at the 5’ and 3’ ends of a mRNA *in vivo*. Since FRET measures interactions in the 1-10 nm range and a typical mRNA is going to have a linear length in excess of 300nm (http://bionumbers.hms.harvard.edu//bionumber.aspx?id=100023&ver=1#), we considered that such a reporter system, with FRET donors tethered to the 5’

and 3' end of the mRNA, might detect RNA circularisation events in either the nucleus or cytoplasm. In order to be able to tether donor and acceptor FRET molecules to an mRNA *in vivo* we took advantage of two sequence specific RNA binding proteins, bacteriophage MS2 and PP7 proteins (Gesnel et al, 2009). Both proteins bind with high specificity to specific short hairpin RNA binding elements, therefore we made reporter constructs as shown **(Figure 3-1)**. The 5' bs construct had multiple copies of the PP7 recognition sequence, close to the 5' end of the mRNA and the 3'bs construct had multiple copies of the MS2 recognition sequence close to the 3' end of the mRNA. Finally the construct called "Reporter" carried 5' PP7 and 3' MS2 recognition sequences. All three constructs carried an intron so would be spliced and the "Reporter" construct and the 3' bs construct also carried a luciferase open reading frame, thus the mRNAs produced from these two latter constructs would be expected to be translated.

To establish that the two constructs carrying the luciferase gene were translated, they were transfected into 293T cells and luciferase activity measured **(Figure 3-2)**. Since these reporters carried MS2 binding sites we also investigated the effects of tethering mRNA export factors to these RNAs since MS2-GFP, MS2-REF and MS2-TAP fusions were available in the

laboratory. All three MS2 fusion proteins produced proteins of the expected size when the expression constructs for these fusions were transfected into 293T cells **(Figure 3-2A)**. When MS2-REF was cotransfected with either the 3' bs construct or the reporter construct we observed approximately a three fold increase in luciferase expression whereas coexpression of MS2-TAP led to approximately a 40 fold increase in lucierase expression. These data indicate that firstly, the constructs containing the luciferase gene can be translated, secondly that the MS2 sites are likely to be functional since the reporters respond to the coexpression of an MS2 fusion protein and thirdly that direct tethering of these mRNA export factors to these reporter constructs in vivo leads to enhanced gene expression. This may be due to more efficient export of these mRNAs.

We next constructed expression vectors for fluorescent proteins fusion with MS2 and PP7 to allow the expression *in vivo* of fusion proteins which when in close proximity would trigger FRET. For this we used cyan fluorescent protein (CFP) which we fused to PP7 and yellow fluorescent protein (YFP) which we fused to MS2. **Figure 3-3A** provides a schematic of how I envisaged the FRET based reporter system would work, the presence of specific binding sites would tether PP7 and therefore CFP at the 5' end of the mRNA and MS2

therefore YFP at the 3' end of the mRNA. If the two fluorescent proteins came into close proximity which might indicate mRNA circularisation, then we would expect to see a FRET signal. A Western blot was used to confirm that the PP7-CFP and MS2-YFP fusions expressed proteins of the expected size **(Figure 3-3B)**.

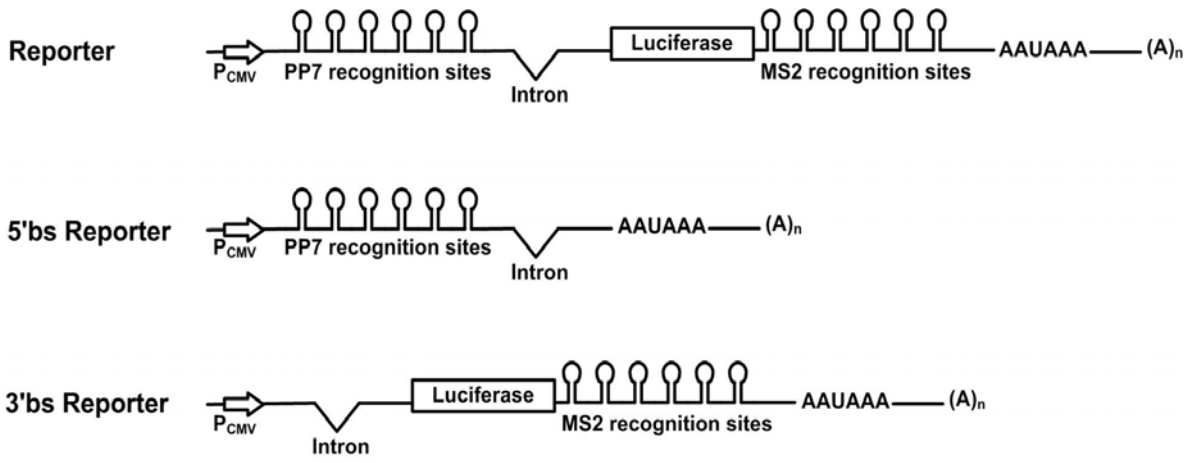

Figure 3-1. Schematics of tethered mRNA reporter constructs.

The six repeated PP7 recognition sites and MS2 recognition sites are designed at either 5' end or at 3' end of the reporter mRNAs. One intron or one cDNA encoding luciferase proteins are included in the constructs. P_{CMV}, a CMV promoter; $(A)_n$, a polyadenylation tail.

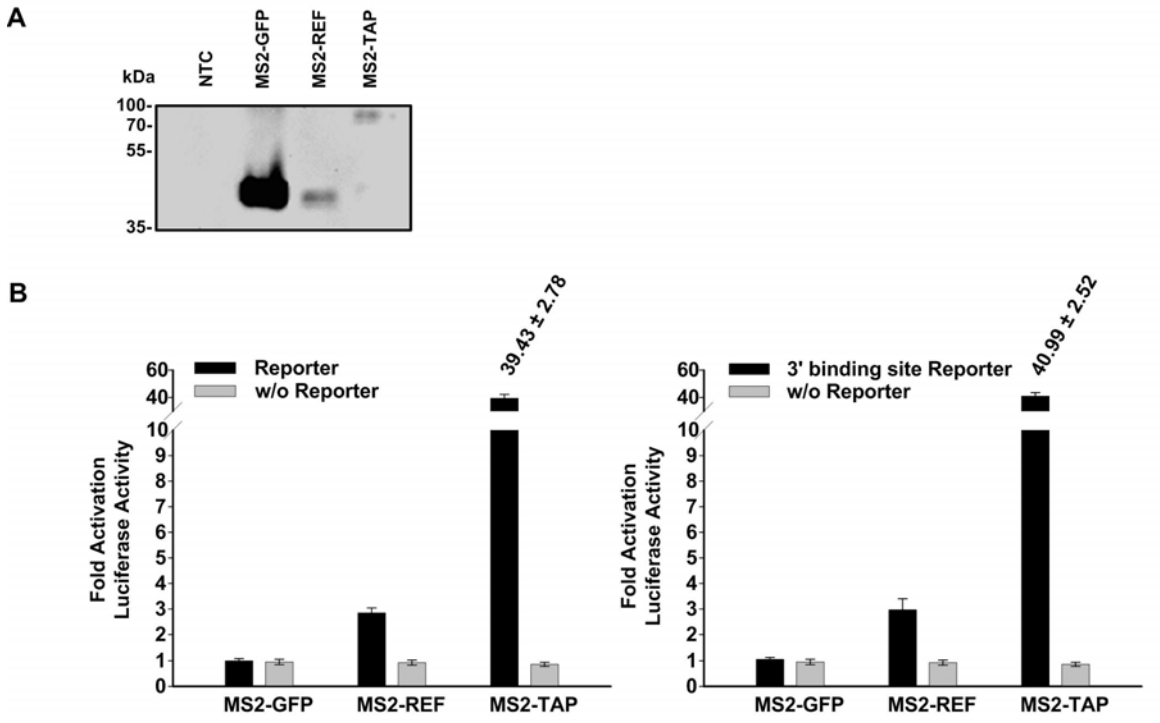

Figure 3-2. Functional analysis of tethered messenger RNA export assay.

(A) Western blots detected for Myc-tagged MS2 fusion proteins in the PP7/MS2 tethering assay are shown by using Myc antibodies. NTC, non-transfected cells. (B) Quantification of luciferase activities in 293T cells expressing the indicated MS2 fusion proteins with reporter constructs or without reporter constructs is determined in the assay. The results of the tethered mRNA export assay are analyzed from at least triplicates in two independent experiments and error bars show the standard errors of the mean.

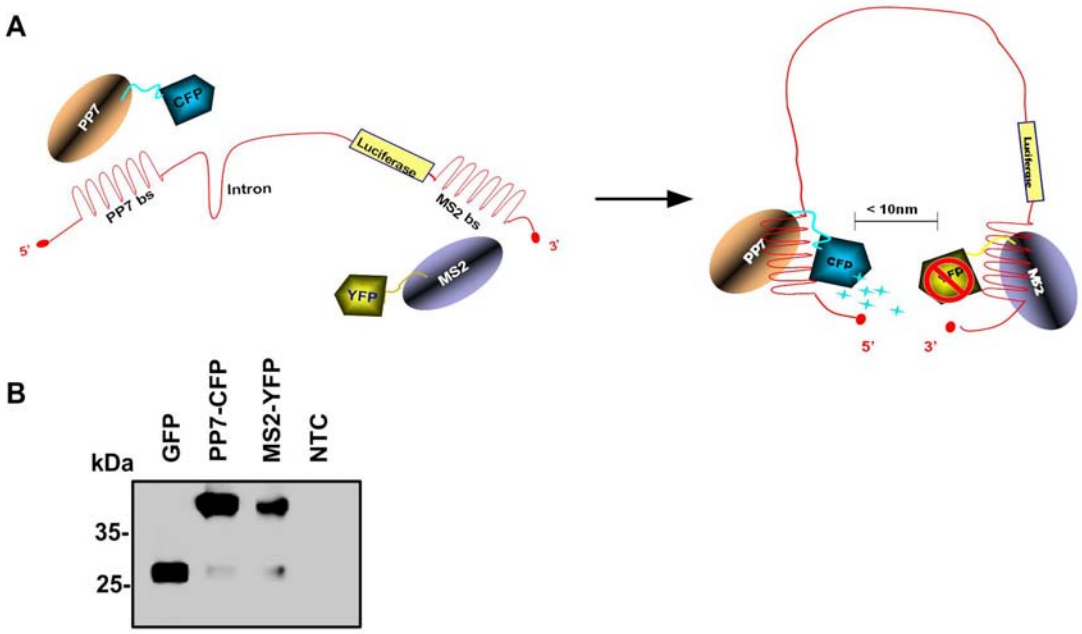

Figure 3-3. A FRET-based RNA reporter system.

(A) A schematic for the detection reporter mRNA by using acceptor photobleaching FRET microscopy. (B) Western blot analysis of HeLa cell extract transfected with PP7-CFP and MS2-YFP coat proteins constructs and proteins were detected with GFP antibody. NTC, non-transfected cells.

In order to assay for FRET I used acceptor photobleaching FRET microscopy following transfection of HeLa cells with various plasmid combinations and the FRET efficiency was monitored for at least ten cells in each condition and individual cell FRET efficiencies were plotted **(Figure 3-4A)** together with cumulative data medians **(Figure 3-4B)**. In each case the nuclear FRET efficiency was monitored as the nucleus was specifically

bleached **(See Figures 3-4A , right panels)**. In the absence of the “reporter construct” the HeLa cells showed a background median FRET efficiency of ~2.0% which presumably arose from occasional random interaction of the YFP and CFP fusion proteins in the nucleus. In contrast, when the reporter RNA was cotransfected with PP7-CFP and MS2-YFP a much higher median nuclear FRET efficiency of ~9% was observed, which was much higher than the background FRET efficiency. These data indicate that when the PP7-CFP is tethered to the 5’ end of an mRNA and MS2-YFP to the 3’ end of an mRNA, FRET can be observed between the YCP and CFP indicating they are in close proximity within the nucleus, which could indicate circularisation of mRNA in the nucleus.

As further controls we also look at the nuclear FRET efficiency with RNA expression constructs which had single binding sites either for PP7-CFP or MS2-YFP **(Figure 3-5)**. Moreover, in a comparison of the nuclear FRET efficiency (%) with various expression vectors, the signals have been averaged in each condition and shown in bar graph **(Figure 3-6)**. Using the 5’ bs or 3’ bs constructs which only harbor binding sites for one of the FRET partners we found that the FRET efficiency was equivalent to background levels without a reporter when both the PP7-CFP and MS2-YFP were

coexpressed in the cell. Finally, we transfected the 5' bs and 3' bs constructs into the same cell together PP7-CFP and MS2-YFP. In this situation, the median FRET efficiency was ~5%, which is considerably higher than background. However, there was a significant range in the FRET efficiencies and the error bars suggest that on the sample size used, there was no significant difference in the FRET efficiency compared with the other controls. However, since the median FRET efficiency was higher with the FRET pair proteins tethered to two separate RNA molecules, we were concerned that there may be an element of FRET occurring *in trans* between the two RNA molecules with PP7-CFP and MS2-YFP tethered on separate molecules. If this was the case then it would make it very difficult to dissect out FRET arising *in trans* between two separate RNA molecules, which would not necessarily by circularising and *in cis* FRET within a single RNA molecule, caused by RNA circularisation. Given these concerns it was decided not to pursue this reporter system further and instead concentrate on the analysis of the interactions between mRNA export factors using FRET based microscopy techniques and this will be discussed in the next results chapter.

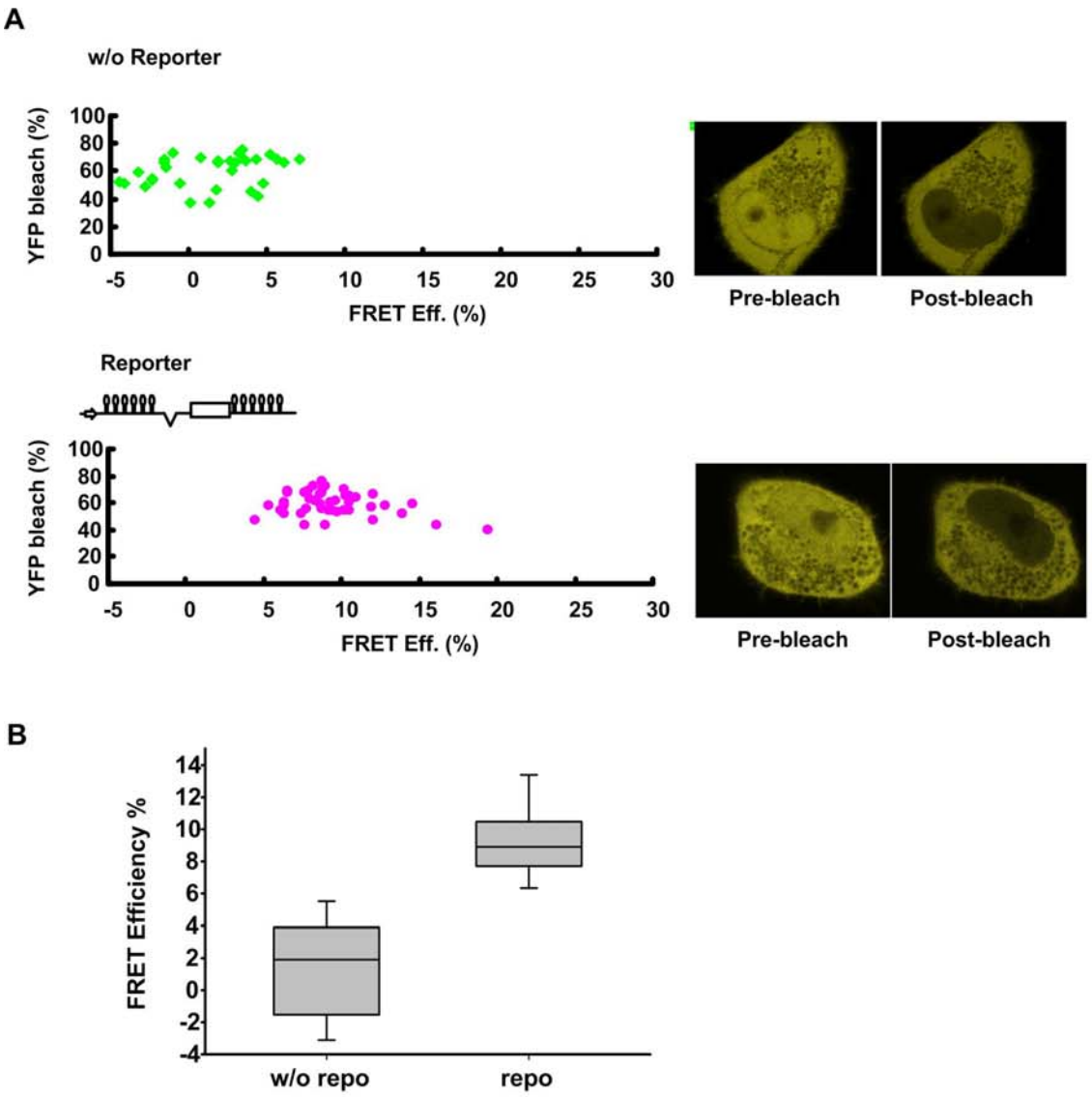

Figure 3-4. An effect of a FRET-based RNA reporter system.

(A) HeLa cells coexpressing PP7-CFP and MS2-YFP with reporter vectors containing 5' and 3' recognition sites or without report vectors are detected by acceptor photobleaching FRET microscopy. The percentage of decreased YFP intensity and corresponding FRET efficiency for a bleached ROI in each condition are plotted. The images for pre-bleached and post-bleached MS2-YFPs are shown to the right of a plot. (B) Quantification of the effect on the percent FRET efficiency in each condition. The boxes contain the 25th to 75th percentile of data, the lines within boxes represent the data median and the upper and lower whiskers indicate the 10th and 90th percentile of data, respectively. Each condition contains at least 10 cells.

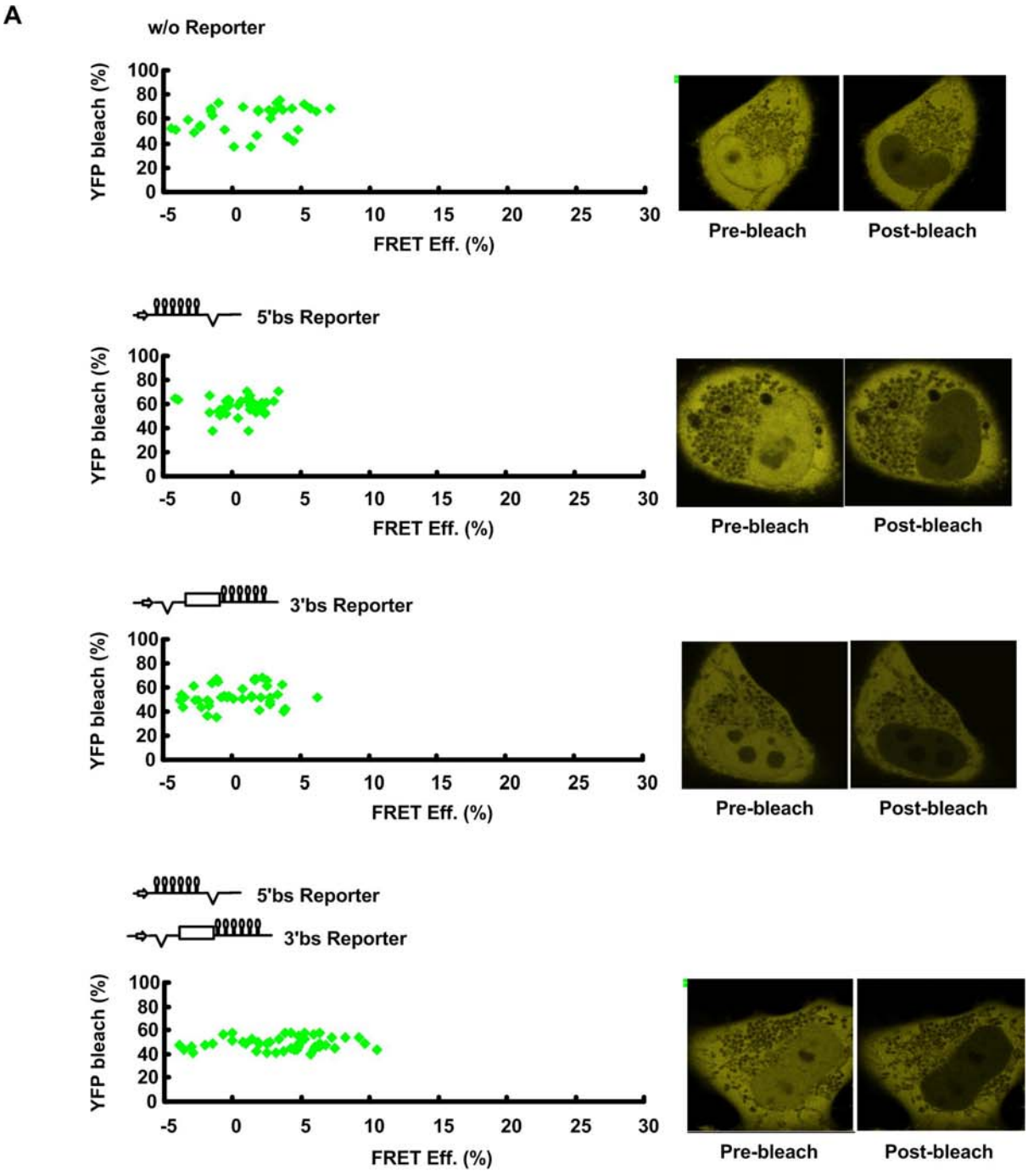
A
w/o Reporter
YFP bleach (%)
FRET Eff. (%)
Pre-bleach
Post-bleach
5'bs Reporter
3'bs Reporter
5'bs Reporter
3'bs Reporter
B
FRET Efficiency %
w/o repo
5'bs
3'bs
5'bs+3'bs

Figure 3-5. An effect in the presence of 5'end or 3'end of reporter mRNA.

(A) HeLa cells coexpressing with PP7-CFP and MS2-YFP with reporter vectors including individual recognition sites or without report vectors are detected by acceptor photobleaching FRET microscopy. The percentage of decreased YFP intensity and corresponding FRET efficiency for a bleached ROI in each condition are plotted. The images for pre-bleached and post-bleached MS2-YFPs are shown to the right of a plot. (B) Quantification of the effect on the percent FRET efficiency in each condition. The boxes contain the 25th to 75th percentile of data, the lines within boxes represent the data median and the upper and lower whiskers indicate the 10th and 90th percentile of data, respectively. Each condition contains at least 10 cells.

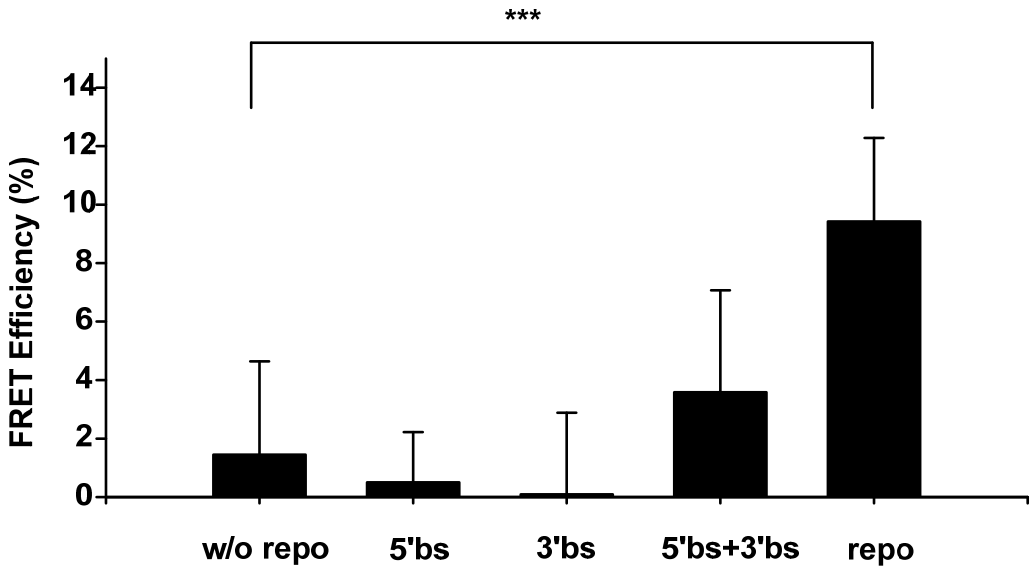

Figure 3-6. A comparison of FRET Efficiency (%) with various expression vectors

HeLa cells coexpressing PP7-CFP and MS2-YFP together with different sets of vectors such as 5' bs or 3' bs constructs, a combination of both 5' bs and 3'bs constructs and reporter constructs or mock constructs. The bar graph of FRET efficiency was analyzed in cells by acceptor photobleaching as mentioned in Figure 3-4 and Figure 3-5. Data presented as mean ± SD and each condition contains at least 10 cells, $^{***}P<0.001$.

CHAPTER IV

4.1 Subnuclear localization of mRNA export proteins

To investigate the subnuclear distribution of mRNA export factors in HeLa cells we performed immunofluorescence microscopy. The Srsf2 (SC35) antibody was used to label the nuclear speckles which coincided with areas of the nucleus that stained poorly with the DNA stain DAPI (Figure 4-1A). The cells were also stained for the TREX subunit Chtop, which was concentrated in and around nuclear speckle domains (Figure 4-1A). Close examination of z-stack sections revealed that whilst the majority of Chtop colocalised with Srsf2 in nuclear speckles, a significant proportion of Chtop localised to the region immediately surrounding the speckle domains (Figure 4-1B).

The majority of Chtop appears to colocalise with poly (A) + RNA in the nuclear speckle domain by using In situ hybridization experiment (Figure 4-2). We also examined the localization of endogenous Nxf1 in HeLa cells and found it had a diffuse nuclear staining with no obvious concentration in nuclear speckle domains (Figure 4-3A). Magnification of the red boxed regions revealed that whilst the majority of Nxf1 localised close to the region surrounding the speckle domains (Figure 4-3B).

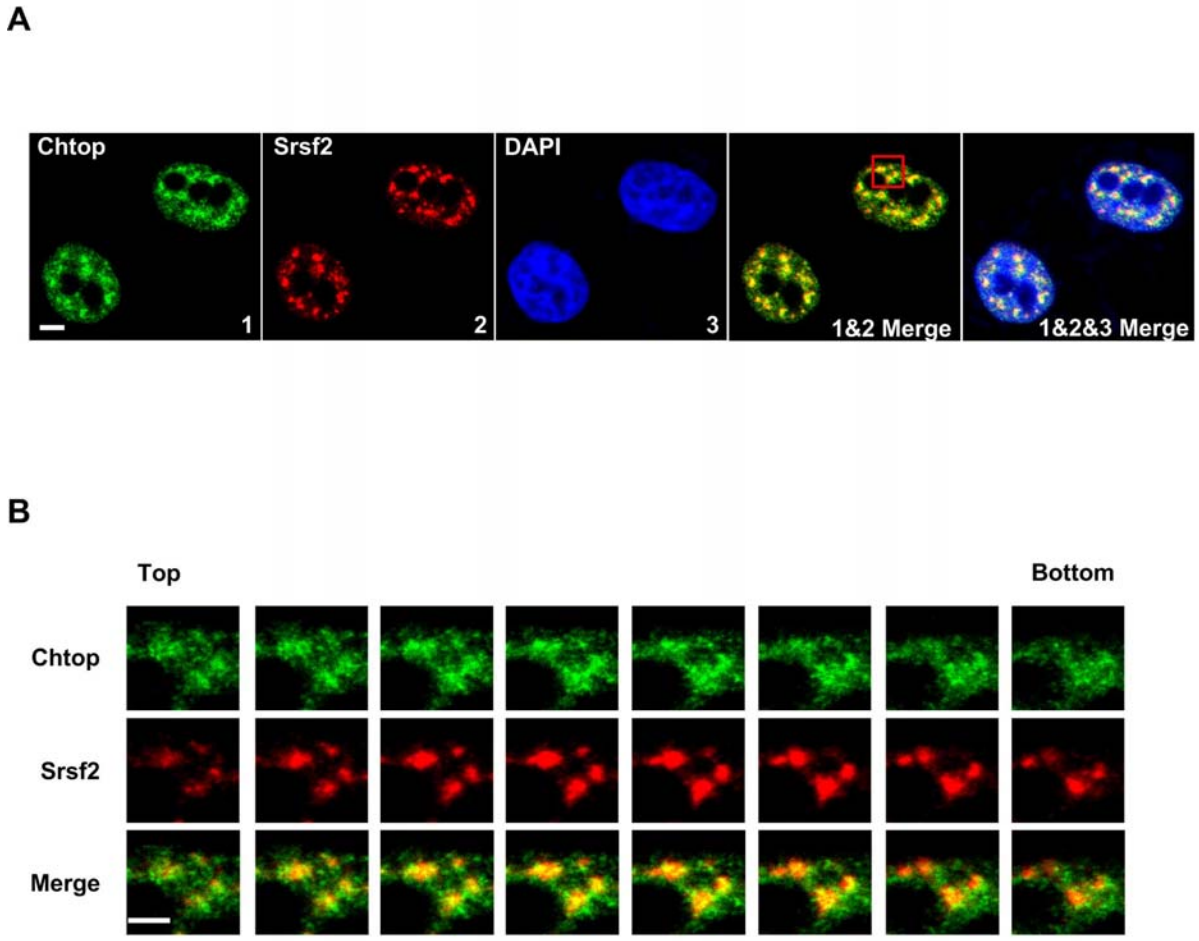

Figure 4-1. mRNA export protein Chtop localizes to the vicinity of nuclear speckles.

(A) HeLa cells were stained with the anti-Chtop antibody (green). Speckles and DNAs were detected with the anti-Srsf2 antibody (red) and DAPI (blue) by immunofluorescence microscopy. Scale bar, 5 μm. (B) Magnification of the boxed region in (A). Images acquired from Z-stack sections were shown from top to bottom. Scale bar, 2 μm.

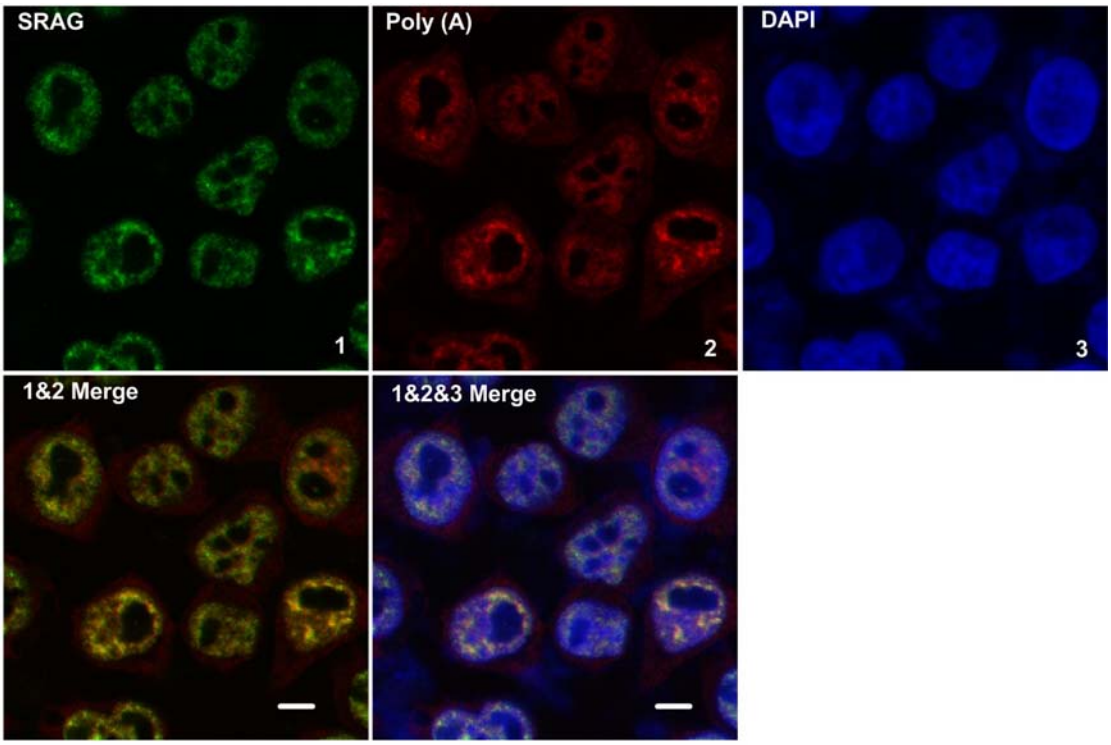

Figure 4-2. Chtop colocalizes with poly (A)+ RNA in nuclear speckle.

HeLa cells were stained with anti-Chtop antibody (green) and poly(A)+ RNA was stained with a fluorescent labeled oligo-d(T) probe (red) by FISH experiments.

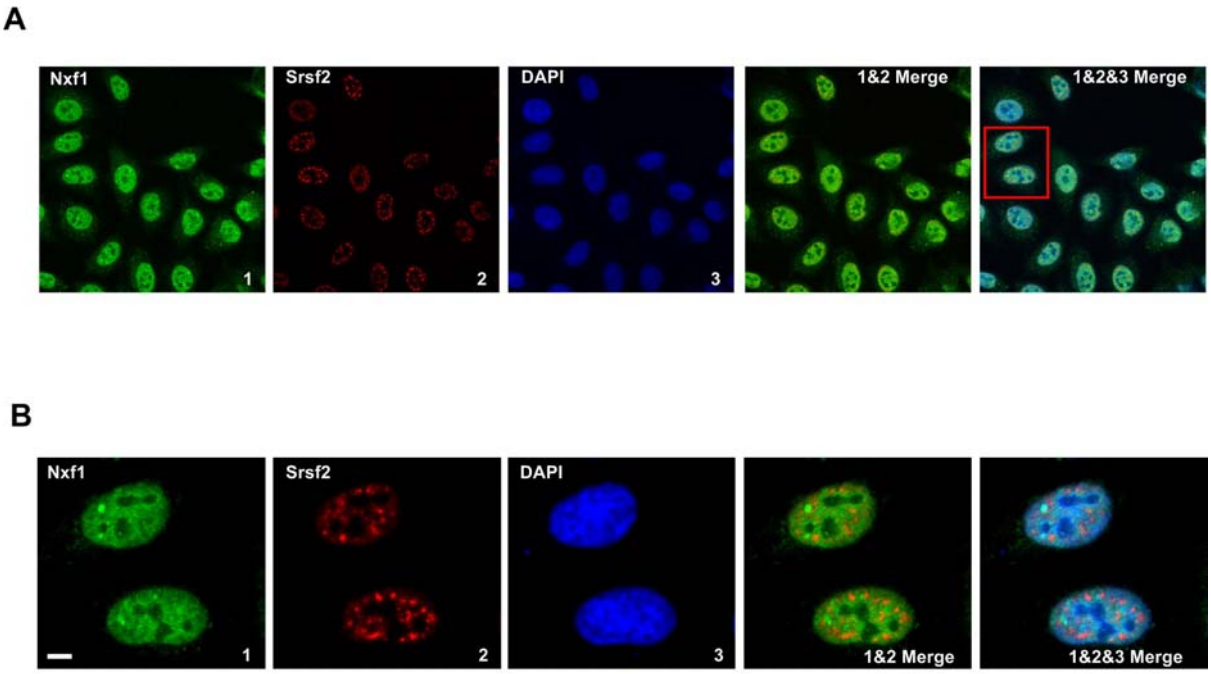

Figure 4-3. Nxf1 localizes to the vicinity of nuclear speckles.

(A) HeLa cells were stained with the anti-Nxf1 antibody (green). Speckles and DNAs were detected with the anti-Srsf2 antibody (red) and DAPI (blue). (B) Magnification of the boxed region in (A). Scale bar, 5 μm.

4.2 Detection of the Chtop:Nxf1 interaction in living cells

To investigate the localization of Chtop in live cells we firstly investigated whether Chtop tagged with a fluorescent protein was capable of interacting with other mRNA export factors. Chtop-GFP was found to co-immunoprecipitate with multiple TREX subunits and Nxf1, indicating that the fluorescent protein tag does not prevent its assembly with these binding partners (Figure 4-4A). Similarly, tagging Nxf1 with GFP did not prevent its association with mRNA export factors since it co-immunoprecipitated with Alyref (Figure 4-4B). To directly examine the interaction of Chtop and Nxf1, we performed sensitized emission FRET in live HeLa cells using Chtop-ECFP as donor and Nxf1-EYFP as acceptor. The normalized FRET (NFRET) measured from the entire nucleus of a cell in control donor:acceptor pairs of ECFP:Nxf1-EYFP, Chtop-ECFP:EYFP and ECFP:EYFP were averaged (Figure 4-5). For all these control samples the averaged NFRET values were below 5.0, indicating this is a baseline value for non-specific NFRET in these conditions. In contrast the Chtop-ECFP:Nxf1-EYFP pair showed an average NFRET signal of 6.78, which is significantly higher than the background (Figure 4-5). Since Chtop interacts with the NTF2-like (NTF2L) domain of Nxf1, we also examined this interaction using a C-terminal fragment of Nxf1

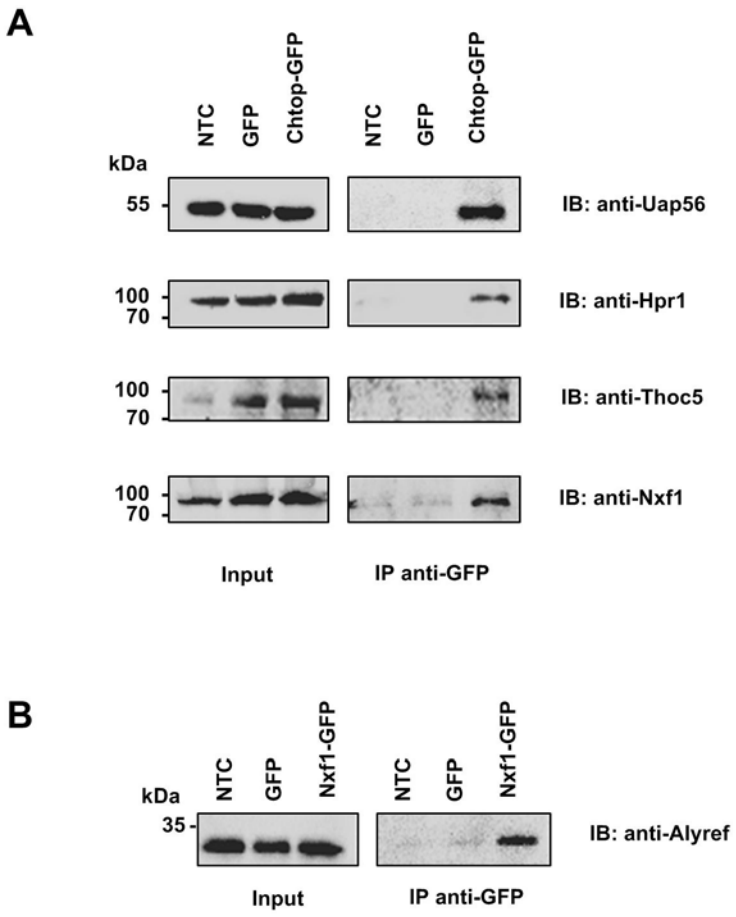

Figure 4-4. Chtop associates with TREX complex.

293T cells transiently expressing Chtop-GFP, GFP or mock transfected were lysed and immunoprecipitated with anti-GFP conjugated protein G Sepharose beads. The bound proteins were detected by western blot with anti-UAP56, anti-Hpr1, anti-Thoc5 or anti-Alyref antibodies.

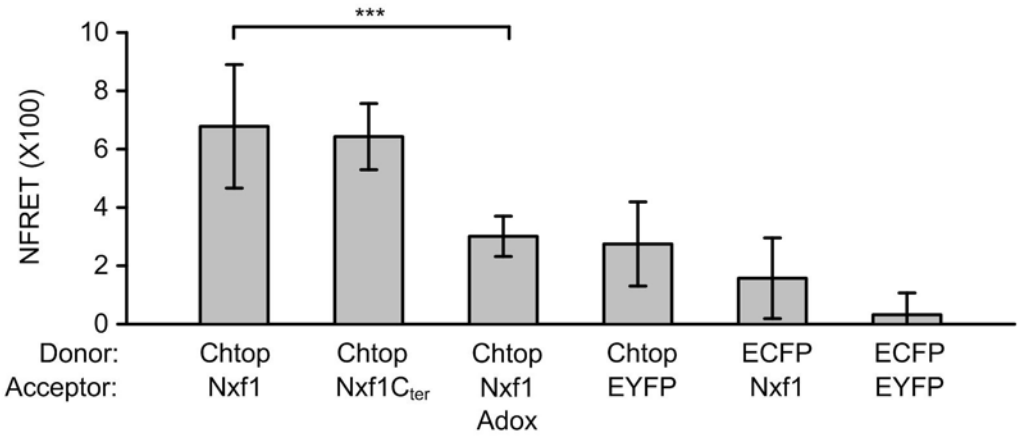

Figure 4-5. Chtop interacts with Nxf1 in living cells.

Quantitative NFRET values were analyzed by sensitized emission FRET. FRET pairs were displayed from left to right in the panel: donor Chtop-ECFP and acceptors Nxf1-EYFP, Nxf1C-terminus-EYFP, Nxf1-EYFP, EYFP; control pairs donor ECFP and acceptors Nxf1-EYFP, EYFP. Data presented as mean ± SD for n= 22 - 25 cells, ***P<0.001.

encompassing the NTF2L domain and found this also gave an NFRET signal significantly higher than the background. The interaction of Chtop with the NTF2L domain of Nxf1 requires methylation of Chtop (Chang et al, 2013). Therefore we also examined the NFRET signal in cells expressing Chtop-ECFP:Nxf1-EYFP in the presence of the methylation inhibitor Adox and found that the NFRET signal was reduced to background levels. Together these data indicate that the FRET signal observed between Chtop-ECFP:Nxf1-EYFP is specific and correlates with previous biochemical experiments used to analyse this interaction (Chang et al, 2013). To spatially map the interaction between Chtop-ECFP and Nxf1-EYFP in the nucleus, NFRET images were displayed in a color-code format (Figure 4-6). Strikingly, the pattern of NFRET signal differed markedly from the localization observed for Chtop-ECFP and Nxf1-EYFP individually. There was a strong NFRET signal at the nuclear periphery together with strong patches of intranuclear signal. Since the most intense Chtop staining in the nucleus in fixed cells corresponds with Srsf2 in the nuclear speckles (Figure 4-1B). We also overlayed the NFRET signal with the Chtop-ECFP signal (Figure 4-6B and 4-6C). This overlay showed that the strong intranuclear patches of NFRET signal do not signficantly overlap with nuclear speckle regions, but some

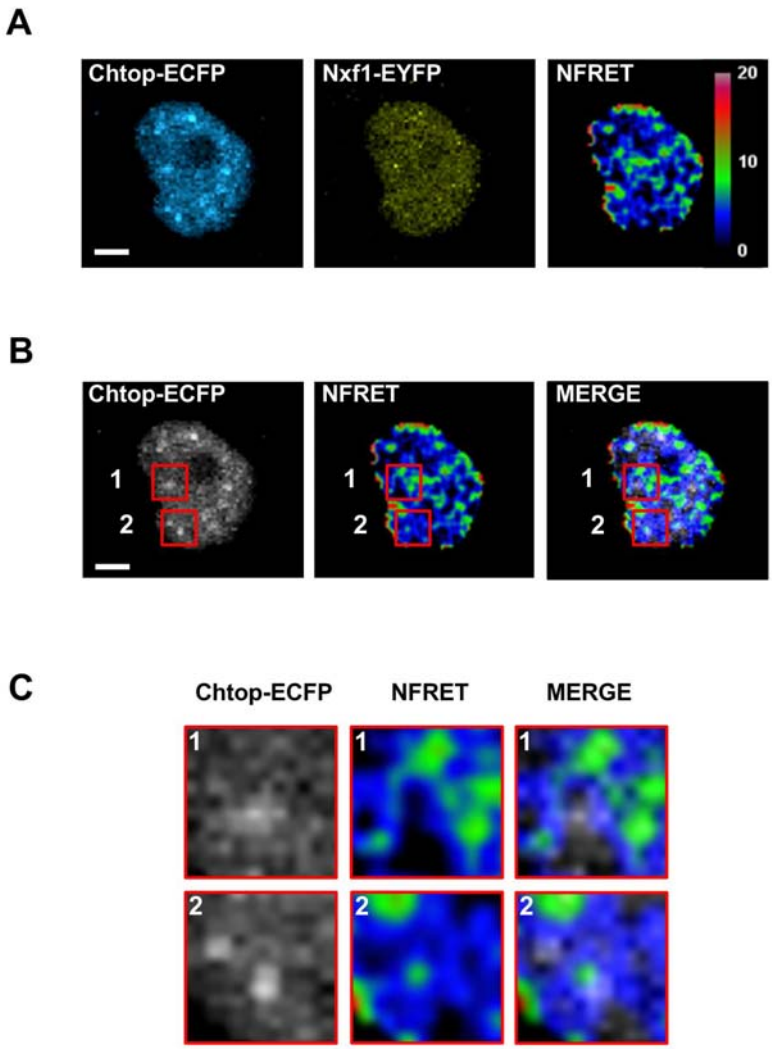

Figure 4-6. Chtop associates with Nxf1 near nuclear speckle.

(A) Representative images of live HeLa cells transiently coexpressing Chtop-ECFP and Nxf1-EYFP were taken in ECFP and EYFP channel and were analyzed by sensitized emission FRET method. The NFRET image was shown in color-code format with percentage value ranges. (B) The merged image combines an ECFP channel and a NFRET image. (C) Magnification of the boxed region in (B). Scale bar, 5μm.

interaction sites lie in close proximity to speckles. The graphic plot from the arrow across the merge image also shows the similar results (Figure 4-7). Together these data suggest that the major sites for interaction of Nxf1 and Chtop are in close proximity to nuclear speckles. There are additional intranuclear sites for strong Nxf1:Chtop interactions mapped by NFRET, not obviously associated with nuclear speckles and some of these may correspond to Chtop and Nxf1 assembled in the mRNP in transit to the nuclear pore. The interaction sites at the nuclear rim may correspond to mRNPs docked at the nuclear pore, in the process of or awaiting translocation through the nuclear pore.

We also assessed the importance of ongoing transcription for the Chtop-ECFP:Nxf1-EYFP interaction and found that there was no significant change to the averaged nuclear NFRET signal intensity when transcription was inhibited by actinomycin D (Figure 4-8A). However, there was a reduction in the strength of the NFRET signals in the intranuclear region, though the NFRET signal at the nuclear periphery was more pronounced (Figure 4-8B). These data suggest that the intranuclear interaction between Chtop and Nxf1 requires ongoing transcription yet the interaction at the nuclear periphery does not.

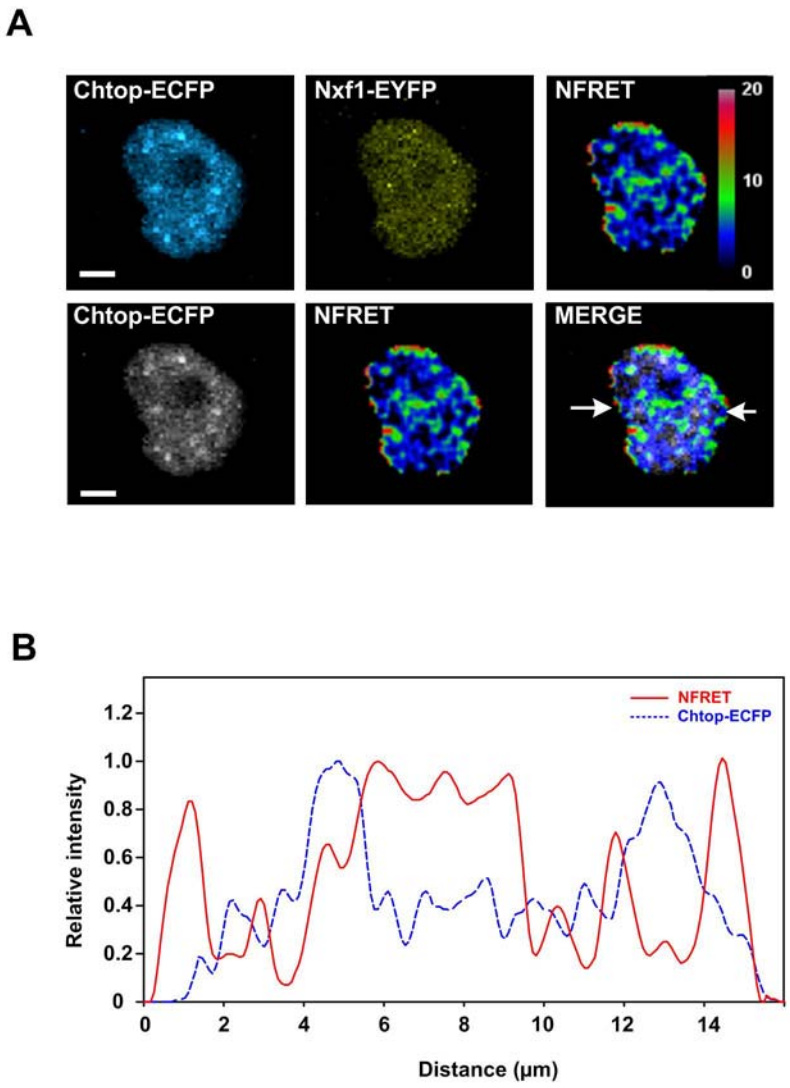

Figure 4-7. Chtop associates with Nxf1 near nuclear speckles.

(A) Representative NFRET images of HeLa cells coexpressing Chtop-ECFP and Nxf1-EYFP. (B) The graphic plot indicates the position of a line scan from the arrow across a MERGE image. Scale bar, 5 μm.

A

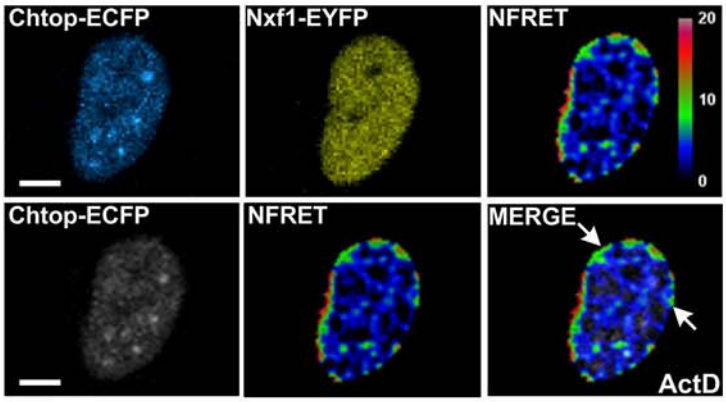

B

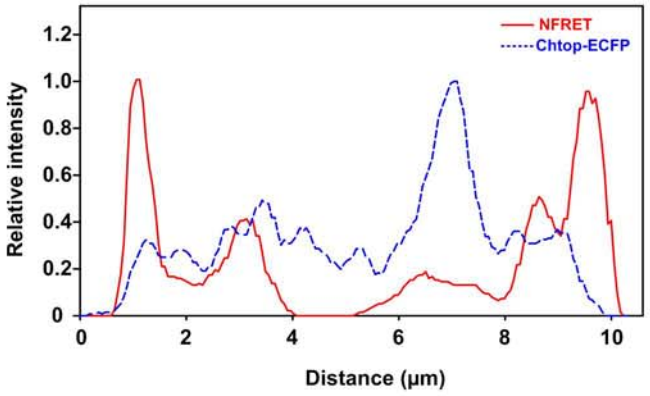

Figure 4-8. mRNA export is coupled to ongoing transcription process near nuclear speckles.

(A) Effect of actinomycin D treatment on the interaction between Chtop-ECFP and Nxf1-EYFP. (B) The graphic plot indicates the position of a line scan from the arrow across a MERGE image. Scale bar, 5 μm.

We also assessed the importance of ongoing transcription for the Chtop-ECFP:Nxf1-EYFP interaction (Figure 4-3A, B). The NFRET signal was quantitated across cells and we found that there was a significant reduction in the intranuclear NFRET signal when cells were treated with actinomycin D. In contrast, the NFRET signal at the nuclear periphery persisted. These data suggest that the intranuclear interaction between Chtop and Nxf1 requires ongoing transcription yet the interaction at the nuclear periphery does not.

4.3 Spatially mapping the interaction between Chtop and Nxf1 by FLIM-FRET

To further characterise the Chtop:Nxf1 interaction *in vivo* we performed FLIM-FRET analysis. When Chtop-ECFP was expressed with EYFP a background average FRET efficiency of 1.59% was observed, whereas when cells expressed both Chtop-ECFP and Nxf1-EYFP the FRET efficiency rose to 9.00% (Figure 4-9). A similar robust interaction was detected for Chtop-ECFP together with a construct expressing the C-terminal half of Nxf1 fused to EYFP. (Figure 4-9). To map the intracellular distribution of the FLIM-FRET signal, images from HeLa cells co-expressing Chtop-ECFP and Nxf1-EYFP were mapped with continuous pseudocolors in each pixel to show mean

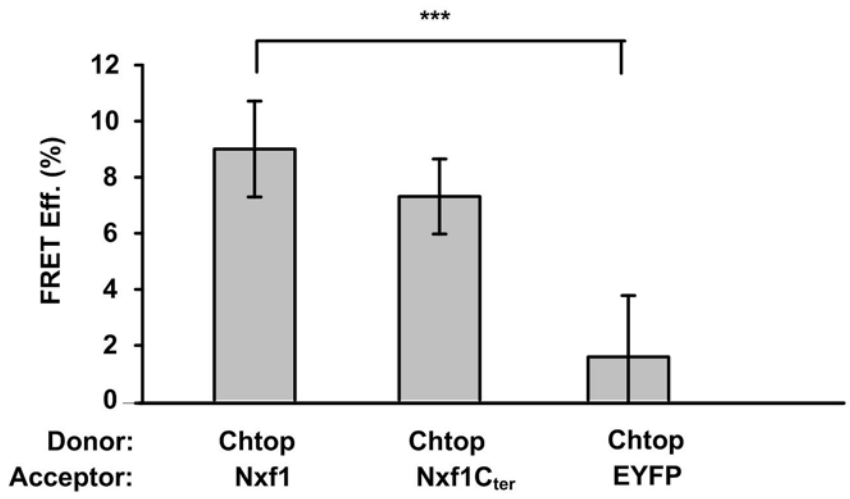

Figure 4-9. The interaction between Chtop and Nxf was analyzed by FLIM-FRET.

HeLa cells were transfected with both donor Chtop-ECFP and indicated acceptors Nxf1-EYFP, Nxf1C-terminus-EYFP, EYFP. Bar graph of FRET efficiency was analyzed by FLIM-FRET. Data presented as mean ± SD for n= 15 - 31 cells, ***P<0.001.

fluorescence lifetime, the percentage of FRET efficiency and FRET population. To establish the background FLIM-FRET signal we analysed Chtop-ECFP co-expressed with EYFP and observed relatively long fluorescence lifetimes throughout the nucleus, thus providing a baseline for non-specific interactions (Figure 4-10). In contrast, Chtop-ECFP co-expressed with Nxf1-EYFP gave an image with much lower fluorescence lifetimes within the nucleus, indicative of a specific interaction (Figure 4-11). The steady state localisation of Chtop overlaps with nuclear speckles and therefore the Chtop-ECFP signal provides a guide as to the location of the nuclear speckles. Strikingly, when the FLIM-FRET signal for Chtop-ECFP:Nxf1-EYFP was overlayed with the Chtop-ECFP signal it became apparent that the main sites for interaction between Chtop-ECFP and Nxf1-EYFP were found in close proximity to the speckle regions, together with additional intranuclear regions not directly associated with speckles. Within the nuclear speckles, there was still evidence of an interaction above background levels but at a much lower level than that seen on the periphery of speckles and at other intranuclear sites. With actinomycin D treatment, the FLIM-FRET efficiency signals between Chtop-ECFP and Nxf1-EYFP were reduced within the nucleus (Figure 4-12) but strong interaction sites were visible around the nuclear periphery as

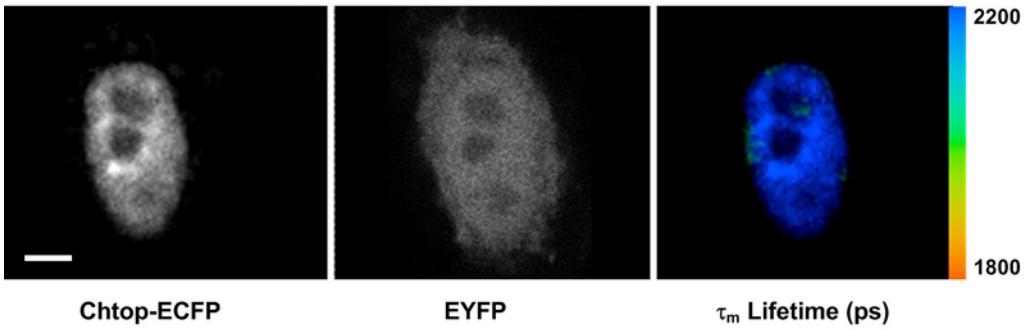

Figure 4-10. The FLIM image of Chtop and EYFP

Representative images of HeLa cells co-expressing Chtop-ECFP and EYFP. The image representing mean fluorescence lifetime (picoseconds) was shown in continuous pseudo-colors with time value range.

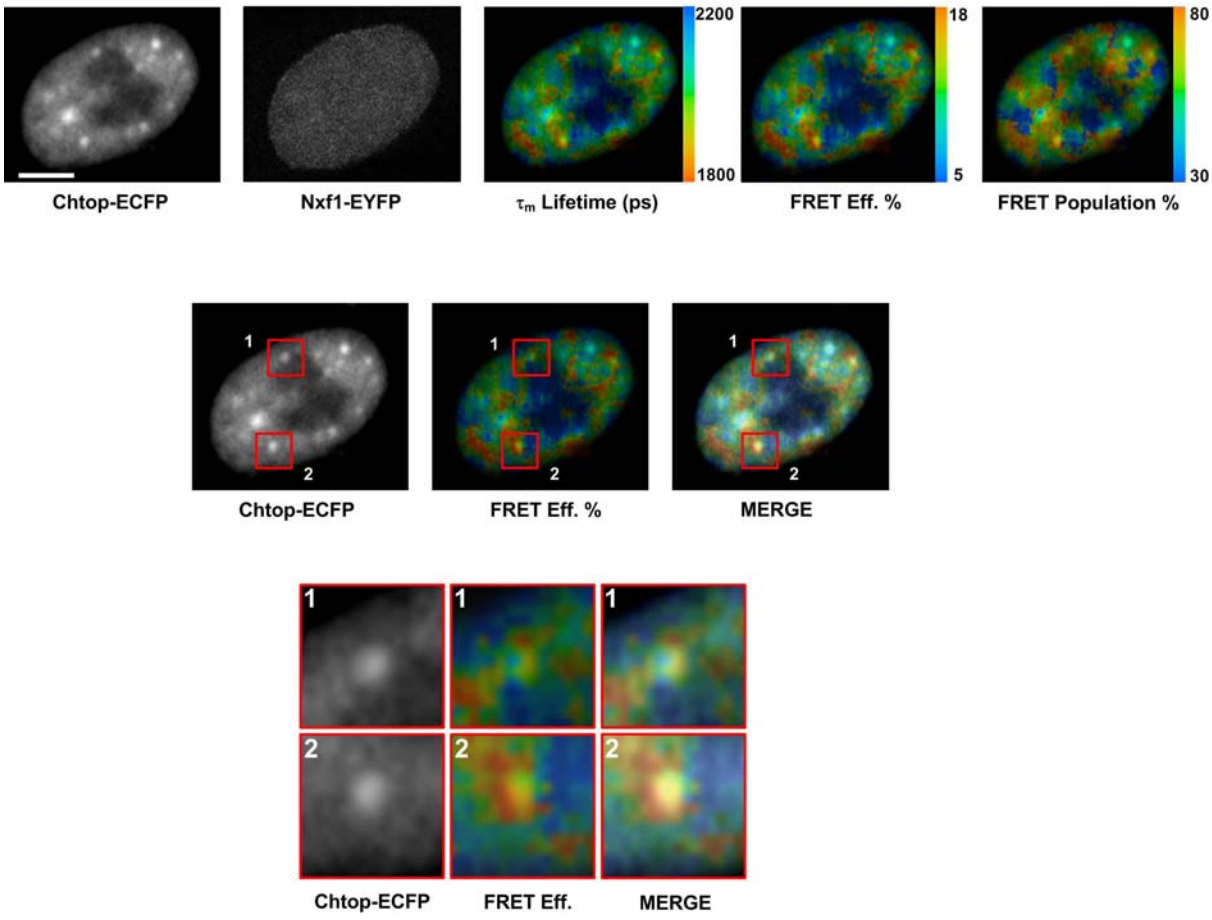

Figure 4-11. The topological relationship between Chtop and Nxf1

Representative images of HeLa cells coexpressing Chtop-ECFP and Nxf1-EYFP. FRET efficiency and FRET population (% of interacting donor molecules) were shown in continuous pseudo-colors with percentage value ranges.

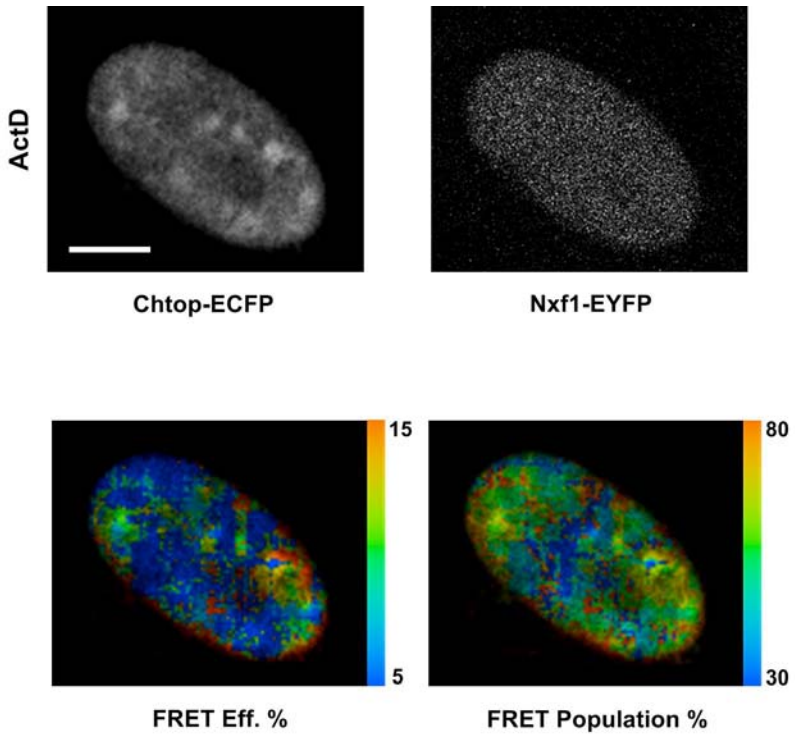

Figure 4-12. The topological relationship between Chtop and Nxf1 following transcription inhibition.

Effect of actinomycin D treatment on the interaction between Chtop-ECFP and Nxf1-EYFP. FRET efficiency and FRET population (% of interacting donor molecules) were shown in continuous pseudo-colors with percentage value ranges. Scale bar, 5 μm.

observed earlier (Figure 4-8). To investigate the FLIM-FRET signal for Chtop-ECFP co-expressing with Nxf1 Cterminus-EYFP and we observed relatively shorter fluorescence lifetimes throughout the nucleus, thus providing a intracellular map for non-specific interactions (Figure 4-13).

4.4 Alyref interacts with Nxf1 in living cells

To establish whether the pattern of interaction observed between Nxf1 and Chtop was a more general property of other mRNA export factors which interact with Nxf1, we also monitored the Alyref-ECFP:Nxf1-EYFP interaction in living cells. Initially we analysed the overall NFRET-signal observed in the nucleus, averaged across multiple cells. When Alyref-ECFP co-expressed with EYFP and ECFP co-expressed with Nxf1-EYFP gave background NFRET signals of 2.06 and 1.57 respectively. In contrast, Alyref-ECFP:Nxf1-EYFP gave a significantly higher NFRET value of 8.14, indicating a robust interaction (Figure 4-14).

We next analysed the distribution of NFRET signals for Alyref-ECFP coexpressed with Nxf1-EYFP. Since Alyref localizes with nuclear speckles at steady state (Zhou et al, 2000), we overlayed the NFRET and Alyref-ECFP images (Figure 4-15). This analysis revealed that the major sites of interaction

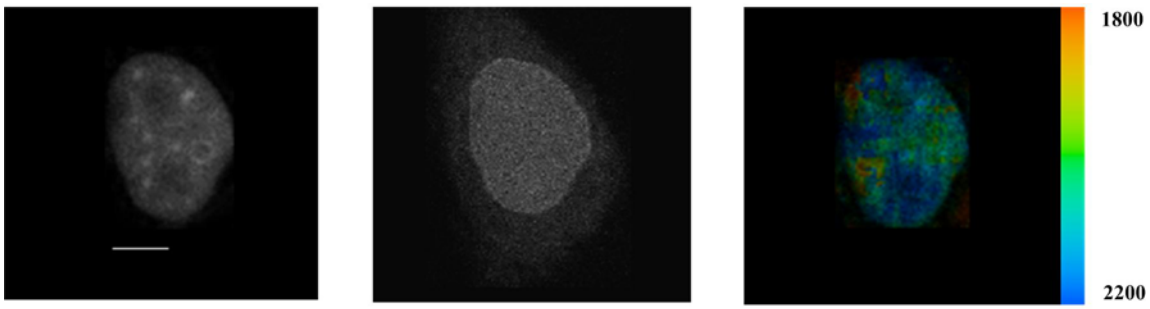

Figure 4-13. FLIM image between Chtop and Nxf1-Cterminus

Representative images of HeLa cells coexpressing Chtop-ECFP and Nxf1-Cterminus-EYFP. FRET efficiency and FRET population (% of interacting donor molecules) were shown in continuous pseudo-colors with percentage value ranges. Scale bar, 5 μm.

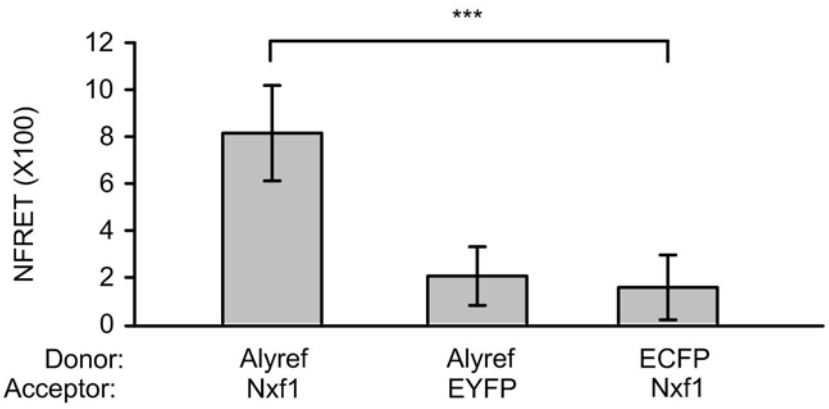

Figure 4-14. Analysis of the Nxf1 and Alyref interaction in living HeLa cells.

Quantitative analysis of NFRET values for different pairs of donor and acceptor in live HeLa cells by sensitized emission FRET (mean ± SD for n= 22 - 32 cells, ***P<0.001).

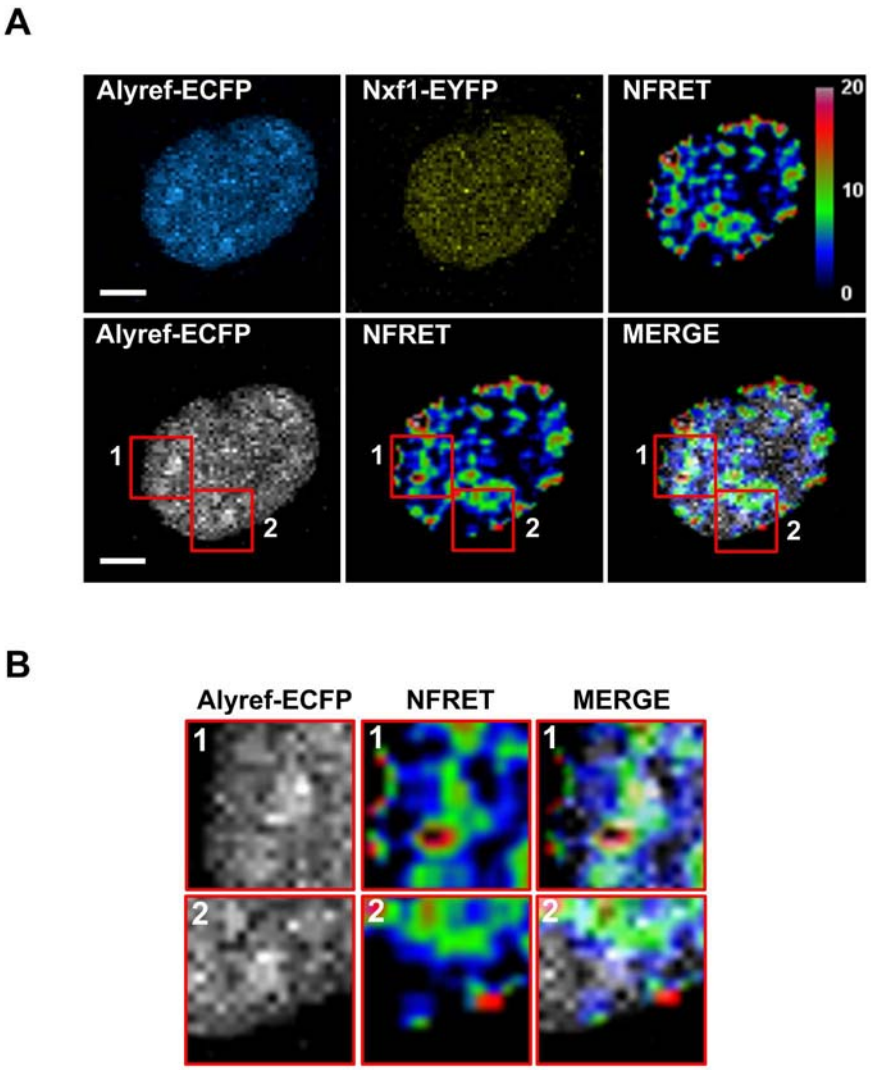

Figure 4-15. FRET images of Nxf1 and Alyref in living HeLa cells.

Representative NFRET images of HeLa cells coexpressing Alyref-ECFP and Nxf1-EYFP. Scale bar, 5μm.

of Alyref-ECFP and Nxf1-EYFP did not coincide with the nuclear speckle regions directly although they were closely associated (Figure 4-15B). We also observed that, actinomycin D treatment reduced the intranuclear NFRET signal for Alyref-ECFP and Nxf1-EYFP, yet a strong signal persisted at the nuclear periphery (Figure 4-16). This striking alteration in the sites of interactions mirrors that observed between Chtop-ECFP and Nxf1-EYFP as well (Figure 4-8). Further analysis of the Alyref-ECFP:Nxf1-EYFP interaction using FLIM-FRET (Figures 4-17) confirmed the specific association of Alyref and Nxf1 in living cells. The major sites of association between Alyref-ECFP and Nxf1-EYFP did not correspond to the speckle regions where Alyref is found at steady state (Zhou et al, 2000) and instead, major interaction sites were found in close proximity to the speckles within the nucleus (Figure 4-18). However, FLIM-FRET detected interactions between Nxf1 and Alyref even within speckle regions, though at much lower levels, consistent with the FLIM-FRET analysis of the Chtop-ECFP:Nxf1-EYFP interaction (Figure 4-11).

4.5 Intermolecular interactions between mRNA export factors Chtop and Alyref *in vivo*

To investigate where TREX assembly occurs in the cell we investigated

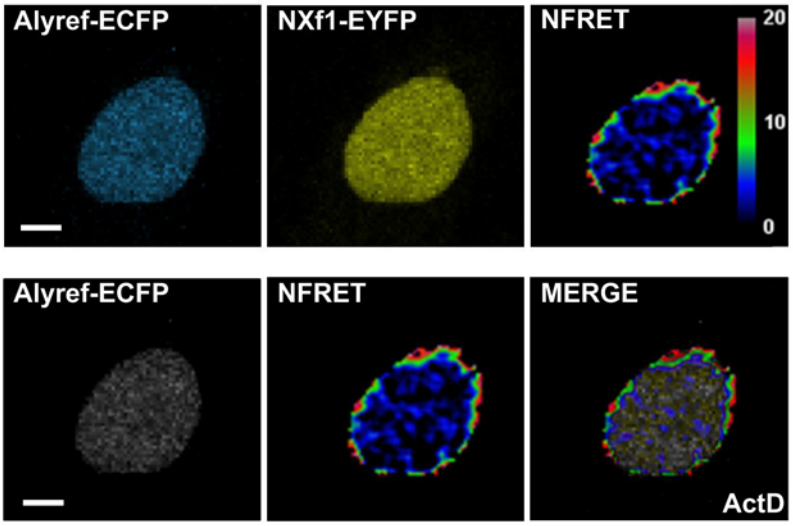

Figure 4-16. FRET images of Nxf1 and Alyref after transcription stops.

Effect of actinomycin D treatment on the interaction of HeLa cells coexpressing Alyref-ECFP and Nxf1-EYFP examined by NFRET. Scale bar, 5μm.

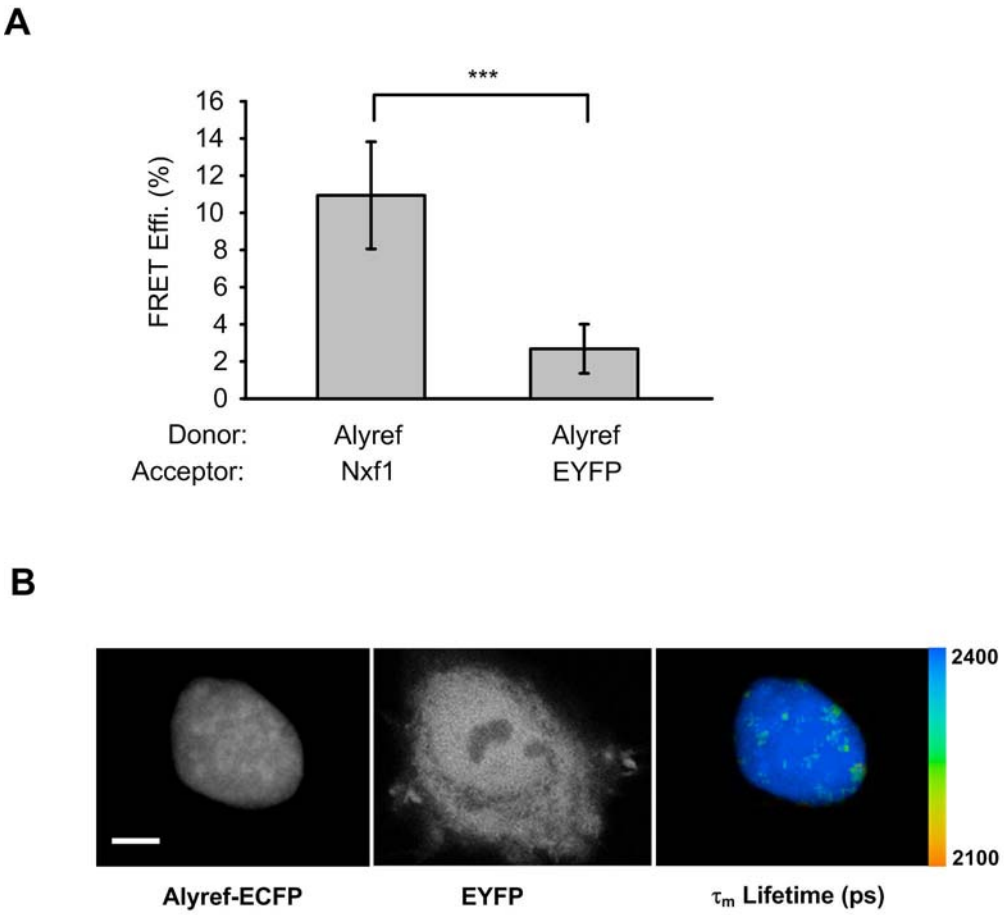

Figure 4-17. The interactions of Nxf1 and Alyref by FLIM-FRET.

(A) Bar graph of FLIM-FRET efficiency of donor Alyref-ECFP with acceptor Nxf1-EYFP or EYFP (mean ± SD for n= 18 - 27 cells, ***P<0.001). (B) Representative FLIM-FRET images of HeLa cells transfected with both Alyref-ECFP and Nxf1-EYFP. Scale bars, 5 μm.

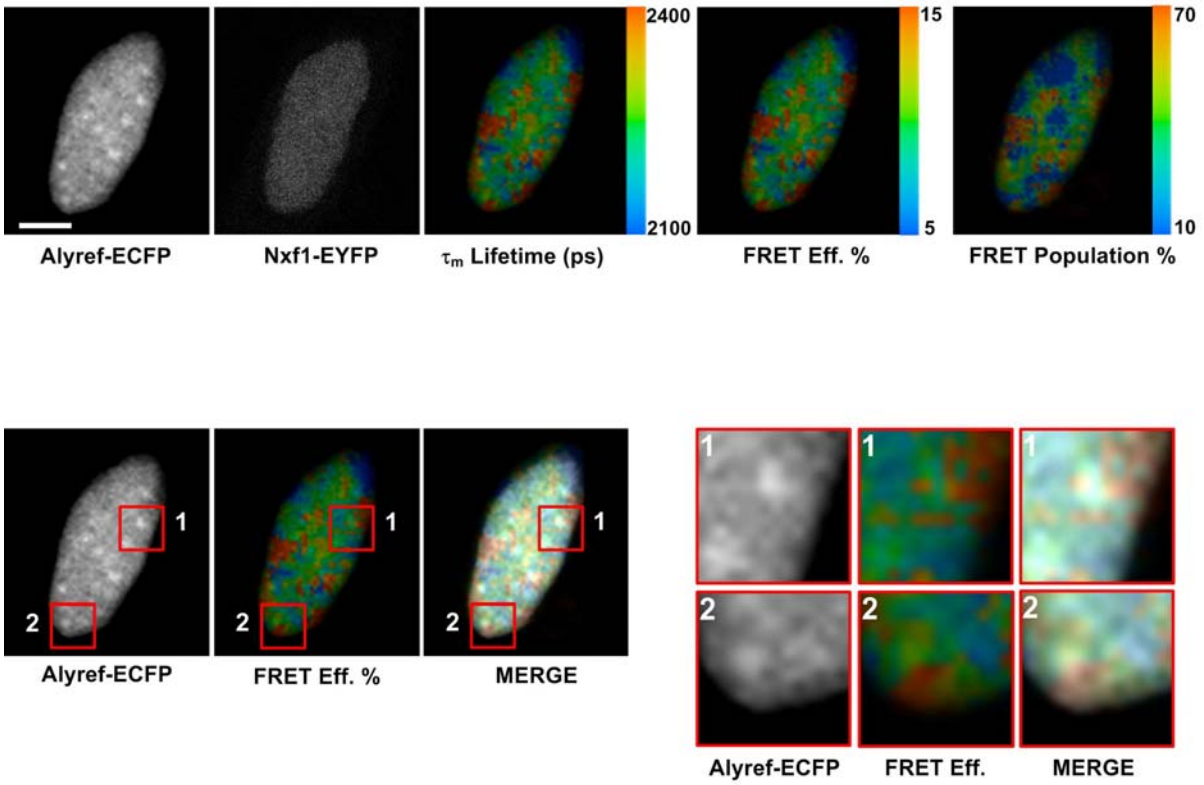

Figure 4-18. The spatial interactions of Nxf1 and Alyref by FLIM-FRET.

Representative FLIM-FRET images of HeLa cells transfected with both Alyref-ECFP and Nxf1-EYFP. Scale bars, 5 μm.

where two TREX subunits Chtop and Alyref interact. Chtop exists in both methylated and unmethylated forms within the nucleus. Its methylation state can regulate the intermolecular interactions with Alyref, Nxf1 and RNA, with unmethylated Chtop selectively binding Alyref and methylated Chtop binding Nxf1 (Chang et al, 2013). We established that Chtop tagged with a fluorescent protein retained the same binding characteristics with Alyref using co-immunoprecipitation (Figure 4-19A). Following treatment with Adox we observed a characteristic shift to a higher mobility form of Alyref in SDS-PAGE which corresponds to the hypomethyalted form (Figure 4-19A), indicating Adox treatment was successfully blocking protein methylation. Following immunoprecipitation with an antibody to GFP we found that Chtop-GFP preferentially immunoprecipitated with Alyref when cells were treated with Adox (Figure 4-19A, right panel), indicating the interaction between these proteins preferentially occurs when they are hypomethylated.

We next investigated the steady state localization of both Chtop and Alyref and found that they showed substantial colocalisation (Figure 4-19B) consistent with their individual colocalisation with nuclear speckles (Figure 4-1A and (Zhou et al, 2000)). We examined where Chtop and Alyref interactions occur in living cells using FLIM-FRET (Figures 4-20). In the

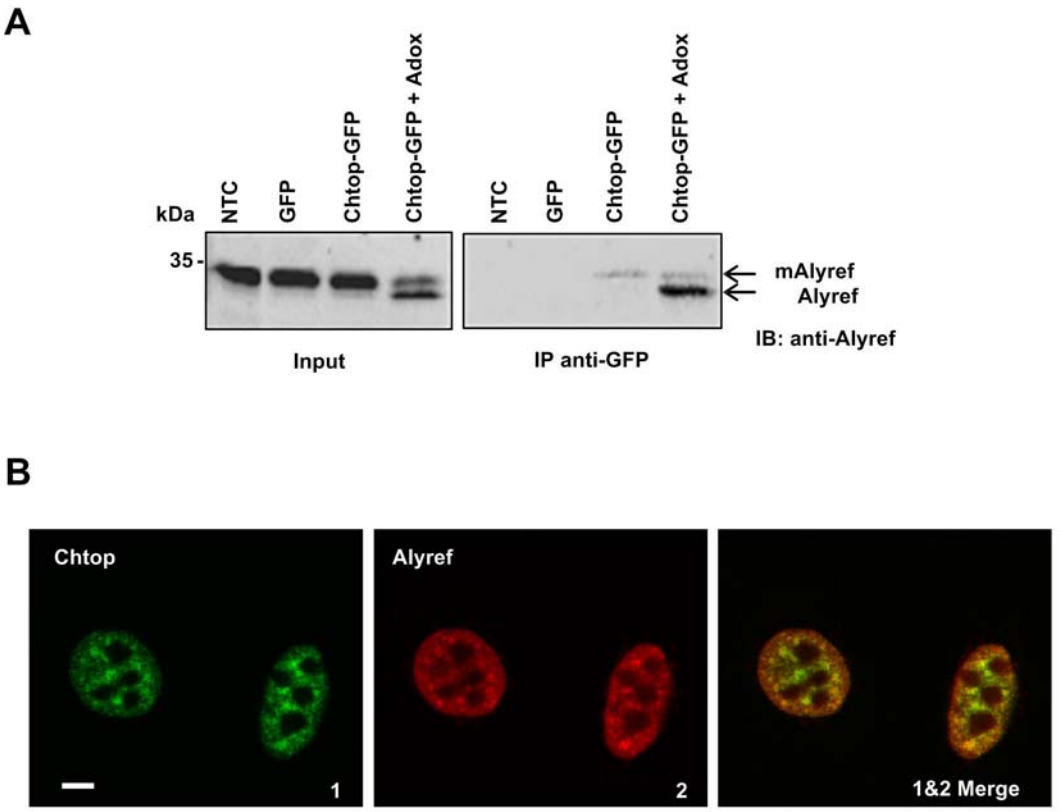

Figure 4-19. The interactions between Chtop and Alyref.

(A) cells extracts from 293T cells transfected with Chtop-GFP, GFP or mock transfected were immunoprecipitated with anti-GFP antibody and detected by Western blot with anti-Alyref antibody. (B) The fixed HeLa cells were stained with anti-Chtop antibody (green) and anti-Alyref antibody (red).

absence of Adox only background signals were observed for Chtop-ECFP:Alyref-EYFP (Figures 4-20B). This suggests that unmethylated Chtop only exists very transiently in cells normally. Following Adox treatment, strong intranuclear interactions were observed by FLIM-FRET (Figure 4-21). The FRET population and FRET efficiency maps showed substantial similarities and when the steady state localization of Chtop-ECFP was compared with the FRET efficiency map it was clear that the major Chtop-ECFP and Alyref-EYFP interactions occur in regions adjacent to nuclear speckles and at additional intranuclear sites. However the FRET efficiencies within regions corresponding to nuclear speckles were above background, though substantially lower than those seen on the periphery of speckles, indicating Chtop and Alyref also associate within nuclear speckles.

We next used sensitized emission FRET to detect the interaction of Chtop-ECFP and Alyref-EYFP in live HeLa cells (Figure 4-22). The more increased NFRET signals can be seen in the nucleus and nuclear periphery in the presence of Adox compared to the signals where without Adox treatment (Figure 4-23). However, we cotransfected with Alyref-ECFP and Chtop-EYFP in HeLa cells, and found that the average NFRET signal did not significantly change with actinomycin D treatment (Figure 4-22). In the presence of

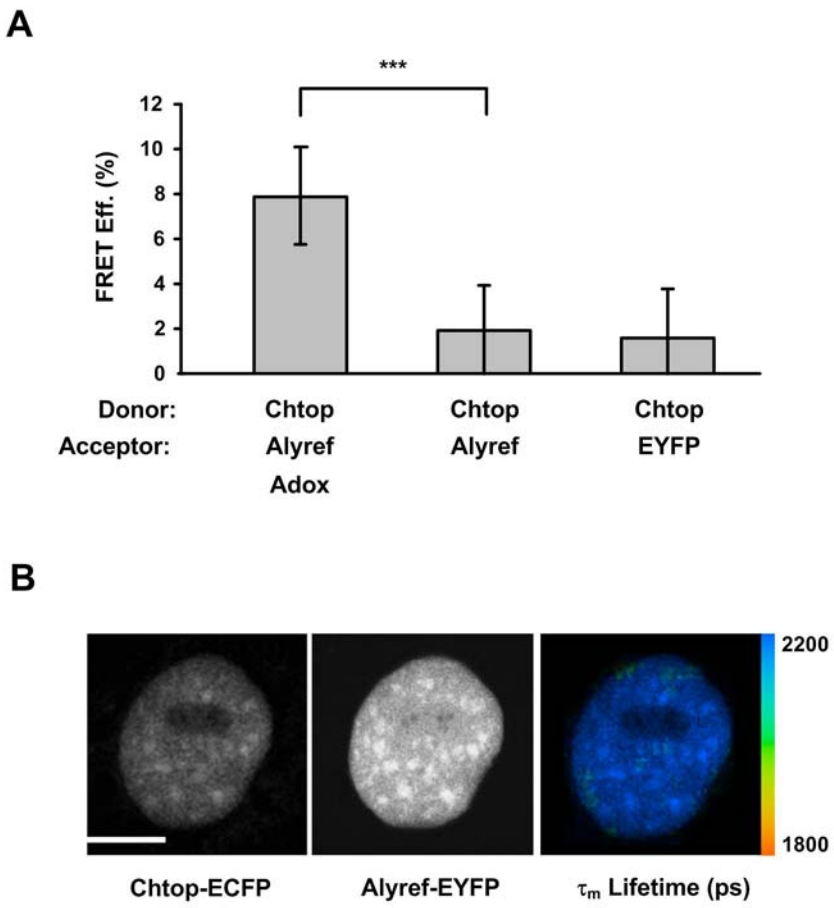

Figure 4-20. The interactions between Chtop and Alyref by FLIM-FRET.

(A) Quantitative FLIM-FRET efficiency of Chtop-ECFP and Alyref-EYFP pair in the presence or absence of Adox treatment (mean ± SD for n= 17 - 25 cells, ***P<0.001). (B) Representative FLIM-FRET images of HeLa cells coexpressing Chtop-ECFP and Alyref-EYFP. Scale bars, 5 μm.

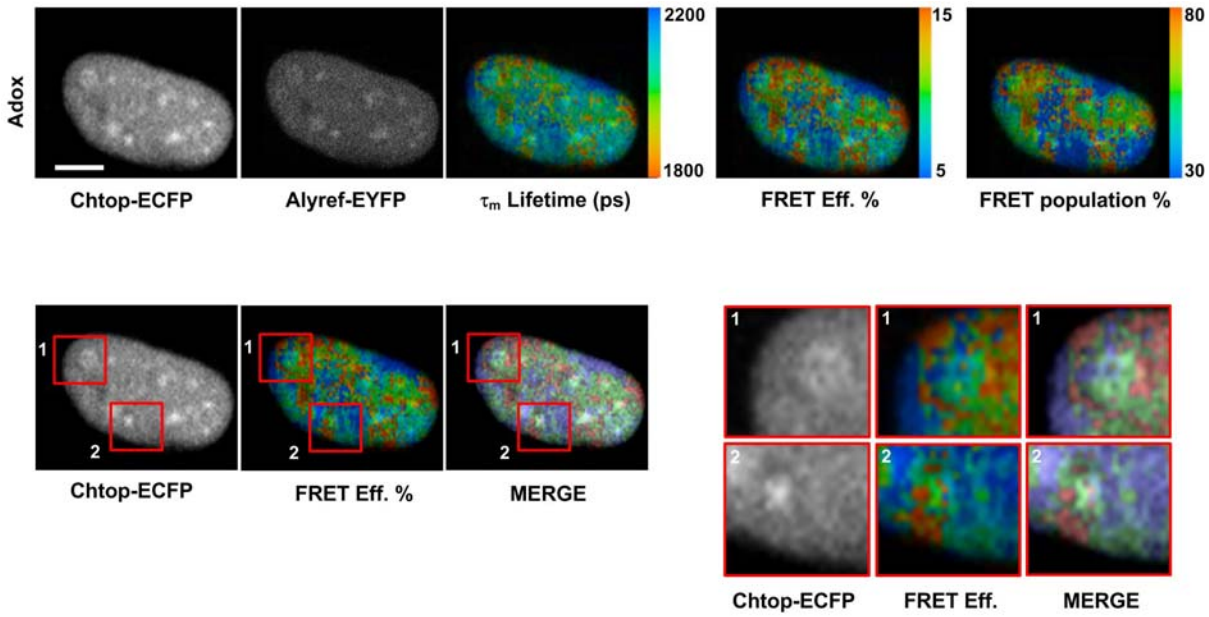

Figure 4-21. The spatial interactions between Chtop and Alyref by FLIM-FRET.

Effect of Adox treatment on the interaction between Chtop-ECFP and Alyref-EYFP. Scale bars, 5 μm.

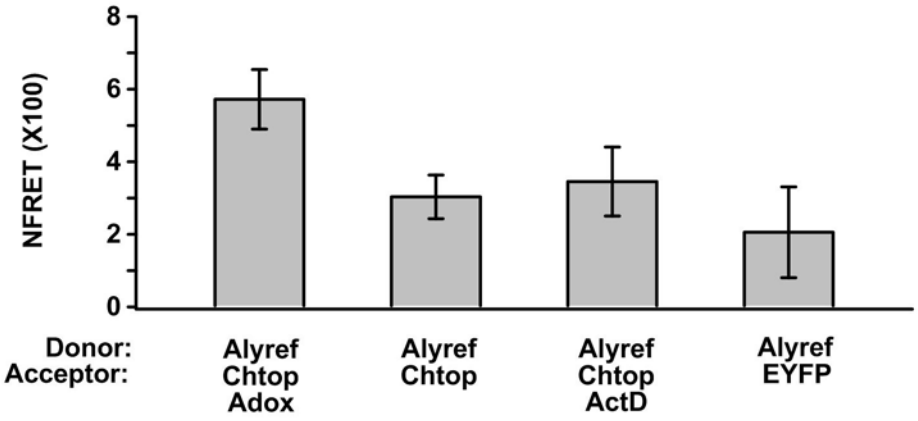

Figure 4-22. The interaction between Alyref and Chtop analyzed by NFRET.

Quantitative analysis of NFRET values for different pairs of donor and acceptor in live HeLa cells by sensitized emission FRET (mean ± SD for n= 17 - 32 cells).

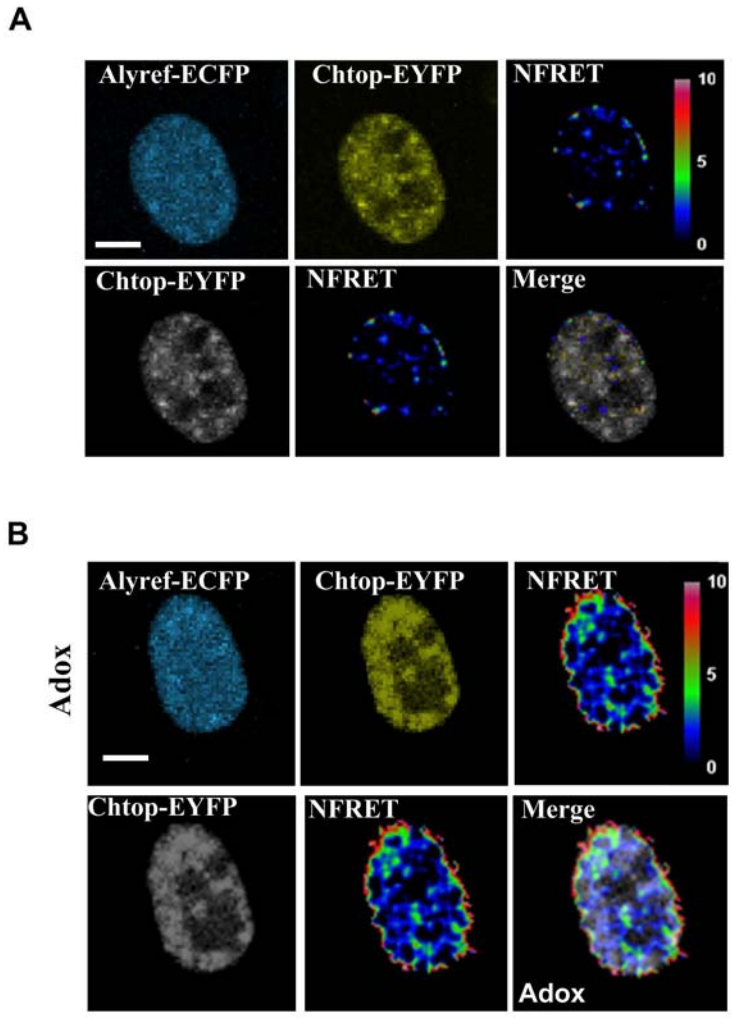

Figure 4-23. The spatial interaction between Alyref and Chtop in living cells.

(A) Representative NFRET images of HeLa cells coexpressing Alyref-ECFP and Chtop-EYFP. (B) Representative NFRET images of HeLa cells coexpressing Alyref-ECFP and Chtop-EYFP in the presence of Adox treatment. Scale bar, 5μm.

actinomycin D, we observed that <5% NFRET signal was distributed intracellularly, showing the binding affinity was reduced intracellularly between Alyref and Chtop, however, some NFRET signal at perinuclear domain maintain >5%, suggesting that the interaction between Alryref and Chtop may have the feedback response in a post-transcriptional pathway (Figure 4-24).

4.6 Nuclear dynamics of mRNA export proteins

To characterize the dynamic behavior of mRNA export proteins in different compartments of the nucleus, we used the fluorescence recovery after photobleaching (FRAP) technique. We measured the half-life of recovery and mobility of mRNA export proteins tagged with GFP within the nuclear speckles and nucleoplasm of live HeLa cells. Chtop-GFP present in the nuclear speckles had a half life for recovery from photobleaching of 141.46 seconds (Table 1) and reached a plateau of fluorescence intensity post-bleaching after 800 seconds (Figure 4-25). In contrast, Chtop-GFP in the nucleoplasm showed a post-bleach half life for recovery of 48.47 seconds and reached a plateau of fluorescence intensity within 300 seconds (Figure 4-25B). These data indicate that Chtop-GFP is significantly less mobile in nuclear speckles than in the nucleoplasm. Earlier FRAP studies on whole nuclei for Chtop-GFP

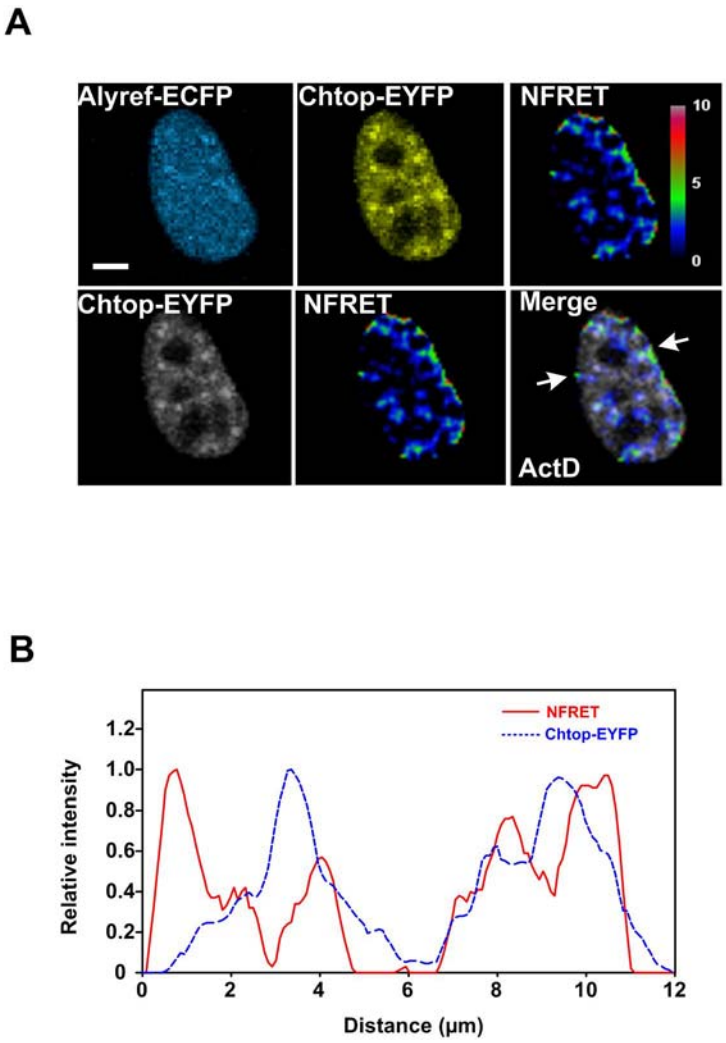

Figure 4-24. The spatial interaction between Alyref and Chtop in living cells.

(A) Representative NFRET images of HeLa cells coexpressing Alyref-ECFP and Chtop-EYFP in the presence of ActD treatment. (B) The graphic plot indicates the position of a line scan from the arrow across a MERGE image. Scale bar, 5 μm.

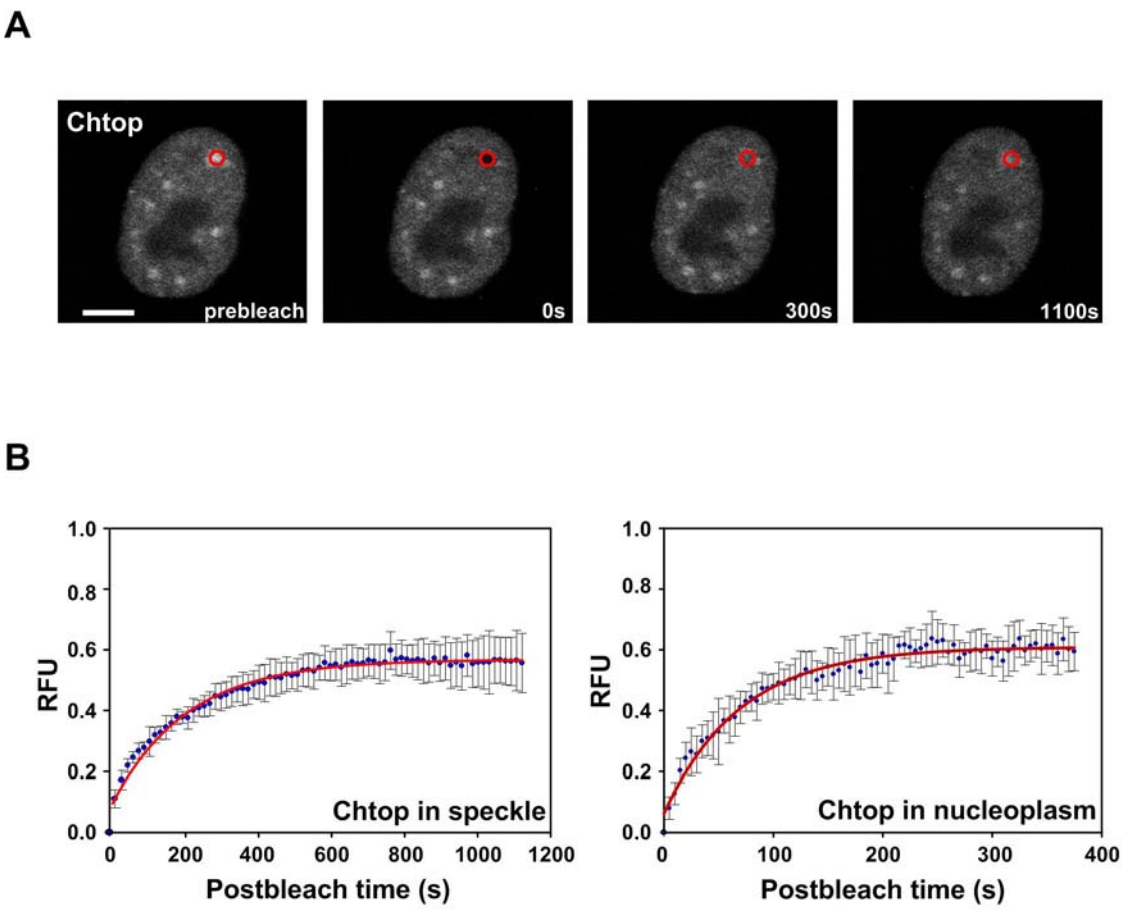

Figure 4-25. Nuclear dynamics of Chtop were measured by FRAP.

(A) Representative images illustrating fluorescence recovery of Chtop-GFP after photobleaching in nuclear speckle (red circle) of live HeLa cells. (B) The plots of time-dependent normalized fluorescence recovery of Chtop-GFP in the bleached speckles and nucleoplasms. RFU, relative fluorescent units; FRAP, fluorescence recovery after photobleaching; Scale bars, 5 μm.

also showed that it took in excess of 800 seconds to reach a post-bleach plateau of fluorescence recovery (van Dijk et al, 2010) which fits with the observation that a large proportion of Chtop-GFP resides in the nuclear speckles. A large fraction of Chtop-GFP was found in the immobile fractions in both the nucleoplasm (39.23%) and nuclear speckles (43.95%) (Table 1), which for nucleoplasmic Chtop is consistent with the observation that it stably associates with chromatin (van Dijk et al, 2010). We also analysed the mobility of two Chtop-GFP fragments comprising residues 1-87 and 93-213 in the nucleoplasm, and found that both these fragments of Chtop had substantially shorter half lives for recovery and lower immobile fractions compared with full length Chtop (Table 1), suggesting that Chtop requires both N and C-terminal regions for interaction with nuclear structures which reduce its mobility. For comparison we also monitored the mobility of two other export factors, Alyref and Nxf1 (Figure 4-26 and Table 1). Alyref-GFP and Nxf1-GFP have very short half lives for recovery post-bleaching compared with Chtop-GFP and much smaller immobile fractions, indicating that these two export factors have far greater mobility within the nucleus than Chtop. Interestingly, Alyref showed reduced mobility in the nuclear speckles compared with the nucleoplasm as did Chtop (Table 1). The increased mobility of Chtop

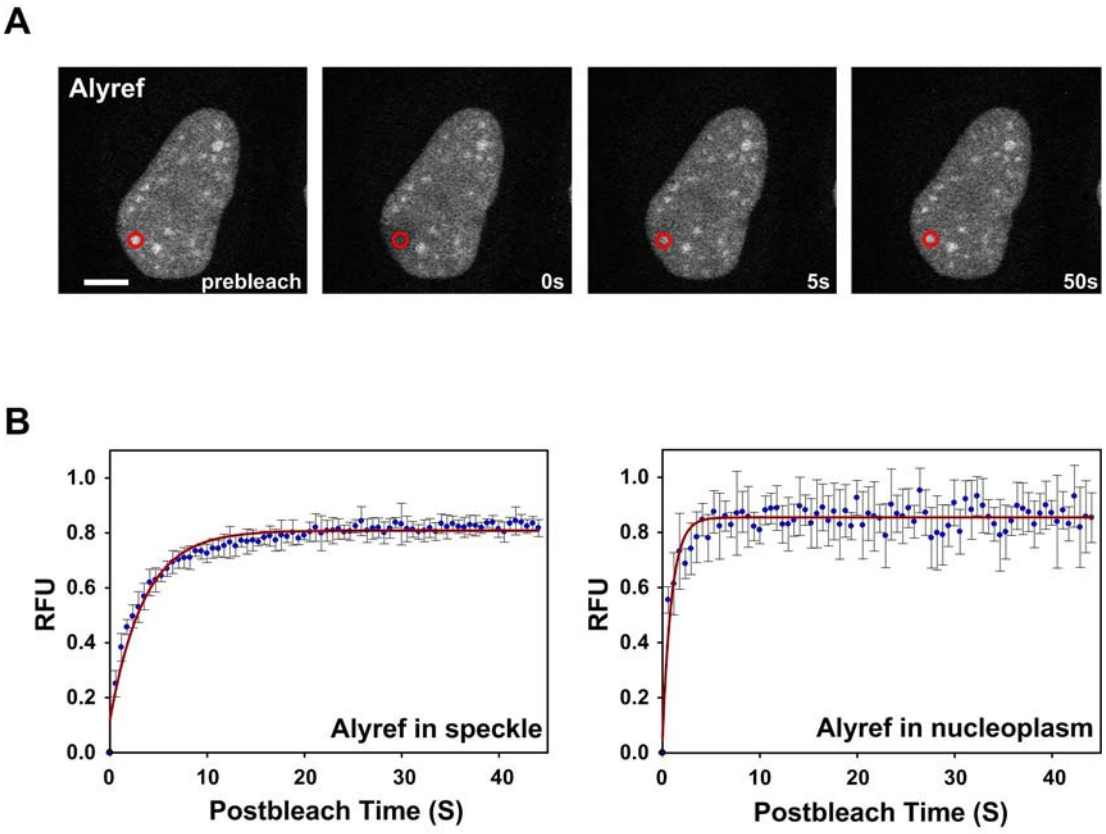

Figure 4-26. Nuclear dynamics of Alyref were measured by FRAP.

(A) Representative images illustrating fluorescence recovery of Alyref-GFP after photobleaching in the nuclear speckle (red circle) of live HeLa cells. (B) The plots of time-dependent normalized fluorescence recovery of Alyref-GFP in the nuclear speckle and nucleoplasm. RFU, relative fluorescent units; FRAP, fluorescence recovery after photobleaching; Scale bars, 5 μm.

	Location	Half- life of recovery	Immobile fraction	Cell numbers
Chtop	speckle	141.46 sec	43.95 ± 4.21 %	7
	nucleoplasm	48.47 sec	39.23 ± 1.38%	7
Chtop1-87	nucleoplasm	3.62 sec	8.43 ± 2.02%	15
Chtop 93-213	nucleoplasm	2.44 sec	13.56 ± 3.69%	8
Alyref	speckle	2.42 sec	17.18 ± 1.29%	8
	nucleoplasm	0.65 sec	13.52 ± 3.30%	6
Nxf1	nucleoplasm	1.43 sec	14.40 ± 2.67%	7

Table 1. FRAP measurement of export factors in living cells

[1]Constructs with GFP fusion protein,

[2]s time of half-life of recovery,

[3]n number of cells from which the FRAP is measured.

and Alyref within the nucleoplasm compared with the nuclear speckles is consistent with the NFRET and FLIM-FRET data which show that a major site for assembly of TREX with Nxf1 occurs around nuclear speckles. Therefore a proportion of the nucleoplasmic Chtop and Alyref may be molecules already assembled with TREX and Nxf1, in the process of export to the cytoplasm.

CHAPTER IV

DISCUSSION

We have spatially mapped the site where TREX subunits associate with each other and the mRNA export receptor Nxf1. We found that the major sites for interaction between two TREX subunits and Nxf1 do not lie within nuclear speckles. This is despite observing significant a concentration of TREX subunits within nuclear speckles. Instead, the major interaction sites are often found in close proximity to the nuclear speckles and these sites of interaction are sensitive to transcriptional inhibition. These data are consistent with an earlier study which used bifluorescence complementation to look at the interaction between Nxf1 and the exon-junction complex component Y14 (Schmidt et al, 2006). In these earlier studies, Nxf1 and Y14 interactions were prominently observed in perispeckle regions, surrounding nuclear speckles in some cells, though weaker interactions were also observed within speckles. We also provide further evidence confirming that methylation of Chtop provides an important control step during assembly and maturation of the mRNA export complex. We have shown that unmethylated Chtop is able to bind Alyref *in vivo* (Figure 4-21). This interaction probably occurs early during TREX assembly since only methylated Chtop subsequently binds Nxf1 within

assembled TREX (Figure 5 and (Chang et al, 2013)).

TREX assembly is coupled with transcription, splicing and polyadenylation, moreover Nxf1 recruitment to mRNA requires an assembled TREX complex (Viphakone et al, 2012). Thus Nxf1 recruitment to TREX might be expected to occur at sites where these processes take place. Nuclear speckles are devoid of DNA and transcription does not take place within the majority of them (Cmarko et al, 1999), though a number of proteins involved in transcription are found associated with nuclear speckles (Spector & Lamond, 2011). Active transcription sites are found at many sites within the nucleus but are enriched in regions surrounding nuclear speckles known as perispeckles (Daguenet et al, 2012). Perispeckles correspond to a doughnut like ring structure found immediately surrounding nuclear speckles and these are the assembly site for the exon junction complex (EJC). This observation fits nicely with the earlier observation that splicing factors feed out from nuclear speckles to adjacent sites of transcription (Misteli et al, 1997) since the EJC assembles on spliced RNA as does TREX. Whilst we have not observed the tight clustering of TREX:Nxf1 assembly sites around nuclear speckles in the same way that EJC components assemble in the perispeckle region, we clearly see extensive interactions in the perispeckle region. Thus the perispeckle region appears to

be a major site for both assembly of TREX and subsequent recruitment of Nxf1.

When we inhibit transcription there is a significant reduction in Nxf1:TREX interactions observed within the nucleus, which suggests that TREX assembly with Nxf1 might occur cotranscriptionally. Consitently, the TREX subunits Hpr1 and Alyref are recruited cotranscriptionally (Li et al, 2005) (Yoh et al, 2007) (Johnson et al, 2009b). The sites of Nxf1:TREX interaction which we observe which are not tightly associated with nuclear speckles may correspond to additional sites of transcription within the nucleus or TREX:Nxf1:mRNA complexes in transit to the cytoplasm. The other striking observation following the inhibition of transcription is the persistence of TREX subunit:Nxf1 interactions at the nuclear periphery. This interaction may represent complexes which have become trapped at the nuclear pore following the transcription block. In yeast, proofreading of mRNPs at the nuclear pore involves the Mlp proteins which can feedback and alter gene transcription in response to defects in the mRNP (Vinciguerra et al, 2005) and such a proofreading mechanisms exists in human cells involving the mammalian orthologue of Mlp1, which is Tpr (Coyle et al, 2011) . Such a proofreading mechanism involving might also stall some preassembled mRNPs at the

nuclear pore when transcription is inhibited. Nxf1 itself appears to stably associate with the nuclear pore since detergent extraction of cells prior to fixation readily reveals a distinctive nuclear rim association for Nxf1, though this association is dependent on the TREX complex (Viphakone et al, 2012). Thus it seems likely that the interaction which persists at the nuclear pore involves assembled TREX association with Nxf1.

TREX deposition on mRNA is coupled with splicing (Masuda et al, 2005) and the majority of splicing occurs co-transcriptionally. The majority of active spliceosomes localize to the periphery of nuclear speckles (Girard et al, 2012) and we see extensive TREX subunit and Nxf1:TREX interactions at the periphery of nuclear speckles which provides further support for the idea that TREX assembly is coupled with splicing. However, approximately 15-20% of active spliceosomes are found within nuclear speckles and these are engaged in post-transcriptional splicing (Girard et al, 2012). Post-transcriptionally spliced mRNA within nuclear speckles require mRNA export factors including Alyref and Uap56 to exit the nuclear speckle domain and for subsequent export to the cytoplasm (Girard et al, 2012) (Dias et al, 2010). Using FLIM-FRET, we are able to see interactions between TREX subunits and TREX:Nxf1 within speckles, indicating that active mRNA export complexes do

form within this domain, but the number of molecules engaged in these is much lower than at the periphery of speckles. This probably reflects the low percentage of transcripts which undergo post-transcriptional splicing.

In conclusion we have provided the first spatial map of mRNA export complex assembly by investigating where TREX assembly takes place and where Nxf1 is recruited to TREX in vivo. The major sites of mRNA export complex assembly coincide with sites involved in transcription, splicing and exon junction complex formation revealing how intimately coupled these processes are likely to be.

In other part, here we include in discussion how to analyse spatial distribution quantitatively (e.g. 3D zones etc). In order to detect the intracellular distribution of RNA or DNA, first of all, cells are pre-incubated with fluorescently labeled secondary antibody such as AlexaFluor 488 or 555 by the methods of fluorescent in situ hybridization (RNA FISH or DNA FISH), allowing to observe the localization of RNAs or DNAs in the cells under confocal microscopy. Secondly, to analyze spatial distribution quantitatively such as 3D zones, the image stacks with micrometer step size are collected step by step using optical confocal microscopes. In the examples of signals for green or red fluorescent staining, the image stacks are obtained from green and red

channel separately. Thirdly, the distance between signals observed from the image stacks are therefore measured or re-constructed in use of image analysis software such as Volocity.

REFERENCE

Abruzzi KC, Lacadie S, Rosbash M (2004) Biochemical analysis of TREX complex recruitment to intronless and intron-containing yeast genes. *EMBO J* 23: 2620-2631

Arts GJ, Kuersten S, Romby P, Ehresmann B, Mattaj IW (1998) The role of exportin-t in selective nuclear export of mature tRNAs. *EMBO J* 17: 7430-7441

Becker W. (2012) Fluorescence lifetime imaging--techniques and applications. *J Microsc*, Vol. 247, pp. 119-136.

Bednenko J, Cingolani G, Gerace L (2003) Nucleocytoplasmic transport: navigating the channel. *Traffic* 4: 127-135

Bernstein E, Caudy AA, Hammond SM, Hannon GJ (2001) Role for a bidentate ribonuclease in the initiation step of RNA interference. *Nature* 409: 363-366

Borchert GM, Lanier W, Davidson BL (2006) RNA polymerase III transcribes human microRNAs. *Nat Struct Mol Biol* 13: 1097-1101

Braun IC, Rohrbach E, Schmitt C, Izaurralde E (1999) TAP binds to the constitutive transport element (CTE) through a novel RNA-binding motif that is sufficient to promote CTE-dependent RNA export from the nucleus. *EMBO J* 18: 1953-1965

Bregman DB, Du L, van der Zee S, Warren SL (1995) Transcription-dependent redistribution of the large subunit of RNA polymerase II to discrete nuclear domains. *J Cell Biol* 129: 287-298

Brown JM, Green J, das Neves RP, Wallace HA, Smith AJ, Hughes J, Gray N, Taylor S, Wood WG, Higgs DR, Iborra FJ, Buckle VJ (2008) Association between active genes occurs at nuclear speckles and is modulated by chromatin environment. *J Cell Biol* 182: 1083-1097

Bucheli ME, He X, Kaplan CD, Moore CL, Buratowski S (2007) Polyadenylation site choice in yeast is affected by competition between Npl3 and polyadenylation factor CFI. *RNA* 13: 1756-1764

Carmody SR, Tran EJ, Apponi LH, Corbett AH, Wente SR (2010) The mitogen-activated protein kinase Slt2 regulates nuclear retention of non-heat shock mRNAs during heat shock-induced stress. *Mol Cell Biol* 30: 5168-5179

Céline Cassé, Federico Giannoni, Van Trung Nguyen, Marie-Françoise Dubois, Olivier Bensaude (1999) The Transcriptional Inhibitors, Actinomycin D and α-Amanitin, Activate the HIV-1 Promoter and Favor Phosphorylation of the RNA Polymerase II C-terminal Domain. *The Journal of Biological Chemistry* 274, 16097-16106.

Chang CT, Hautbergue GM, Walsh MJ, Viphakone N, van Dijk TB, Philipsen S, Wilson SA (2013) Chtop is a component of the dynamic TREX mRNA export complex. *EMBO J* 32: 473-486

Chen IH, Li L, Silva L, Sandri-Goldin RM (2005) ICP27 recruits Aly/REF but not TAP/NXF1 to herpes simplex virus type 1 transcription sites although TAP/NXF1 is required for ICP27 export. *J Virol* 79: 3949-3961

Chen IH, Sciabica KS, Sandri-Goldin RM (2002) ICP27 interacts with the RNA export factor Aly/REF to direct herpes simplex virus type 1 intronless mRNAs to the TAP export pathway. *J Virol* 76: 12877-12889

Cheng H, Dufu K, Lee CS, Hsu JL, Dias A, Reed R (2006) Human mRNA export machinery recruited to the 5' end of mRNA. *Cell* 127: 1389-1400

Cmarko D, Verschure PJ, Martin TE, Dahmus ME, Krause S, Fu XD, van Driel R, Fakan S (1999) Ultrastructural analysis of transcription and splicing in the cell nucleus after bromo-UTP microinjection. *Mol Biol Cell* 10: 211-223

Conti E, Izaurralde E (2001) Nucleocytoplasmic transport enters the atomic age. *Curr Opin Cell Biol* 13: 310-319

Coyle JH, Bor YC, Rekosh D, Hammarskjold ML (2011) The Tpr protein regulates export of mRNAs with retained introns that traffic through the Nxf1 pathway. *Rna* 17: 1344-1356

Cronshaw JM, Krutchinsky AN, Zhang W, Chait BT, Matunis MJ (2002)

Proteomic analysis of the mammalian nuclear pore complex. *J Cell Biol* 158: 915-927

Cook PR (2010) A model for all genomes: the role of transcription factories. *J Mol Biol* 395:1-10.

Custodio N, Carvalho C, Condado I, Antoniou M, Blencowe BJ, Carmo-Fonseca M (2004) In vivo recruitment of exon junction complex proteins to transcription sites in mammalian cell nuclei. *RNA* 10: 622-633

Daguenet E, Baguet A, Degot S, Schmidt U, Alpy F, Wendling C, Spiegelhalter C, Kessler P, Rio MC, Le Hir H, Bertrand E, Tomasetto C (2012) Perispeckles are major assembly sites for the exon junction core complex. *Mol Biol Cell* 23: 1765-1782

Das R, Yu J, Zhang Z, Gygi MP, Krainer AR, Gygi SP, Reed R (2007) SR proteins function in coupling RNAP II transcription to pre-mRNA splicing. *Mol Cell* 26: 867-881

Dias AP, Dufu K, Lei H, Reed R (2010) A role for TREX components in the release of spliced mRNA from nuclear speckle domains. *Nat Commun* 1: 97

Doyle O, Corden JL, Murphy C, Gall JG (2002) The distribution of RNA polymerase II largest subunit (RPB1) in the Xenopus germinal vesicle. *J Struct Biol* 140: 154-166

Dufu K, Livingstone MJ, Seebacher J, Gygi SP, Wilson SA, Reed R (2010) ATP is required for interactions between UAP56 and two conserved mRNA export proteins, Aly and CIP29, to assemble the TREX complex. *Genes Dev* 24: 2043-2053

Dundr M, Hoffmann-Rohrer U, Hu QY, Grummt I, Rothblum LI, Phair RD, Misteli T (2002) A kinetic framework for a mammalian RNA polymerase in vivo. Science 298:1623-1626.

Edelman LB, Fraser P (2012) Transcription factories: genetic programming in three dimensions. *Curr Opin Genet Dev* 22 (2):110-4.

Fahrenkrog B, Stoffler D, Aebi U (2001) Nuclear pore complex architecture and functional dynamics. *Curr Top Microbiol Immunol* 259: 95-117

Fakan S (1994) Perichromatin fibrils are in situ forms of nascent transcripts. *Trends Cell Biol* 4: 86-90

Fribourg S, Braun IC, Izaurralde E, Conti E (2001) Structural basis for the recognition of a nucleoporin FG repeat by the NTF2-like domain of the TAP/p15 mRNA nuclear export factor. *Mol Cell* 8: 645-656

Gatfield D, Izaurralde E (2002) REF1/Aly and the additional exon junction complex proteins are dispensable for nuclear mRNA export. *J Cell Biol* 159: 579-588

Gesnel MC, Del Gatto-Konczak F, Breathnach R (2009) Combined use of MS2 and PP7 coat fusions shows that TIA-1 dominates hnRNP A1 for K-SAM exon splicing control. *J Biomed Biotechnol* 2009: 104853

Gilbert W, Guthrie C (2004) The Glc7p nuclear phosphatase promotes mRNA export by facilitating association of Mex67p with mRNA. *Mol Cell* 13: 201-212

Girard C, Will CL, Peng J, Makarov EM, Kastner B, Lemm I, Urlaub H, Hartmuth K, Luhrmann R (2012) Post-transcriptional spliceosomes are retained in nuclear speckles until splicing completion. *Nat Commun* 3: 994

Gorlich D, Kutay U (1999) Transport between the cell nucleus and the cytoplasm. *Annu Rev Cell Dev Biol* 15: 607-660

Grande MA, van der Kraan I, de Jong L, van Driel R (1997) Nuclear distribution of transcription factors in relation to sites of transcription and RNA polymerase II. *J Cell Sci* 110 (Pt 15): 1781-1791

Graveley BR (2000) Sorting out the complexity of SR protein functions. *RNA* 6: 1197-1211

Gwizdek C, Hobeika M, Kus B, Ossareh-Nazari B, Dargemont C, Rodriguez MS (2005) The mRNA nuclear export factor Hpr1 is regulated by

Rsp5-mediated ubiquitylation. *J Biol Chem* 280: 13401-13405

Gwizdek C, Iglesias N, Rodriguez MS, Ossareh-Nazari B, Hobeika M, Divita G, Stutz F, Dargemont C (2006) Ubiquitin-associated domain of Mex67 synchronizes recruitment of the mRNA export machinery with transcription. *Proc Natl Acad Sci U S A* 103: 16376-16381

Hall LL, Smith KP, Byron M, Lawrence JB (2006) Molecular anatomy of a speckle. *Anat Rec A Discov Mol Cell Evol Biol* 288: 664-675

Hautbergue GM, Hung ML, Walsh MJ, Snijders AP, Chang C, Jones R, Ponting CP, Dickman MJ, Wilson SA (2009a) UIF, a New mRNA Export Adaptor Which Works Together with REF/ALY, Requires FACT for Recruitment to mRNA. *Curr Biol* 19: 1918-1924

Hautbergue GM, Hung ML, Walsh MJ, Snijders AP, Chang CT, Jones R, Ponting CP, Dickman MJ, Wilson SA (2009b) UIF, a New mRNA export adaptor that works together with REF/ALY, requires FACT for recruitment to mRNA. *Curr Biol* 19: 1918-1924

Hellmuth K, Lau DM, Bischoff FR, Kunzler M, Hurt E, Simos G (1998) Yeast Los1p has properties of an exportin-like nucleocytoplasmic transport factor for tRNA. *Mol Cell Biol* 18: 6374-6386

Hieronymus H, Silver PA (2003) Genome-wide analysis of RNA-protein interactions illustrates specificity of the mRNA export machinery. *Nat Genet* 33: 155-161

Ho JH, Kallstrom G, Johnson AW (2000) Nmd3p is a Crm1p-dependent adapter protein for nuclear export of the large ribosomal subunit. *J Cell Biol* 151: 1057-1066

Hobeika M, Brockmann C, Iglesias N, Gwizdek C, Neuhaus D, Stutz F, Stewart M, Divita G, Dargemont C (2007) Coordination of Hpr1 and ubiquitin binding by the UBA domain of the mRNA export factor Mex67. *Mol Biol Cell* 18: 2561-2568

Huang S, Deerinck TJ, Ellisman MH, Spector DL (1994) In vivo analysis of the

stability and transport of nuclear poly(A)+ RNA. *J Cell Biol* 126: 877-899

Huang Y, Yario TA, Steitz JA (2004) A molecular link between SR protein dephosphorylation and mRNA export. *Proc Natl Acad Sci U S A* 101: 9666-9670

Huber J, Cronshagen U, Kadokura M, Marshallsay C, Wada T, Sekine M, Luhrmann R (1998) Snurportin1, an m3G-cap-specific nuclear import receptor with a novel domain structure. *EMBO J* 17: 4114-4126

Huertas P, Aguilera A (2003) Cotranscriptionally formed DNA:RNA hybrids mediate transcription elongation impairment and transcription-associated recombination. *Mol Cell* 12: 711-721

Hung ML, Hautbergue GM, Snijders AP, Dickman MJ, Wilson SA (2010a) Arginine methylation of REF/ALY promotes efficient handover of mRNA to TAP/NXF1. *Nucleic Acids Res* 38: 3351-3361

Hung ML, Hautbergue GM, Snijders AP, Dickman MJ, Wilson SA (2010b) Arginine methylation of REF/ALY promotes efficient handover of mRNA to TAP/NXF1. *Nucleic Acids Res*

Iborra FJ, Pombo A, Jackson DA, Cook PR (1996) Active RNA polymerases are localized within discrete transcription ‘factories’ in human nuclei. *J Cell Sci* 109, 1427–1436.

Iglesias N, Stutz F (2008) Regulation of mRNP dynamics along the export pathway. *FEBS Lett* 582: 1987-1996

Iglesias N, Tutucci E, Gwizdek C, Vinciguerra P, Von Dach E, Corbett AH, Dargemont C, Stutz F (2010) Ubiquitin-mediated mRNP dynamics and surveillance prior to budding yeast mRNA export. *Genes Dev* 24: 1927-1938

Jackson BR, Boyne JR, Noerenberg M, Taylor A, Hautbergue GM, Walsh MJ, Wheat R, Blackbourn DJ, Wilson SA, Whitehouse A (2011) An interaction between KSHV ORF57 and UIF provides mRNA-adaptor redundancy in herpesvirus intronless mRNA export. *PLoS Pathog* 7: e1002138

Jackson DA, Iborra FJ, Manders EM, Cook PR (1998) Numbers and organization of RNA polymerases, nascent transcripts, and transcription units in HeLa nuclei. *Mol. Biol. Cell* 9, 1523–1536.

Jackson DA, Pombo A, Iborra F (2000) The balance sheet for transcription: an analysis of nuclear RNA metabolism in mammalian cells. *FASEB J.* 14, 242–254.

Jackson DA (2003) The principles of nuclear structure. *Chromosome Res* 11(5):387-401.

Jackson DA (2003) The anatomy of transcription sites. *Curr Opin Cell Biol* 15(3):311-7.

Jackson DA (2005) The amazing complexity of transcription factories. *Brief Funct Genomic Proteomic* 4(2): 143-57.

Jensen TH, Boulay J, Olesen JR, Colin J, Weyler M, Libri D (2004) Modulation of transcription affects mRNP quality. *Mol Cell* 16: 235-244

Johnson C, Primorac D, McKinstry M, McNeil J, Rowe D, Lawrence JB (2000) Tracking COL1A1 RNA in osteogenesis imperfecta. splice-defective transcripts initiate transport from the gene but are retained within the SC35 domain. *J Cell Biol* 150: 417-432

Johnson LA, Li L, Sandri-Goldin RM (2009a) The cellular RNA export receptor TAP/NXF1 is required for ICP27-mediated export of herpes simplex virus 1 RNA, but the TREX complex adaptor protein Aly/REF appears to be dispensable. *J Virol* 83: 6335-6346

Johnson LA, Sandri-Goldin RM (2009) Efficient nuclear export of herpes simplex virus 1 transcripts requires both RNA binding by ICP27 and ICP27 interaction with TAP/NXF1. *J Virol* 83: 1184-1192

Johnson SA, Cubberley G, Bentley DL (2009b) Cotranscriptional recruitment of the mRNA export factor Yra1 by direct interaction with the 3' end processing factor Pcf11. *Mol Cell* 33: 215-226

Johnson SA, Kim H, Erickson B, Bentley DL (2011) The export factor Yra1 modulates mRNA 3' end processing. *Nat Struct Mol Biol* 18: 1164-1171

Katahira J, Inoue H, Hurt E, Yoneda Y (2009) Adaptor Aly and co-adaptor Thoc5 function in the Tap-p15-mediated nuclear export of HSP70 mRNA. *EMBO J* 28: 556-567

Kelly SM, Leung SW, Apponi LH, Bramley AM, Tran EJ, Chekanova JA, Wente SR, Corbett AH (2010) Recognition of polyadenosine RNA by the zinc finger domain of nuclear poly(A) RNA-binding protein 2 (Nab2) is required for correct mRNA 3'-end formation. *J Biol Chem* 285: 26022-26032

Kelly SM, Pabit SA, Kitchen CM, Guo P, Marfatia KA, Murphy TJ, Corbett AH, Berland KM (2007) Recognition of polyadenosine RNA by zinc finger proteins. *Proc Natl Acad Sci U S A* 104: 12306-12311

Kim Guisbert K, Duncan K, Li H, Guthrie C (2005) Functional specificity of shuttling hnRNPs revealed by genome-wide analysis of their RNA binding profiles. *RNA* 11: 383-393

Kimura H, Sugaya K, Cook PR (2002) The transcription cycle of RNA polymerase II in living cells. *J Cell Biol* 159: 777-782

Kiseleva E, Goldberg MW, Allen TD, Akey CW (1998) Active nuclear pore complexes in Chironomus: visualization of transporter configurations related to mRNP export. *J Cell Sci* 111 (Pt 2): 223-236

Kohler A, Hurt E (2007) Exporting RNA from the nucleus to the cytoplasm. *Nat Rev Mol Cell Biol* 8: 761-773

Kress TL, Krogan NJ, Guthrie C (2008) A single SR-like protein, Npl3, promotes pre-mRNA splicing in budding yeast. *Mol Cell* 32: 727-734

Kutay U, Lipowsky G, Izaurralde E, Bischoff FR, Schwarzmaier P, Hartmann E, Gorlich D (1998) Identification of a tRNA-specific nuclear export receptor. *Mol Cell* 1: 359-369

Lamond AI, Spector DL (2003) Nuclear speckles: a model for nuclear

organelles. *Nat Rev Mol Cell Biol* 4: 605-612

Le Hir H, Gatfield D, Izaurralde E, Moore MJ (2001) The exon-exon junction complex provides a binding platform for factors involved in mRNA export and nonsense-mediated mRNA decay. *EMBO J* 20: 4987-4997

Le Hir H, Izaurralde E, Maquat LE, Moore MJ (2000) The spliceosome deposits multiple proteins 20-24 nucleotides upstream of mRNA exon-exon junctions. *EMBO J* 19: 6860-6869

Lee Y, Ahn C, Han J, Choi H, Kim J, Yim J, Lee J, Provost P, Radmark O, Kim S, Kim VN (2003) The nuclear RNase III Drosha initiates microRNA processing. *Nature* 425: 415-419

Li Y, Wang X, Zhang X, Goodrich DW (2005) Human hHpr1/p84/Thoc1 regulates transcriptional elongation and physically links RNA polymerase II and RNA processing factors. *Mol Cell Biol* 25: 4023-4033

Longman D, Johnstone IL, Caceres JF (2003) The Ref/Aly proteins are dispensable for mRNA export and development in Caenorhabditis elegans. *RNA* 9: 881-891

Luo ML, Zhou Z, Magni K, Christoforides C, Rappsilber J, Mann M, Reed R (2001) Pre-mRNA splicing and mRNA export linked by direct interactions between UAP56 and Aly. *Nature* 413: 644-647

Masuda S, Das R, Cheng H, Hurt E, Dorman N, Reed R (2005) Recruitment of the human TREX complex to mRNA during splicing. *Genes Dev* 19: 1512-1517

Mattaj IW, Englmeier L (1998) Nucleocytoplasmic transport: the soluble phase. *Annu Rev Biochem* 67: 265-306

Martin S, Pombo A (2003) Transcription factories: quantitative studies of nanostructures in the mammalian nucleus. *Chromosome Res.* 11, 461–470
.
Melnik S, Deng B, Papantonis A, Baboo S, Carr IM, Cook PR (2011) The proteomes of transcription factories containing RNA polymerases I, II or III. *Nature Methods* 8, 963–968

Melcak I, Cermanova S, Jirsova K, Koberna K, Malinsky J, Raska I (2000) Nuclear pre-mRNA compartmentalization: trafficking of released transcripts to splicing factor reservoirs. *Mol Biol Cell* 11: 497-510

Misteli T, Caceres JF, Clement JQ, Krainer AR, Wilkinson MF, Spector DL (1998) Serine phosphorylation of SR proteins is required for their recruitment to sites of transcription in vivo. *J Cell Biol* 143: 297-307

Misteli T, Caceres JF, Spector DL (1997) The dynamics of a pre-mRNA splicing factor in living cells. *Nature* 387: 523-527

Moen PT, Jr., Johnson CV, Byron M, Shopland LS, de la Serna IL, Imbalzano AN, Lawrence JB (2004) Repositioning of muscle-specific genes relative to the periphery of SC-35 domains during skeletal myogenesis. *Mol Biol Cell* 15: 197-206

Mortillaro MJ, Blencowe BJ, Wei X, Nakayasu H, Du L, Warren SL, Sharp PA, Berezney R (1996) A hyperphosphorylated form of the large subunit of RNA polymerase II is associated with splicing complexes and the nuclear matrix. *Proc Natl Acad Sci U S A* 93: 8253-8257

Nickels BE, Mukhopadhyay j, Garrity SJ, Ebright RH, Hochschild A (2004) The σ^{70} subunit of RNA polymerase mediates a promoter-proximal pause at the lac promoter. *Nat Struct Mol Biol* 11: 544–550.

Nissan TA, Bassler J, Petfalski E, Tollervey D, Hurt E (2002) 60S pre-ribosome formation viewed from assembly in the nucleolus until export to the cytoplasm. *EMBO J* 21: 5539-5547

Noordermeer D, Branco MR, Splinter E, Klous P, van Ijcken W, Swagemakers S, Koutsourakis M, van der Spek P, Pombo A, de Laat W (2008) Transcription and chromatin organization of a housekeeping gene cluster containing an integrated betaglobin locus control region. *PLoS Genet* 4:e1000016.

Ohno M, Segref A, Bachi A, Wilm M, Mattaj IW (2000) PHAX, a mediator of U snRNA nuclear export whose activity is regulated by phosphorylation. *Cell* 101: 187-198

Osborne CS, Chakalova L, Brown KE, Carter D, Horton A, Debrand E, Goyenechea B, Mitchell JA, Lopes S, Reik W, Fraser P (2004) Active genes dynamically colocalize to shared sites of ongoing transcription. *Nature Genetics* 36 (10): 1065–71.

Papantonis A, Takahide Kohro T, Baboo S, Larkin JD, Deng B, Patrick, Short P, Tsutsumi S, Taylor S, Kanki Y, Kobayashi M, Li G, Poh HM, Ruan X, Aburatani H, Ruan Y, Kodama T, Wada Y, Cook PR (2012) TNFα signals through specialized factories where responsive coding and miRNA genes are transcribed. *EMBO J* 31(23): 4404–4414

Papantonis A, Cook PR (2010) Genome architecture and the role of transcription. *CURRENT OPINION IN CELL BIOLOGY* 22:271–276

Pemberton LF, Blobel G, Rosenblum JS (1998) Transport routes through the nuclear pore complex. *Curr Opin Cell Biol* 10: 392-399

Proudfoot N (2004) New perspectives on connecting messenger RNA 3' end formation to transcription. *Curr Opin Cell Biol* 16: 272-278

Rappsilber J, Ryder U, Lamond AI, Mann M (2002) Large-scale proteomic analysis of the human spliceosome. *Genome Res* 12: 1231-1245

Reed R, Cheng H (2005) TREX, SR proteins and export of mRNA. *Curr Opin Cell Biol* 17: 269-273

Reed R, Hurt E (2002) A conserved mRNA export machinery coupled to pre-mRNA splicing. *Cell* 108: 523-531

Rehwinkel J, Herold A, Gari K, Kocher T, Rode M, Ciccarelli FL, Wilm M, Izaurralde E (2004) Genome-wide analysis of mRNAs regulated by the THO complex in Drosophila melanogaster. *Nat Struct Mol Biol* 11: 558-566

Ribbeck K, Gorlich D (2001) Kinetic analysis of translocation through nuclear pore complexes. *EMBO J* 20: 1320-1330

Ribbeck K, Gorlich D (2002) The permeability barrier of nuclear pore

complexes appears to operate via hydrophobic exclusion. *EMBO J* 21: 2664-2671

Rodrigues JP, Rode M, Gatfield D, Blencowe BJ, Carmo-Fonseca M, Izaurralde E (2001) REF proteins mediate the export of spliced and unspliced mRNAs from the nucleus. *Proc Natl Acad Sci U S A* 98: 1030-1035

Rodriguez-Navarro S, Hurt E (2011) Linking gene regulation to mRNA production and export. *Curr Opin Cell Biol* 23: 302-309

Rodriguez MS, Dargemont C, Stutz F (2004) Nuclear export of RNA. *Biol Cell* 96: 639-655

Rout MP, Aitchison JD (2001) The nuclear pore complex as a transport machine. *J Biol Chem* 276: 16593-16596

Rout MP, Aitchison JD, Magnasco MO, Chait BT (2003) Virtual gating and nuclear transport: the hole picture. *Trends Cell Biol* 13: 622-628

Rout MP, Aitchison JD, Suprapto A, Hjertaas K, Zhao Y, Chait BT (2000) The yeast nuclear pore complex: composition, architecture, and transport mechanism. *J Cell Biol* 148: 635-651

Sacco-Bubulya P, Spector DL (2002) Disassembly of interchromatin granule clusters alters the coordination of transcription and pre-mRNA splicing. *J Cell Biol* 156: 425-436

Sadowski M, Dichtl B, Hubner W, Keller W (2003) Independent functions of yeast Pcf11p in pre-mRNA 3' end processing and in transcription termination. *EMBO J* 22: 2167-2177

Saitoh N, Spahr CS, Patterson SD, Bubulya P, Neuwald AF, Spector DL (2004) Proteomic analysis of interchromatin granule clusters. *Mol Biol Cell* 15: 3876-3890

Sandri-Goldin RM (2004) Viral regulation of mRNA export. *J Virol* 78: 4389-4396

Sapra AK, Anko ML, Grishina I, Lorenz M, Pabis M, Poser I, Rollins J, Weiland EM, Neugebauer KM (2009) SR protein family members display diverse activities in the formation of nascent and mature mRNPs in vivo. *Mol Cell* 34: 179-190

Schmidt U, Richter K, Berger AB, Lichter P (2006) In vivo BiFC analysis of Y14 and NXF1 mRNA export complexes: preferential localization within and around SC35 domains. *J Cell Biol* 172: 373-381

Schwarz DS, Hutvagner G, Du T, Xu Z, Aronin N, Zamore PD (2003) Asymmetry in the assembly of the RNAi enzyme complex. *Cell* 115: 199-208

Sciabica KS, Dai QJ, Sandri-Goldin RM (2003) ICP27 interacts with SRPK1 to mediate HSV splicing inhibition by altering SR protein phosphorylation. *EMBO J* 22: 1608-1619

Sekar RB, Periasamy A (2003) Fluorescence resonance energy transfer (FRET) microscopy imaging of live cell protein localizations. *J Cell Biol* 160: 629-633

Shopland LS, Johnson CV, Byron M, McNeil J, Lawrence JB (2003) Clustering of multiple specific genes and gene-rich R-bands around SC-35 domains: evidence for local euchromatic neighborhoods. *J Cell Biol* 162: 981-990

Spector DL (1993) Macromolecular domains within the cell nucleus. *Annu Rev Cell Biol* 9: 265-315

Spector DL (2003) The dynamics of chromosome organization and gene regulation. *Annu Rev Biochem* 72: 573-608

Spector DL, Lamond AI (2011) Nuclear speckles. *Cold Spring Harbor perspectives in biology* 3

Strasser K, Bassler J, Hurt E (2000) Binding of the Mex67p/Mtr2p heterodimer to FXFG, GLFG, and FG repeat nucleoporins is essential for nuclear mRNA export. *J Cell Biol* 150: 695-706

Strasser K, Hurt E (2000) Yra1p, a conserved nuclear RNA-binding protein,

interacts directly with Mex67p and is required for mRNA export. *EMBO J* 19: 410-420

Strasser K, Hurt E (2001) Splicing factor Sub2p is required for nuclear mRNA export through its interaction with Yra1p. *Nature* 413: 648-652

Strasser K, Masuda S, Mason P, Pfannstiel J, Oppizzi M, Rodriguez-Navarro S, Rondon AG, Aguilera A, Struhl K, Reed R, Hurt E (2002) TREX is a conserved complex coupling transcription with messenger RNA export. *Nature* 417: 304-308

Stutz F, Bachi A, Doerks T, Braun IC, Seraphin B, Wilm M, Bork P, Izaurralde E (2000) REF, an evolutionary conserved family of hnRNP-like proteins, interacts with TAP/Mex67p and participates in mRNA nuclear export. *RNA* 6: 638-650

Sutherland H, Bickmore WA (2009) Transcription factories: gene expression in unions? *Nat Rev Genet* 10:457-466.

Thiry M (1995) The interchromatin granules. *Histol Histopathol* 10: 1035-1045

Tran EJ, Zhou Y, Corbett AH, Wente SR (2007) The DEAD-box protein Dbp5 controls mRNA export by triggering specific RNA:protein remodeling events. *Mol Cell* 28: 850-859

Valencia-Sanchez MA, Liu J, Hannon GJ, Parker R (2006) Control of translation and mRNA degradation by miRNAs and siRNAs. *Genes Dev* 20: 515-524

Van Hijum SA, Medema MH, Kuipers OP (2009) Mechanisms and evolution of control logic in prokaryotic transcriptional regulation. *Microbiol Mol Biol Rev.* 73(3):481-509.

van Dijk TB, Gillemans N, Stein C, Fanis P, Demmers J, van de Corput M, Essers J, Grosveld F, Bauer UM, Philipsen S (2010) Friend of Prmt1, a novel chromatin target of protein arginine methyltransferases. *Mol Cell Biol* 30: 260-272

Vinciguerra P, Iglesias N, Camblong J, Zenklusen D, Stutz F (2005)

Perinuclear Mlp proteins downregulate gene expression in response to a defect in mRNA export. *Embo J* 24: 813-823

Viphakone N, Hautbergue GM, Walsh M, Chang CT, Holland A, Folco EG, Reed R, Wilson SA (2012) TREX exposes the RNA-binding domain of Nxf1 to enable mRNA export. *Nat Commun* 3: 1006

Wade JT, Roa DC, Grainger DC, Hurd D, Busby SJ, Struhl K, Nudler E (2006) Extensive functional overlap between sigma factors in *Escherichia coli*. *Nat Struct Mol Biol* 13:806–814.

Walsh MJ, Hautbergue GM, Wilson SA (2010) Structure and function of mRNA export adaptors. *Biochem Soc Trans* 38: 232-236

Wei X, Somanathan S, Samarabandu J, Berezney R (1999) Three-dimensional visualization of transcription sites and their association with splicing factor-rich nuclear speckles. *J Cell Biol* 146: 543-558

Wells SE, Hillner PE, Vale RD, Sachs AB (1998) Circularization of mRNA by eukaryotic translation initiation factors. *Mol Cell* 2: 135-140

Wong CM, Tang HM, Kong KY, Wong GW, Qiu H, Jin DY, Hinnebusch AG (2010) Yeast arginine methyltransferase Hmt1p regulates transcription elongation and termination by methylating Npl3p. *Nucleic Acids Res* 38: 2217-2228

Xu M, Cook PR (2008) Similar active genes cluster in specialized transcription factories. *J Cell Biol* 181, 615–623.

Yao W, Roser D, Kohler A, Bradatsch B, Bassler J, Hurt E (2007) Nuclear export of ribosomal 60S subunits by the general mRNA export receptor Mex67-Mtr2. *Mol Cell* 26: 51-62

Yoh SM, Cho H, Pickle L, Evans RM, Jones KA (2007) The Spt6 SH2 domain binds Ser2-P RNAPII to direct Iws1-dependent mRNA splicing and export. *Genes Dev* 21: 160-174

Zenklusen D, Vinciguerra P, Wyss JC, Stutz F (2002) Stable mRNP formation

and export require cotranscriptional recruitment of the mRNA export factors Yra1p and Sub2p by Hpr1p. *Mol Cell Biol* 22: 8241-8253

Zhao R, Bodnar MS, Spector DL (2009) Nuclear neighborhoods and gene expression. *Curr Opin Genet Dev* 19: 172-179

Zhou Z, Licklider LJ, Gygi SP, Reed R (2002) Comprehensive proteomic analysis of the human spliceosome. *Nature* 419: 182-185

Zhou Z, Luo MJ, Straesser K, Katahira J, Hurt E, Reed R (2000) The protein Aly links pre-messenger-RNA splicing to nuclear export in metazoans. *Nature* 407: 401-405